MASTER OF SCIENCE BY RESEARCH

Power-train control and design for a stable and driveable hybrid electric vehicle

Kode, Hugues Komi

Award date:
2011

Awarding institution:
Coventry University

Power-train Control and Design for a Stable and Driveable Hybrid Electric Vehicle

by

Hugues Komi KODE

A thesis

submitted in partial fulfilment

of the University's requirements for the degree of

MSc by Research

Control Theory and Applications Centre (CTAC)

Coventry University, United Kingdom, *April, 2011*

Author's declaration

I hereby certify that this thesis contains no material previously published or written by another person. All material borrowed from other persons are fully referenced. This is a true copy of the thesis, including any required final revisions, as accepted by my examiners. I understand that my thesis may be made electronically available to the public.

Abstract

The price of oil has been increasing since the oil crisis of 1970. Indeed oil, often imported, lies at the heart of the transportation industries of the richest countries in the world (this earth). In the transportation industry there are vehicles (cars and trucks), which use large quantities of fuel (oil), which in turn produce pollutants (CO, CO_2, NO_x ...). These pollutants constitute an additive problem of environmental pollution, which today is reaching a level, which threatens the climate of the planet. This document will focus on the hybrid electrical vehicle (HEV), in particular a four-wheel drive vehicle. The work carried out in this research is essentially power-train control, with the development of a power-train controller platform. This platform can be 'plugged' into different HEV power-trains. The outcome of the simulation results shows that the developed platform needs to be re-configured properly for each power-train for satisfactory simulation results of the flow of the power and the vehicle handling. The main topics in this thesis are HEV, design, modelling and control.

Acknowledgements

Firstly I would like to say many thanks to my Supervisor and Mentor Professor Keith J. Burnham, Director of the CTAC (Control Theory and Applications Centre) for his valuable information, advice and support. Many thanks go to Jaguar-Land Rover for funding this work.

I give many thanks to Miss M. Williamson and President Mandela for their philosophy, which definitely has strengthened my personal mastery and mental model. Many thanks go to MathWorks for help and valuable and information about the modelling tool box. I give many thanks as well to Mr. O. Maganga a PhD student, Mr. A. Fofana a part-time PhD student and Mr. J. Mahtani, Programme Manager, MSc courses in Systems and Control at Coventry University, for their valuable advice and information. I would like to say many thanks to Mr. V. Ersanilli a PhD student and Dr. A. Koshkouei researcher and lecturer at Coventry University for their valuable advice and information. My thanks go also to Mr. J. Herring a PhD student without forgetting Dr. S. Oleksowicz and Mr. N. Phillip for providing some data. I would like to thank Mr. T. Aizad and Mr. L. Birek, a PhD student, for their advice. I will also like to thank Dr. T. Larkowski Lecturer, System identification, errors-in-variables, parameter estimation, signal processing at Coventry University for his advice. I also want to thank my friends who helped me mentally, financially to finish this MSc. Many thanks go to all CTAC staff for their valuable information.

Dedication

To my mother ***Elisabeth A. Soukou***

and

my step small brother ***Afianke K. Ayebou***

who have given me the

courage to do this Master's degree.

Man, who will do everything to reach his goal is great this man can only be noble. Our deepest fear is not to be unfits. But to be powerful beyond measure. It is our own light and not our darkness, which frightens us most. Sometimes we ask ourselves, Who am I to be brilliant, talented, fabulous? Playing small does not serve the world neither your people. We are all born to make difference and impact the world and shine like Stars. That Glory is not just in some of us; it's in everyone. As we let our own light shine, we unconsciously allow others to do the same. As we are liberated from our own fear, our presence alone can liberate others.

Contents

List of Variables

LCV: Low carbon vehicle.

LCEV: Low carbon emission vehicle

HEV: Hybrid electric vehicle.

EV: Electric vehicle.

PS: Power-split.

FC: Fuel cell.

S HEV: Series hybrid electric vehicle.

P HEV: Parallel hybrid electric vehicle.

PHEV: Plug-in hybrid electric vehicle.

PS HEV: Power-split hybrid electric vehicle.

FC HEV: Fuel cell hybrid electric vehicle.

SOC: Sate of charge.

DOH: Degree of hybridisation.

PID: Proportional integral and derivative.

EM: Electrical motor.

Gen.: Generator.

ICE: Internal combustion engine.

ESS: Energy storage systems.

Driver: Driver acceleration profile.

EM_Crtl: EM control action.

Gen._Crtl: Generator control action.

ICE_Crtl: ICE control action.

EM_Tork: Replicated physical mechanical EM torque in $[Nm]$.

ICE_Tork: Replicated physical mechanical ICE torque in $[Nm]$.

Drive Shaft FC: Replicated physical mechanical EM torque, which drives four-wheel drive FC HEV.

Drive Shaft S: Replicated physical mechanical EM torque, which drives four-wheel drive S HEV.

Drive Shaft P1: Replicated physical mechanical EM torque, which drives the two front-wheel of four-wheel drive P HEV.

Drive Shaft P2: Replicated physical mechanical ICE torque, which drives the two rear wheels of four-wheel drive P HEV.

Drive Shaft PS: the summation of the replicated physical mechanical EM torque and the Physical (mechanical) ICE torque, which drives four-wheel drive PS HEV.

EM_spd: EM speed in $[rpm]$.

ICE_Gen._spd: ICE speed in $[rpm]$.

Vbat: Replicated physical electrical input and output of the high voltage battery in $[V]$.

Vdc: Replicated physical electrical input and output of the DC/DC converter in $[V]$.

Vgen: Replicated physical electrical output of the Gen. in $[V]$.

Vem: Replicated physical electrical input and output of the EM in $[V]$.

List of Tables

List of Figures

Chapter 1

Introduction and outline of the thesis

In recent years, fuel economy has been one of the dominant challenges facing the automotive industry. Much research work in the automotive industry over last decades has been focused on sustainable transportation systems. Emerging technologies to achieve satisfactory fuel efficiency, which in return reduces pollutants in vehicles using an internal combustion engine (ICE), are an electric vehicle (EV) or a hybrid electric vehicle (HEV). Basically a HEV is an electric power-train coupled to a ICE power-train. Indeed, a conventional vehicle power-train (the ICE power-train) regroups an engine, transmission, differential and controllers. The HEV power-train operates as described as follows: the controller translates a request (torque) from the driver into inputs to the engine and transmission and this produces the desired torque. It is generally known that electric motors (EMs) are much more efficient than the ICE. Additionally, the EMs are pollutant free. In

other words they are considered to be more environmentally friendly. The power-train control is one of the most interesting and challenging aspect of hybridisation. This is because the energy efficiency of HEVs depends on the power-train control strategy. This is in fact the control strategy or energy management of the hybrid electrical vehicle (HEV). Therefore, the performance of such a system depends on the control method, which should be robust (independent from uncertainties and always guaranteeing the stability of the vehicle) and of course reliable. However, the HEVs power-train control is a complex task compared to a conventional ICE power-train control. This complexity is due to the additional components and to the coupling among these components. These additional components also increase the number of states to be controlled.

The HEV aims to:

- Maximise fuel economy
- Minimise emission of pollutants
- Minimise cost of the propulsion system
- Maintain state of charge (SOC) at a safe level (improve energy storage system (ESS))
- Finally produce an acceptance performance

1.1 Aims and Objective

Essentially the problems are: How to design a computer based HEV power-train? How to control the computer based HEV power-train? How to design a stable and driveable HEV power-train?

In other words: how to manage the flow of power in a HEV power-train and having acceptable handling of the vehicle on the road?

The aim in this research is to design a re-configurable power-train controller (a platform to plug into different power-trains).

The objective within this work is to evaluate the developed power-train controller platform in four different power-trains.

This work is concerned only with a four-wheel drive vehicle, with a petrol engine as the internal combustion engine.

1.2 Contribution

The main contribution in this thesis is the development of a simulation platform, which has been designed to be modular in order to allow ease of comparison of different HEV types.

To demonstrate the effectiveness of the proposed platform, four HEV types are evaluated and their potential assessed when a single controller configuration, both supervisory and component level, is applied.

Whilst, the controllers (supervisory and component level) have not been optimised or tuned to obtain the best performance for each individual HEV power-train, the results obtained are able to provide a preliminary 'benchmark' upon which to improve.

The main attributes of each HEV drivetrains have been highlighted and their individual merits have been discussed. It is left for further work to obtain the best performance for each individual HEV system.

1.3 Organisation of thesis

This thesis is organised as follows:

Chapter 2 provides a literature review, where four different types of HEV are considered. These types are: series HEV, parallel HEV, power-split HEV and fuel cell HEV. Various energy storage systems (ESS) such as a battery and ultra-capacitor are also reviewed. Finally a number of existing control strategies are reviewed.

Chapter 3 describes different HEV architectures, which are proposed and will be implemented. It also deals with Simulink modelling of these architectures. Finally, the re-configurable power-train control strategy, which is going to be implemented will be introduced.

Chapter 4 covers the analysis of simulation results. It aims to verify the goals set in this thesis, which are: designing a HEV power-train, control the HEV power train with a re-configurable power-train controller, finally having a stable and driveable HEV under the proposed power-train controller platform.

Chapter 5 deals with the general conclusions of the work carried out in this research. Also, some further work, which may need to be done for improving the results, is presented and aspects of implementation are considered.

Appendixes A to D give more information about for example the definitions of some of the technical terms and expressions and also include some mathematical formulation used in this document. The implementations of the different subsystems of the HEVs in Simulink are also explained.

Chapter 2

Literature review

This Chapter of the thesis presents the background knowledge of the HEV technologies. In effect it deals with different power-train architectures and power-train components, which are used in the design, and especially the energy storage system. Different control strategies for energy management will also be presented.

2.1 Low carbon vehicle (LCV), general concepts and applications

This Section deals with various types of low carbon emission vehicle (LCEV). The goal here is to introduce different LCEV technologies which already exist. In return it will propose different power-trains design and control strategies. LCEV can be interpreted differently, but here it is restricted to: electric vehicle (EV), hybrid electric vehicle (HEV), plug-in hybrid electric vehicle (PHEV) and fuel cell hybrid

electric vehicle (FC HEV). The LCEV is classified according to the traction power source of the vehicle, which are mainly the ICE and the electric motor (EM) in the HEV case. in other words the sources in question use fuel and electricity to power the EM, which drives the vehicle.

2.1.1 Electric vehicle (EV)

The EV uses batteries to provide the power to the EM. The problem with EV is in the energy storage systems. Here, the energy is mostly stored in a high voltage battery. EV requires to be recharged often (by plug-in electric grid) and the charging times maybe long. To solve the energy storage and charging time problems, HEVs are proposed [1, 2, 3, 4].

2.1.2 Internal combustion engine (ICE) based HEV

In an ICE based HEV, the ICE is coupled with the EM. This combination creates an integrated mechanical and electric drivetrain (see Definition 1 in Appendix A). Here, both ICE and EM drive the vehicle. As a consequence the ICE operates efficiently, because the energy storage system (ESS) provides power to the EM to compensate the ICE power sometimes, or versa. In this type of hybrid, fuel (oil), remains one of the energy sources for the HEV. The introduction of the EM in the HEV power-train, allows reducing the ICE size, and therefore, pollution reduction. As a consequence, the ICE in a HEV, operates more efficiently than in a conventional ICE power-train. The emissions and the fuel consumption of the HEV are tremendously lower in the ICE based HEV than in conventional vehicles [1, 2, 3,

4, 5, 6, 7, 8]. Most of the commercialised HEV are currently ICE based.

2.1.3 Fuel cell (FC) based HEV

FC HEV use only electric power to drive the vehicles. In fact, a fuel cell system is an electric power-generating plant, which is based on controlled electrochemical reactions, the so called proton exchange membrane. The fuel cell continuously produces electric power to run the electric motor and store the energy in an energy storage device (battery). Indeed, the power flow in the electric power-train (see Definition 2 in Appendix A) allows the FC HEV to drive. In principle, fuel cells are more efficient in energy conversion. Besides, it produces zero emissions, because the electrochemical reaction produces water and heat as emissions. FC HEV has advantages such as low operational temperature, compact structure, quick start-up and it is environmentally friendly [1, 10, 11, 12, 13]. However, similar to all the atomic reactions, it needs energy (electricity) to start. The fuel cell is an ideal power source for automotive application. Note that FC HEV is an EV, which derives its electricity from fuel cells activities.

2.2 Architectures of hybrid electric vehicles

A HEV propulsion system (power-train) comprises basically the ICE, a number of electric energy storage devices such as batteries, ultra-capacitors, EM, power converters, a transmission and different driveline links. The classification of the HEV is based on the configuration of the vehicle drivetrain (see Definition 1 in Appendix A). This Section, allows a familiarisation with various HEV architectures

and terminologies. series, parallel and series-parallel combine (power-split) are introduced.

2.2.1 Series hybrid electric vehicle

In this configuration, the tractive power is supplied directly by EM. The series configuration is one of the relatively simple mechanical structures of HEV. Here, the ICE is mainly used to generate electricity through a generator for the purpose of charging the high voltage battery. The electric power produced by the generator goes to either the EM or to the energy storage systems (ESS) [1, 14, 15, 16]. There is no mechanical connection between the EM and the ICE. When the battery charge is low: under a certain value of the state of charge (SOC), the ICE starts charging the battery at the same time powering the EM, through the generator. When the battery is fully charged, the ICE shuts off. In the series configuration, the ICE runs efficiently. The series hybrid vehicle architectures are used in vehicles such as trucks and locomotives [17]. The ICE operation in a series hybrid configuration tends to have a high efficiency. However, the weight of the vehicle increases. The size of the power electronic unit is also excessive [1]. The main disadvantage of this configuration is that there are energy losses during the conversion of energy from fuel energy to electricity and from electricity to mechanical energy.

Figure 2.1 describes the series HEV architecture in the simplest way. This configuration is used in BMW 3 series and Honda Insight.

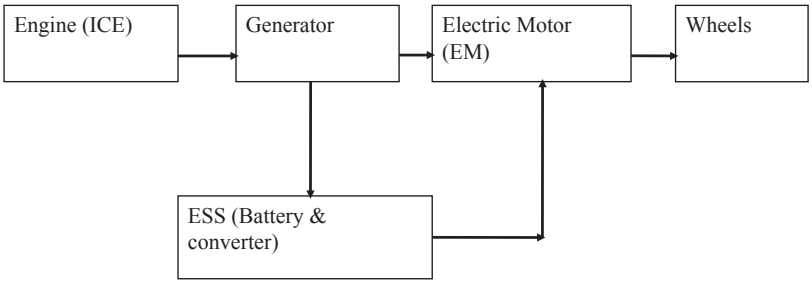

Figure 2.1: A series HEV configuration [1, 14, 16, 18]

FC HEV's architecture in Figure 2.2 is a series configuration. In effect in FC HEV configuration, the fuel cell replaces both of the ICE and the electricity generator. Most importantly the fuel cells generate electric power, rather than mechanical power. To sum-up, the fuel cells function as a power generator [1]. Note that each block corresponds to a component (subsystem) of the series HEV power-train. The arrows indicate the flow of energy through the drivetrain.

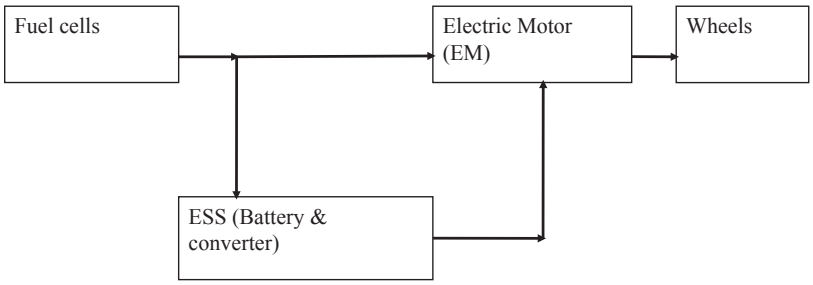

Figure 2.2: FC HEV series configuration [1, 18]

2.2.2 Parallel hybrid electric vehicle

In parallel configurations, both the ICE and the EM provide traction power to the wheels. In fact the ICE and EM are coupled in a parallel manner. If the charge of the battery is low, the EM acts as a generator to recharge the battery. This possibility to couple both the ICE and the EM allows the parallel hybrid architecture to be more viable with lower costs and acceptable efficiency. This configuration exists in the BMW 518 [1, 19]. Note that in the parallel hybrid configuration the gearbox is the same as in the conventional vehicles, either in manual or automatic transmissions. However, the gearbox position in the power-train defines the type of parallel HEV. Therefore, there are configuration called $pre-transmission$ parallel and another called $post-transmission$ parallel. Figure 2.3 and Figure 2.4 show respectively $pre-transmission$ parallel and $post-transmission$ parallel hybrid configurations. Note that a disconnect device such as a clutch is used to disengage the gearbox when running the ICE independently. However, the explanations given previously are literally a literature review based explanation. In effect, parallel hybrid electric vehicle, which is going to be designed is basically a four-wheel drive vehicle. The vehicle is driven by two motors (EM and ICE). The ICE drives the two rear wheels and the EM drives the two front wheels. It is this architecture which is proposed and implemented in software for simulation purpose.

Figure 2.3 shows the $pre-transmission$ parallel configuration. In this configuration, the gearbox is located on the main drive shaft just after the torque coupler. The power flow is added at the gearbox. Then the torque from the EM is added to the torque from the ICE at the input shaft of the gearbox. The gear speed ratios is applied on both the ICE and the EM.

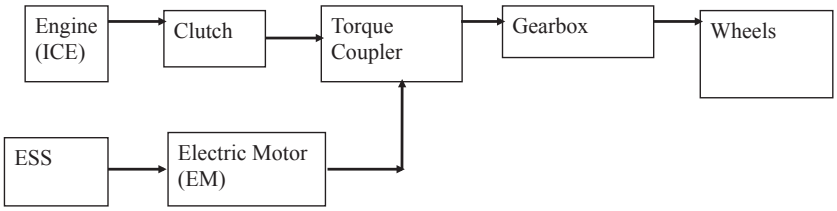

Figure 2.3: A $pre-transmission$ parallel HEV configuration [1, 11, 18]

Figure 2.4 shows the $post-transmission$ parallel configuration. In this configuration, the gearbox is located on the engine shaft prior to the torque coupler. The torque from the EM is added to the torque from the ICE. Then, the torque is delivered on the output shaft of the gearbox. Consequently, the gearbox speed ratios are applied on the ICE only.

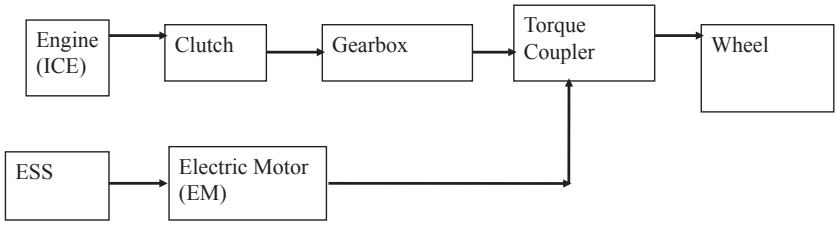

Figure 2.4: A $post-transmission$ parallel HEV configuration [1, 13, 14, 15, 18, 20]

2.2.3 Series-parallel configurations (power-split) HEV

In this configuration, the vehicle can operate as a series hybrid, a parallel hybrid, or indeed a combination of both. Within this architecture the connections between the ICE and the EM can be both electrical and mechanical. The planetary gear plays a crucial role in the power coupling and splitting. In effect, the planetary gear allows coupling of the mechanical torque from the ICE and the torque from EM. This mechanism is called the power-splitting mechanism. One advantage of a series-parallel configuration such as this one is that the ICE speed can be decoupled from the vehicle speed [1]. This advantage offsets partially the additional losses in the power conversion. This configuration is used in the Toyota Pruis [21]. Note that the explanations given previously are based on a literature review. In effect, power-split hybrid electric vehicle (PS HEV) is a four wheel vehicle, which is driven by two motors (EM and ICE), which provide the driven torque to drive the four wheels (two at front and two at rear). Basically in this type of HEV, the ICE is used to provide the extra torque to compensate the EM torque in order to drive the PS HEV power-train. In other word the torque, which drives this four-wheel drive PS HEV is the summation of the ICE torque and the EM torque. It is this architecture which is going to be proposed and implemented latter in software for simulation purpose.

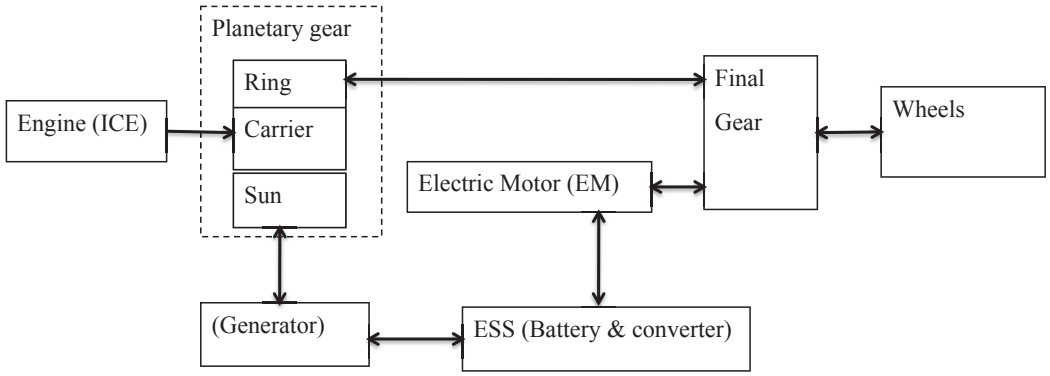

Figure 2.5: Power-split configuration [1, 14, 15, 16, 18]

2.3 Energy storage system (ESS)

This Section deals with energy storage system, where different techniques to store the energy to power the vehicle are presented. There are different types of ESS for each HEV. The EV uses ESS as the only energy source. The ESS on an EV is usually a high voltage battery pack, which is only charged from the electric grid (i.e. a plug in type). The ICE, FC and regenerative braking (see Definition 3 in Appendix A) charge the high voltage battery in the ESS. However, what is challenging here is to find an optimal ESS design. A design, which can satisfy the special characteristics of the vehicle power requirement and efficiency. In this Section, the performance of various ESS technologies will be compared. Note that when discussing ESS, it concerns the converter and the high voltage battery, which allows driving the vehicle by the EM.

2.3.1 ESS for a hybrid electric vehicle

In HEV, the ESS is sized differently depending on the degree of hybridisation (DOH), (see Definition 4 in Appendix A) and power management strategy of the vehicle. The high voltage battery life affects the battery SOC. The battery will operates at a narrow SOC. In [22] it shows that shallow cycle life can greatly satisfy consumer expectation for a HEV. Because its life cycle is much longer, the ultra-capacitor has the potential to be used in a HEV. Note that, it is difficult to standardise the generic power demand for a HEV. Another energy storage device is the mechanical flywheel, where the energy is stored in a spinning wheel. Simply, the kinetic energy is converted into useful energy, with a perspective to charge the high voltage battery. However, this kind of energy storage can be quite large, consequently volume consuming. Therefore, it has been argued that it may not be a good idea as an energy storage for HEV [23].

2.3.2 ESS for a plug-in hybrid electric vehicle

In the PHEV, the ESS is charged either by the on board power source, such as an ICE and FC, or the stationary grid power (plug-in). Sizing the ESS for a plug-in hybrid electric vehicle is not trivial because: firstly, for all electric range, the battery is the only source of power for most operations. Secondly, the depths of charge and discharge affect the battery life. Therefore, it is difficult to satisfy energy and power requirements with a reasonable life expectancy of the ESS [1, 24].

2.3.3 Battery technologies

Presently, three types of batteries are widely used in HEV design. These include lead acid (L-A), Ni-MH, and lithium-ion (Li-ion) batteries. These batteries, respectively, incrementally, improve: performance, energy density, and increased cost. L-A batteries are used in the first generation of EV, because it is inexpensive. Today Ni-MH is mainly used in HEV design. Li-ion batteries, are promising to be the appropriate technology. Most importantly batteries have a number of drawbacks: including

- large size
- power density limit
- thermal impact
- low efficiency
- long charging time and relatively short life.

2.3.3.1 Sealed lead acid battery (SLA)

The SLA is a battery currently used to power electric bicycles, probably because it is not expensive. This battery, besides its robustness, it is durable when it used properly. The self-discharge rate of a SLA battery is also low (if it is not used). The SLA battery does not have a memory effect like the NiCad battery. The weaknesses of this technology are low power and energy densities, and can harm potentially the environment [1].

2.3.3.2 Nickel metal hydride battery (Ni-MH)

Presently, this battery is mainly used to power electric automobiles. The Ni-MH battery has a more satisfactory energy density compared to a SLA battery. Its specific energy can be up to many times the energy from a SLA battery [1]. This battery is also relatively environmentally friendly. Because, it contains materials, which are recyclable. Their weaknesses are: they are expensive; they take a longer time to charge than a SLA battery and they generate a lot of heat during the charging process, it is also more difficult to determine when the Ni-MH battery is fully charged than with the SLA battery case. The recent effort of improving Ni-MH for HEV applications has been focused on reducing the resistance and increasing the power capability. The trade-off will likely be a lower energy density than those used on an EV [1, 22].

2.3.3.3 Lithium ion battery (Li-ion)

Many automotive companies are in the process of developing advanced Li-ion battery technologies for vehicle related applications. In fact much interest is focused on high power batteries for HEV and high-energy batteries for EV. For instance, the high voltage battery can have a energy up to 150 Wh/kg compared to a Ni-MH battery which can be 70 Wh/kg [1]. The major concern of using a Li-ion battery on a hybrid vehicle is the over-heating problem during recharging [24].

2.3.3.4 Ultra-capacitors

Ultra-capacitors are electrochemical capacitors. Here, the energy is stored in the double layer formed at a solid/electrolyte interface [25]. Many advanced research in new ultra-capacitor designs have tremendously improved the energy storage device capability and its cost. By comparing the ultra-capacitor with the conventional capacitor, the ultra-capacitor allows storing more energy (factor of 20 times) [26]. The advantages of the ultra-capacitor are: its maintenance is cost free, its life cycle is longer, and it is insensitive to environmental temperature variation.
Unfortunately, the energy density of this device is still limited compared to batteries. The goal for the ultra-capacitor development is an specific energy of 5 Wh/kg for high power discharge [27]. Carbon-carbon ultra-capacitor devices are commercially available from several companies, including Maxwell, Ness [1, 28]. An experimental test was carried on a series hybrid Ford Escort with and without an ultra-capacitor as load-levelling devices for the batteries [1, 28, 29] and the results were satisfactory and promising.

2.4 Control strategy for hybrid electric vehicles

This Section deals with different control strategies, which are tested on HEV. Indeed, a number of these controls strategies are presented. The focus of HEV design is mostly on power-train efficiency. for example in a hybrid vehicle (HV), an automated power-train controller coordinates the power flows (energy management) between the electric or thermal energy storage devices and the environment, which responds to the drivers power demand. The main objectives of the controller are to

improve fuel economy, reduce emissions and maintain different subsystems such as the high voltage battery in their desired state. As a consequence, the control strategies play a critical role in determining the performance and efficiency of a HEV. Assuming that the driving cycle is known, a global optimal solution for energy consumption can be a dynamic programming control strategy [30, 31]. However, note that practical solutions cannot assume such knowledge of the driving cycle. Some of the control strategies for HEV are based on the principle that the main propulsion power source is the ICE. Here, the EM assists and gives or takes the difference in power at the drivetrain. Note that such a control strategy allows achieving the required performance from the hybrid system [16]. The control strategy is based on rules, where these rules are defined by the designer, according to his knowledge of the power-train. Here is an example of a rule:

$$if\ Battery\ Charge\ is\ low\ then\ Electric\ Motor\ Traction\ Torque\ = 0 \qquad (2.1)$$

For instance this rule can be used to maintain the battery charge higher than a desirable level in an HEV. A rule-based control strategy (a fuzzy control) comprises a large number of logical statements similar to (2.1). Such a fuzzy control strategy is also termed heuristics based[16] and such techniques are commonly used in industrial applications. The efficacy of the heuristic control relies strongly on the calibration of the rules. However, developing an efficient rule-based supervisory control strategy can be a burden. This is because it can be a time consuming processes. However, some benefit of this type of control strategy is its flexibility in the sense that new rules can be introduced (added) into an existing strategy

(rule-based). This does not require an important change in the control algorithm structure. Another control strategy such as the equivalent consumption minimisation control strategy (ECMCS) uses a model-based instantaneous fuel minimisation technique [30, 32,33]. This can be useful for HEV. This control strategy utilises a weighted cost function of electric and fuel energy. Its performance is usually improved by adaptively tuning an equivalence ratio between the two forms of energy (fuel and electricity). This is a ratio, which can be tuned according to the driving conditions. It also can be corrected as necessary to compensate for large deviations in the battery SOC [30, 34]. This method to control the HEV is named the real time control strategy (RTCS). It uses a principle similar to the ECMCS to calculate the optimal torque split [35]. In this strategy, a target performance consists of energy consumption and emission minimisation. In effect, it aims to minimise the energy consumption over permissible ICE and EM torque demands. The solution is then adjusted according to battery SOC considerations. Also, it demonstrates stochastic control strategy for the HEV energy management problem [36, 37]; where an optimal energy management is computed by solving a stochastic dynamic program over an infinite horizon [36]. The resulting controller is implemented in the form of a static state feedback controller. In such a control strategy, the power requested by the driver is modelled as a random Markov process (see Definition 5 in Appendix A) in order to accurately represent the nondetermistic nature of the variable [16]. Other relevant work on the HEV control strategy uses the shortest path stochastic control approach for energy management [37]. The main advantages of the previous control strategies compare to the method presents in [36] are due to the battery SOC control technique. It also reduces the number of

tuning parameters involved in the design [16]. The control strategy in [36] allows the battery SOC to freely vary from its nominal value until the vehicle turns off, but this could penalise the SOC's continuous deviations. It also suggests that better fuel economy is obtained as a result of the relaxed SOC constraint using the control technique described in [37].

The advantages and disadvantages of heuristic control strategy and real-time optimisation techniques for HEV control are listed respectively in Table 2.1 and Table 2.2.

Table 2.1: Advantage and disadvantage of heuristic control strategy for HEV control [16]

Advantages	**Disadvantages**
Simple algorithm development	No guarantee for optimality
Intuitive calibration	Time-consuming calibration
Modest need for computational resources	Performance dependent on vehicle architecture

Table 2.2: Advantage and disadvantage of real-time optimisation techniques for HEV control [16]

Advantages	**Disadvantages**
Leads to quasi optimal control	Requires accurate component models
Small number of calibration parameters	Calibration may be non-intuitive
Easy to adapt to different architectures	Computation burden

For the energy management control, other techniques such as optimal sliding control, robust control and model predictive control are also proposed, respectively, in [38], [39] and [40]. For an optimal sliding control, a fixed power demand is assumed. This work shows that, an optimal solution (if it exists) also satisfies the battery SOC constraint. It can be obtained by fast switching between the specified operating points of the ICE. The H∞ controller strategy is also proposed for energy management in HEV [39]. Unfortunately, the complexity of the technique, especially the computational burden and large number of tuneable parameters makes the design of a H∞ controller technique impractical for real-time HEV

control [16]. The dynamic programming problem can be solved within the model predictive control framework by using predicted future driving conditions over a short driving horizon [39]. However, this strategy also requires extensive computational resources since the finite horizon dynamic programming problem should be solved online at every time step [16].

2.4.1 Supervisory power-train controller

The supervisory power-train controller plays a crucial role in coordinating overall vehicle systems, maximising the potential for improving the fuel economy, reducing the exhaust emissions. It needs to include the following key functions:

- Scheduling engine start-stop for performing, fuel economy, driveability and emissions requirements. Although some of these conditions may be determined using model-based techniques. But others are inevitably imposed by the rules in a rule-based and are tuned to achieve desired performance.

- Enabling driveability and stability specific controls: in certain vehicle traction controls and driveline controls individual controllers are required to be activated as necessary. The supervisory controller handles these controllers based on some predefined transition conditions.

- Enabling driver controls demands: If the driver manually interrupts normal operation, the supervisory controller engages the vehicle into the desired mode of operation.

- Ensuring safe vehicle operation: The supervisory controller reconfigures the control system if a critical power-train fault is detected.

Note that the main objective of the supervisory control strategy design is to develop an optimal and practical power management strategy. A technique, which determines the proper torque split and gear selection. It also satisfies the following constraints:

- Meet the power demand from the driver
- Maintain the SOC at its desired state
- Achieve certain driveability requirements

2.4.2 Power management strategy

The term power management refers to the design of the higher-level control algorithm. The controller, which determines the proper power (torque) to be generated and its splitting between the EM and the ICE while satisfying the power (torque) request from the driver. Also, without forgetting to maintain the energy storage system at a reasonable level. Note that the power management could be either a torque-based or a power-based strategy. It depends on the type of application. Since the ICE and the EM both accept the torque command, the torque-based strategy is used in this situation. The dashed line in the block diagram of Figure 2.6 is the request from the operator (driver). The doted line corresponds to the control action from the power-train components controllers. Finally the full solid line is the power flow through the drivetrain.

Figure 2.6: Hierarchical control architecture of a hybrid electric vehicle [29].

2.5 HEV configuration comparisons

This Section is concerned with the different characteristics of the various LCEV. It is basically the summary of the LCEV technologies, which has been presented previously.

Some of the main characteristics of LCEV are presented in Table 2.3. Note that PHEV (different than P HEV) stands for Plug-in HEV.

Table 2.3: Characteristics of various HEV

Types of LCEV	**EV**	**HEV and PHEV**	**FC HEV**
Propulsion	- Electric motor drives	- Electric motor drives - Internal combustion engine (ICE)	- Electric motor drives
Energy system	- Battery -ultra-capacitor	- Battery - ultra-capacitor - ICE generating unit	- Fuel cells -Need battery ultra-capacitor to enhance power density for starting
Energy source and infrastructure	- Electric grid charging facilities (PHEV)	- Electric grid charging facilities - Gasoline stations	- Hydrogen production transportation and infrastructure
Characteristics	- Emission free - High energy efficiency - Independence - Limited driving range - Commercially available	- Low emission - Max fuel economy - Dependence on fuel (no PHEV) - Long driving range - Commercially available	- Emission free - High energy efficiency - Independence - Satisfied drive range - Very expensive, in development
Major problems	- Battery and its management - Charging facilities cost	- Multiple energy sources control optimisation and management	- Fuel cells cost, cycle life and reliability - Hydrogen infrastructure

2.6 Conclusions

This Chapter has summarised different HEVs and their architectures. In effect the background knowledge of S HEV, P HEV, PS HEV and FC HEV drivetrains architecture were reviewed. It was mentioned a clear difference between the four different drivetrains, which were presented. It also presented different energy storage systems especially the battery. Three types of high voltage batteries (SLA, Ni-MH and Li-ion) technologies were introduced with their advantages and weakness. The ultra-capacitor technology was also presented. Finally it discussed different control strategies. Control strategies such as heuristic based approach, dynamics programming approach, RTCS, ECMCS, power management technique were introduced. The advantages and disadvantages of these control methods were presented as well. The next Chapter will deal with Systems modelling and Control without forgetting the re-configurable power-train control strategy, which will be implemented. Basically four different HEV architectures will be proposed and modelled. These propositions are based on the background knowledge of the HEVs Systems reviewed in Chapter 2. The high voltage battery, which will be used for the four proposed architectures, is Lithium Ion. In fact the next Chapter will be using different information presented in this Chapter 2.

Chapter 3

System Modelling and Control

This Chapter will deal with power-train design, modelling and control. In effect various power-trains (relating to four different HEVs) will be presented. Different control strategies will be introduced and implemented. The HEVs models used in this research work are not derived from first principles. Instead, a Simulink block based modelling approach is used to model the different power-trains. In effect, Simulink tool boxes such as SimpowerSim, SimMechanics, and SimScap are mainly used to build the proposed power-train models. Basically, these Simulink models are based on a mixture of the replicated physical components (components with a replicated mechanical, replicated electrical inputs/outputs) in Simulink and normal standard Simulink components (which support the signals of any numeric data type as inputs/outputs).

3.1 Systems modelling

This Section is about various types of LCEV modelling. The main idea is to propose different architectures, based on the literature review knowledge. In effect from various power-trains introduced previously, different power-trains will be proposed and implemented. The goal is to evaluate different power-trains under the proposed power-train control strategy. As mentioned before, there are various types of LCEV: EV, HEV, PHEV and FC HEV. The classification of LCEV is essentially based on the vehicle power source.

3.1.1 Series power-train (S HEV)

The block diagram in Figure 3.1 shows the architecture of the S HEV power-train, which will be implemented in Simulink later in this thesis. The energy flow in both directions is indicated by the line with arrows on both ends. The arrow between the battery and the DC/DC converter corresponds to the battery charging and discharging: the arrow towards the battery indicates charge of the battery, similarly the arrow, which points to the DC/DC converter represents discharge of the battery. Note that each component (block) of this proposed power-train architecture, will be implemented in Simulink as a subsystem. The characteristics of each component (subsystem) in this proposed power-train are displayed in order to understand the specification of this proposed power-train, without forgetting to evaluate its DOH (Degree Of Hybridization). The units of input/output of subsystems will be presented in this report.

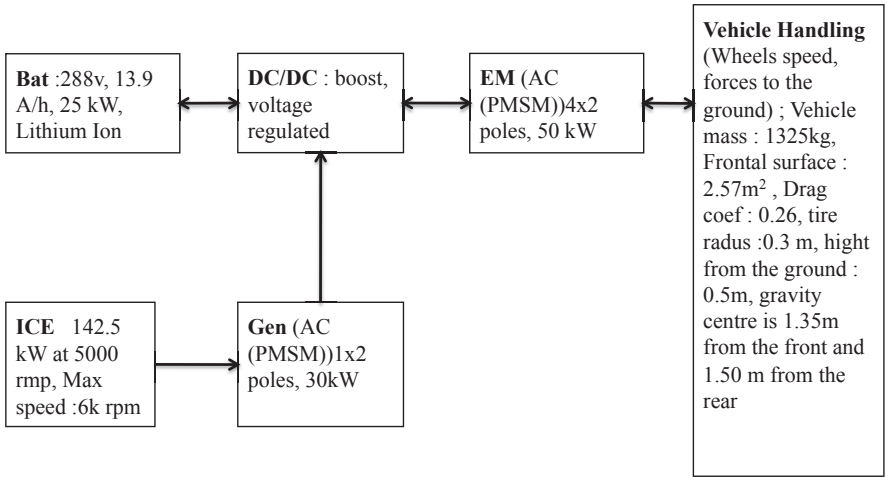

Figure 3.1: Architecture of proposed S HEV

Figure 3.2 displays the Simulink implementation of the model of a S HEV power-train. There are three mains subsystems:

- 'Controllers Unit it' contains the supervisory controller and different components controllers.

- 'Vehicle engine' constitutes the ICE unit and electrical subsystem.

- 'Vehicle Dynamics' is a four-wheel drive vehicle which is implemented. Figure 3.14 shows the composition of this 'Vehicle Dynamics' subsystem.

The subsystem termed 'Driver' allows the simulation of the acceleration requested by the driver when the accelerator is activated. This request lies in the range [-1 1], where the value of 1 correspond to full acceleration request, and -1 is full braking request.

The input to the subsystem termed 'Controllers Unit' is the driver acceleration request. It is a value without units. The output of this subsystem are:

- EM control action, 'EM_Crtl' is either current in $[A]$ or voltage $[V]$.

- ICE control action, 'ICE_Crtl' is either speed in $[rpm]$ or torque in $[Nm]$.

- Generator control action, 'Gen_Crtl' is either speed in $[rpm]$ or torque in $[Nm]$.

- The output of the 'Vehicle Engine' subsystem, 'EM_Tork' is the replicated EM physical mechanical torque in $[Nm]$, to drive the physical wheels of four-wheel drive HEV, which is the 'Vehicle dynamics' subsystem.

- The input of subsystem termed 'Vehicle Dynamics', 'Drive Shaft S' is the replicated EM physical mechanical torque in $[Nm]$, which drive the physical wheels of four-wheel drive HEV, which is in this 'Vehicle dynamics'.

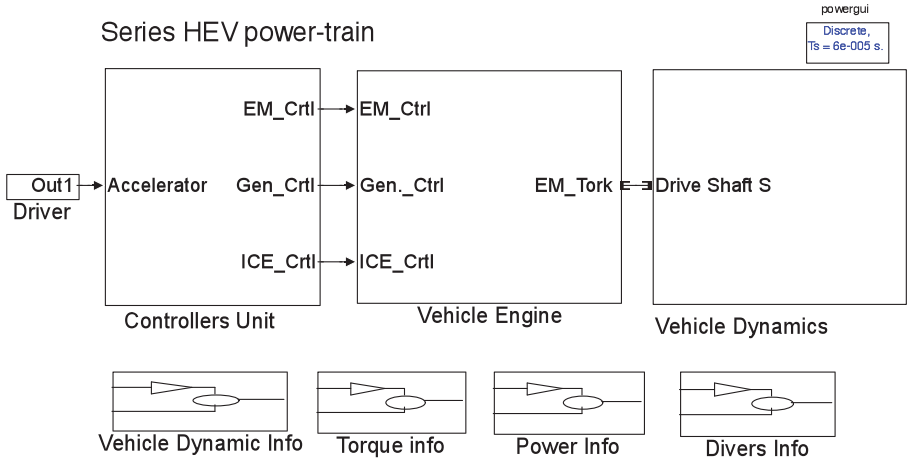

Figure 3.2: S HEV simulink model implementation

Figure 3.3 shows the composition of the vehicle engine subsystem, which is presented in Figure 3.2. There are two main subsystems:

- Electrical subsystem: it contains EM and ESS. Basically it is the electrical part of the proposed series power-train.

- ICE the Internal combustion and fuel-air dynamics are implemented by using some

of the models from MathWorks.

In this model, the ICE (Engine) has a power of $142.5kW$ at $5000rpm$. The input to the ICE is a throttle signal, which lies in the range [0 100]. This signal, technically, it is a control signal for the Engine speed. Note that the ICE Simulink model, which has got a replicated physical mechanical output, does not include the air-fuel mixture dynamics. But fuel-rate control used will be taken from MathWorks and modified, in order to model the fuel-air mixture dynamics.

Note also that in the subsystem 'ICE and fuel consuption', the ICE is implemented ICE with the aire-fuel dynamics to evaluate fuel consumption. The output of the 'ICE and fuel consuption' subsystem is a replicated physical mechanical torque to drive the generator in producing electricity to charge the high voltage battery and power the EM. In fact the 'Electrical Subsystem' subsystem has three inputs with one is a replicated physical mechanical. The replicated physical mechanical output, "EM_Tork" is the torque, which drives four-wheel drive the S HEV.

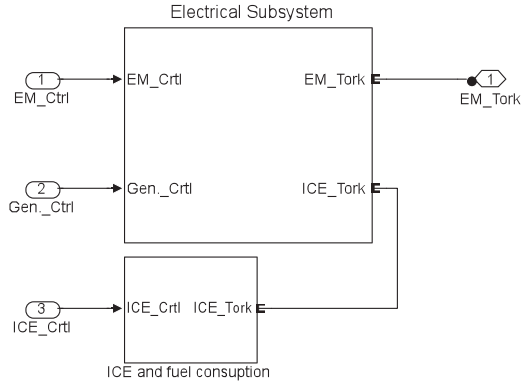

Figure 3.3: S HEV power-train

Figure 3.4 displays the composition of the electrical subsystem, which is presented in Figure 3.3. This shows the design of the electrical part of the proposed series power-train. The characteristic of each component such as the ESS ('Battery' and 'DC/DC converter'); the generator and the EM, which drives the vehicle are displayed in Figure 3.1.

Note that the connection between the 'Battery' subsystem and the 'DC/DC Converter' subsystem in practice are physical electrical connections. The input to the generator is the replicated physical mechanical torque of the ICE in $[Nm]$. This input corresponds to the generator reference input. There are two replicated physical electrical outputs from the 'Gen.' subsystem. In effect the electrical outputs of the generator drive the produced electricity from the generator to the high voltage battery through the DC/DC converter, and power the EM.

Note also that the 'Battery' subsystem implementation is shown in Appendix B. The implementation of the 'DC/DC Converter' subsystem is shown in Appendix B. Also, in the Appendix B it is shown the 'EM' subsystem implementation. Finally, the 'Gen.' subsystem is displayed in Appendix B.

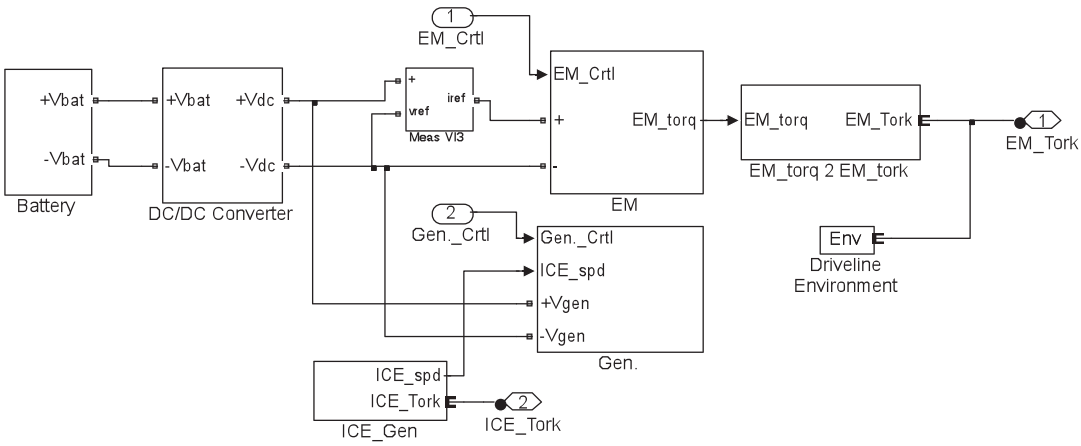

Figure 3.4: 'Electrical Subsystem' of HEV power-trains

3.1.2 Parallel power-train (P HEV)

Figure 3.5 shows the block diagram of the proposed P HEV power-train architecture, which will be implemented later. The energy flow in both directions is indicated by the line with arrows on both sides. For example between the EM and the DC/DC converter, the arrow towards the DC/DC converter corresponds to the regenerative braking, when the EM is transformed to a generator in order to provide power to charge the battery. The dashed arrow corresponds to the ICE torque, which drives the rear wheels. Likewise the arrow in the opposite direction indicates that the EM is driving the vehicle. Note that each component (block) within this proposed power-train will be implemented in Simulink as a subsystem. The characteristics of each component (subsystem) is displayed in order to allow evaluating the DOH of this proposed power-train, if there is need.

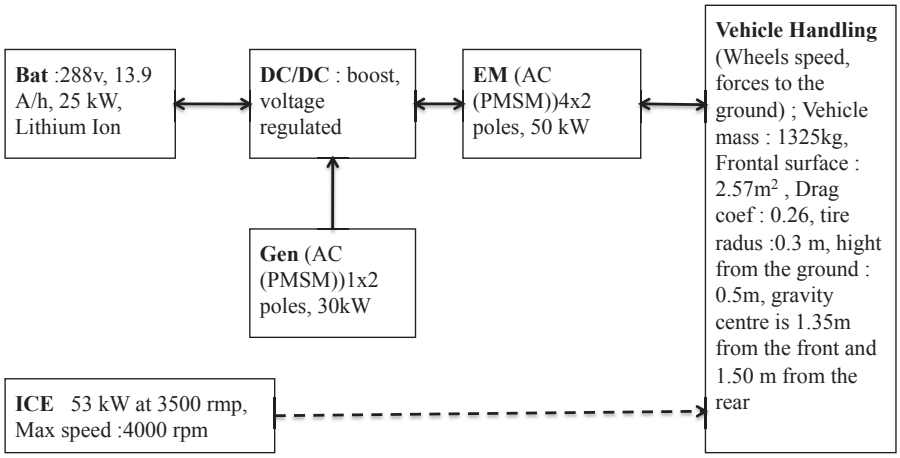

Figure 3.5: Architecture of proposed P HEV

The Simulink block diagram in Figure 3.6 shows the implementation of the P HEV power-train, which is proposed in Figure 3.5. The difference between this Figure 3.6 and Figure 3.2 is in the configuration, in that there are two drive shafts ('Drive Shaft P1' and 'Drive Shaft P2'). In effect, the ICE drives the two rears wheels of the four-wheel drive vehicle, and the EM drives the two front wheels. EM can become generator during braking. This processes is termed regenerative braking.
The two outputs of the 'Vehicle Engine' subsystem are:
- 'EM_Tork', which is a replicated physical mechanical torque in $[Nm]$, which drives the two front wheels of the four-wheel drive HEV in the 'Vehicle dynamics' subsystem.
- 'ICE_Tork' is a replicated physical mechanical torque in $[Nm]$, which drives the two rear wheels of four-wheel drive P HEV located in the 'Vehicle dynamics' subsystem.
The two inputs of the 'Vehicle Dynamics' subsystem are:
- 'Drive Shaft P1', which is a replicated physical mechanical torque in $[Nm]$, which drives the two front wheels of the four-wheel drive HEV in the 'Vehicle dynamics' subsystem.
- 'Drive Shaft P2', is a replicated physical mechanical torque in $[Nm]$, which drives the two rear wheels of four-wheel drive P HEV located in the 'Vehicle dynamics' subsystem.

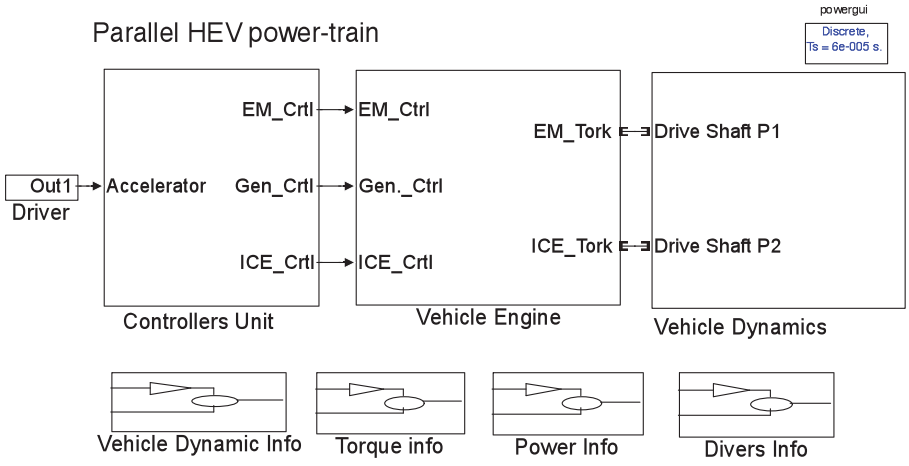

Figure 3.6: P HEV Simulink model implementation

Figure 3.7 shows the composition of the vehicle engine subsystem, which is shown in Figure 3.6. There are two main power sources for this P HEV power-train. Those sources are: the ICE and the electrical system, which is the ESS and the EM. The ICE has a power of $53kW$ at $3500rpm$; it drives the rear wheels. The input to the ICE is a throttle signal, which lies in the range [0 100]. It is a control signal for the Engine speed. The ICE model here is a replicated physical ICE in Simulink, which does not include the dynamics of the air-fuel mixture. The EM drives the two front wheels of the four-wheel drive vehicle. The electrical subsystem within this power-train is quasi similar to that described in Figure 3.4.

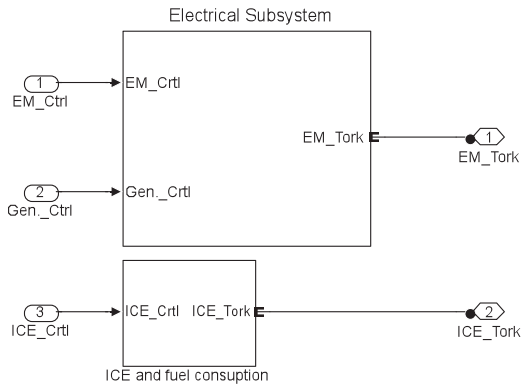

Figure 3.7: P HEV power-train

3.1.3 Power split power-train (PS HEV)

Figure 3.8 shows the block diagram of the architecture of the Power split HEV power-train, which is implemented in Simulink. The observable difference between this Figure 3.8 and others (Figure 3.1 and Figure 3.5) is the planetary gear. The arrow between the battery and the DC/DC converter corresponds to the battery charge and discharge. The arrow towards the battery indicates charging of the battery, whilst the arrow pointing to the DC/DC converter represents the discharge of the battery. Note that the power-train components are different from those used in the series and parallel power-trains previously introduced. Nevertheless components such as battery (Bat), generator (Gen.), converter DC/DC and the vehicle handling are unchanged.

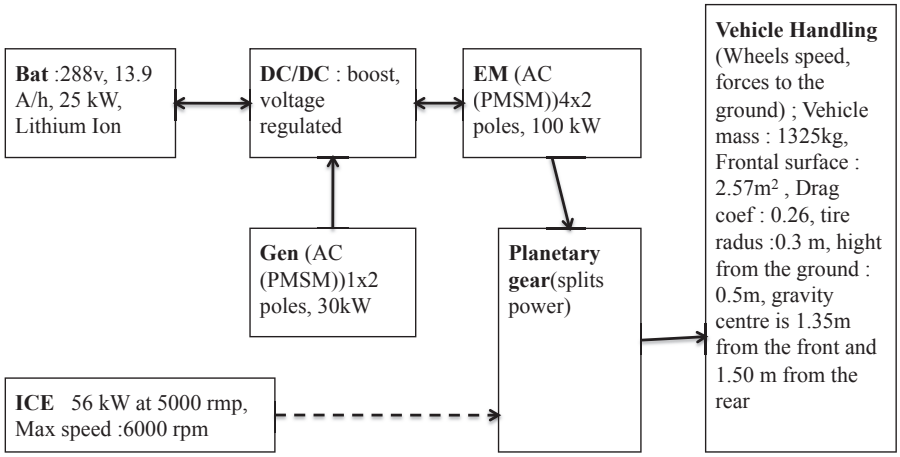

Figure 3.8: Architecture of the proposed PS HEV power-train

Figure 3.9 shows the model of the proposed power split HEV power-train Simulink implementation. The ICE has a power of $56kW$ at $5000rpm$. In this architecture the ICE works if there is need to compensate the EM power to meet the requested power. The EM can take the role of a generator during braking.

Note that the output of the 'Vehicle Engine' subsystem is the replicated physical torque in $[Nm]$, which is provided by the EM and the ICE to drive the wheels of four-wheel drive PS HEV located in the 'Vehicle dynamics' subsystem. In fact, The replicated physical mechanical output termed 'EM_ICE_Tork' is the summation the both torque from (EM and ICE) in $[Nm]$. 'Drive Shaft PS', is a replicated physical mechanical torque in $[Nm]$, which drives the four-wheel drive PS HEV located in the 'Vehicle dynamics' subsystem.

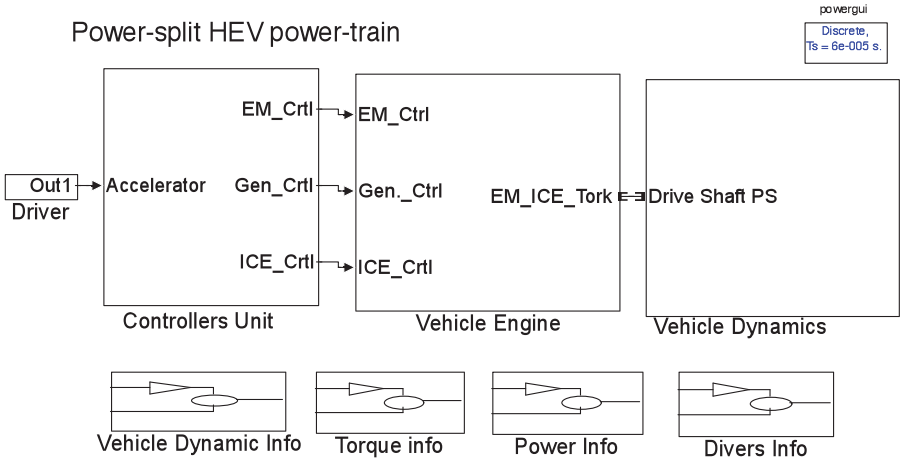

Figure 3.9: PS HEV Simulink model, implemented

Figure 3.10 shows the composition of the vehicle engine subsystem in Figure 3.9. It can be seen that the ICE and electrical subsystem is similar to other electrical system shown in Figure 3.4. The planetary gear allows coupling the ICE and EM torque in order to meet the requested torque by the driver.

To make the planetary gear work properly, it would be better to connect the ICE to the carrier gear, the EM to the ring gear and the generator to the sun gear. Note that when using set up, the sun gear must be connected.

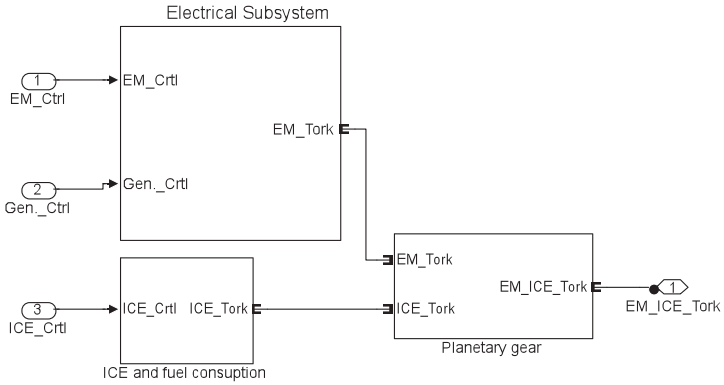

Figure 3.10: PS HEV power-train

3.1.4 Fuel cell power-train (FC HEV)

Figure 3.11 shows the architecture of a fuel cell power-train, which is proposed. This power-train architecture is implemented in Simulink. The characteristic of each component (subsystem) involved in design is displayed.

The energy flow in both directions is indicated by the line with arrows on both ends. The arrow between the battery and the DC/DC converter corresponds to the battery charging and discharging. Note that this architecture is like a series one but without the ICE.

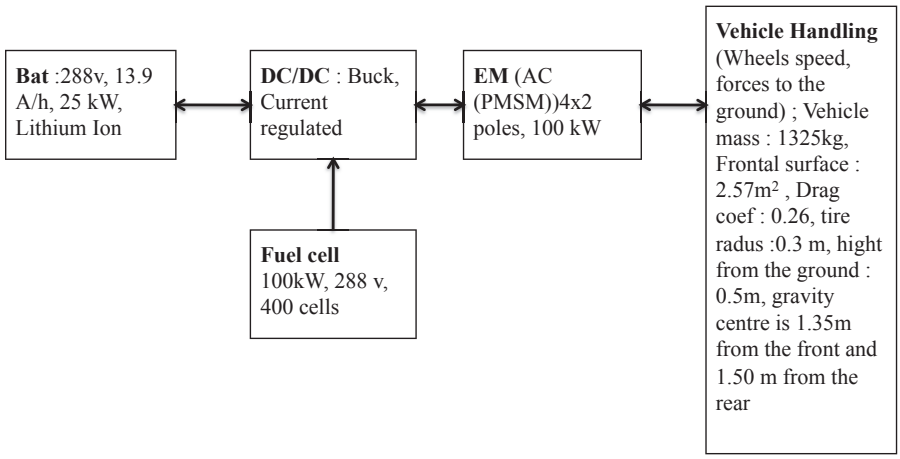

Figure 3.11: Architecture of FC HEV proposed

Figure 3.12 shows the Simulink implementation of a FC HEV power-train, which is proposed. The EM (only) drives the vehicle. Note that the EM takes a generator role during braking.

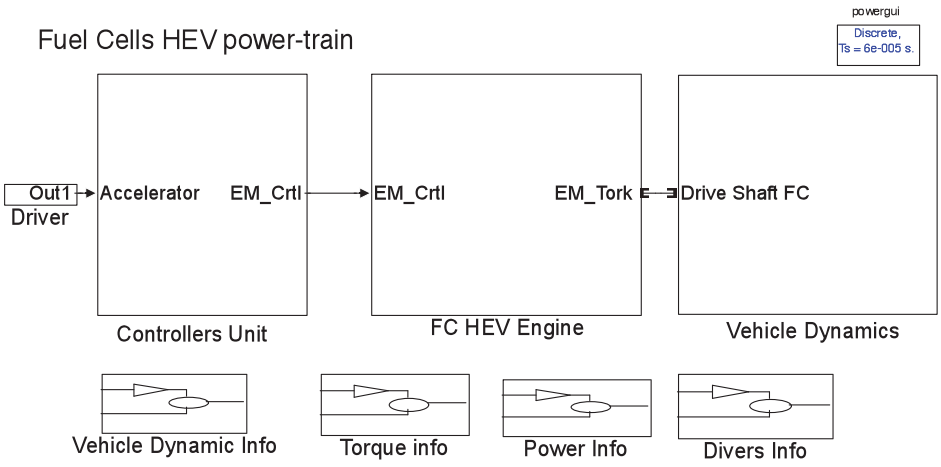

Figure 3.12: FC HEV Simulink model, implementation

Figure 3.13 describes the composition of the FC HEV engine subsystem, which is presented in Figure 3.12. It shows: the fuel cell power source, DC/DC converter, the high voltage battery and the EM which drives the vehicle.
Note that the 'FC reaction' subsystem implementation is shown in Appendix C. The implementation of the 'DC/DC Converter' is presented in Appendix C. In the end, the 'EM' subsystem is shown in Appendix C.

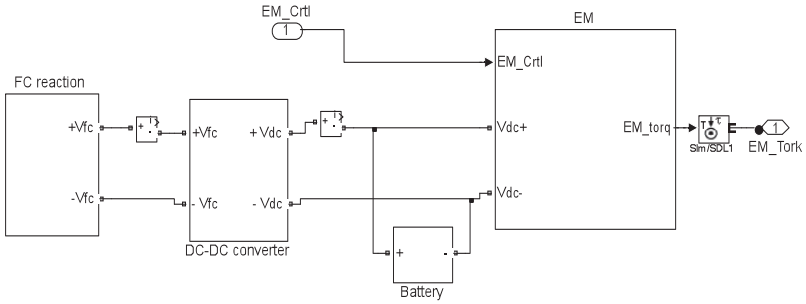

Figure 3.13: FC HEV power-train

3.1.5 Vehicle dynamics

Vehicle Dynamics subsystem models the mechanical parts of a four wheel vehicle. This model includes tyres and the vehicle body. The implemented model is shown in Figure 3.14. The Simulink block:

- Single gear: it reduces the motor's speed and increases the torques

- Differential: it splits the input torque in two equal torque for wheels

- Viscous friction: it aims to model all the losses of the mechanical system.

It assumes that the car is driven on a horizontally in a straight line. Therefore the road angle is equal to zero.

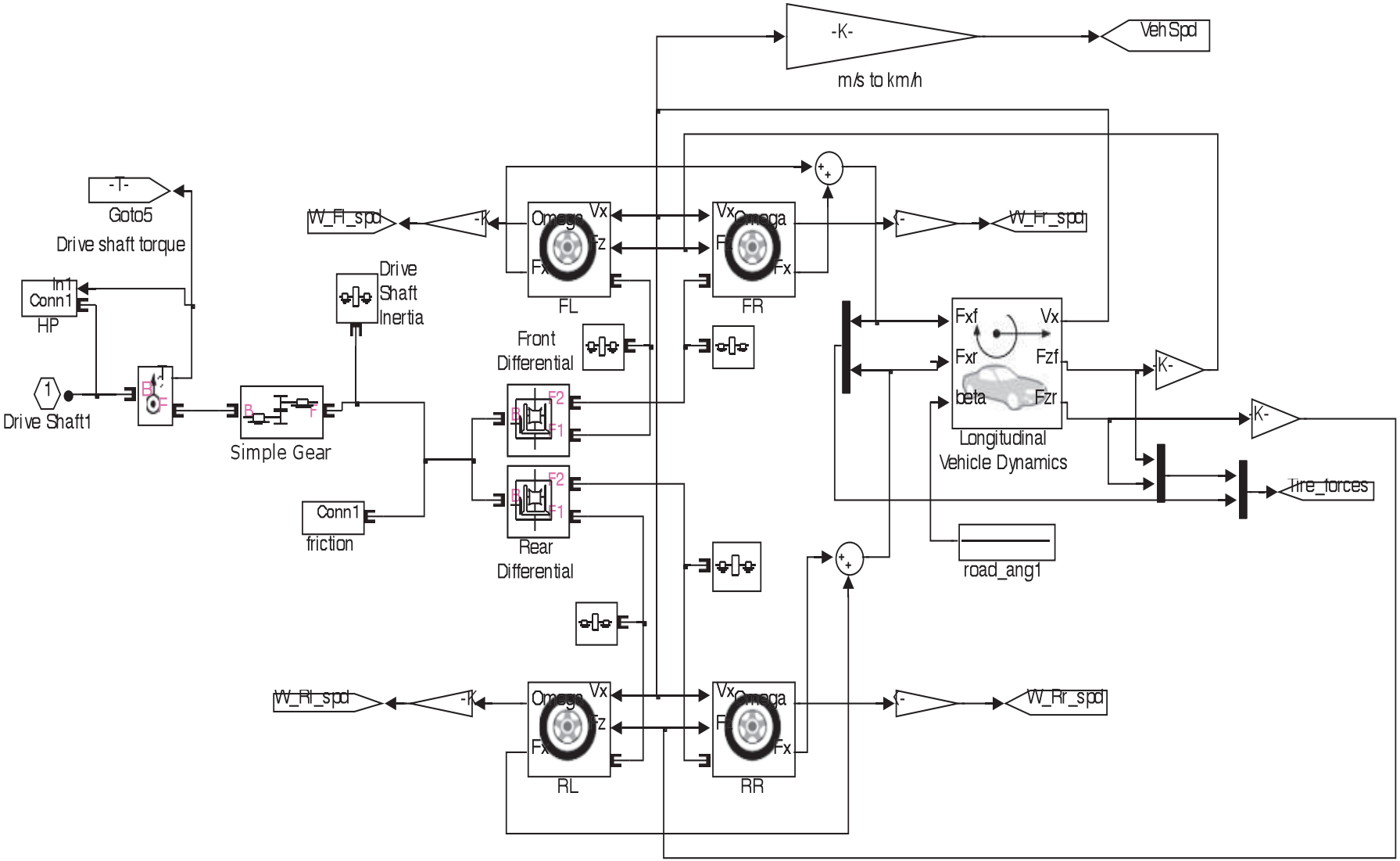

Figure 3.14: Vehicle dynamics, Simulink model

Note that this subsystem will allow analysing the vehicle stability and driveability, which corresponds to the vehicle handling. In effect when talking about vehicle handling, it is about analysing these variables present in Figure 3.15. (F_z, F_x, F_d and Tyre speed). The dashed arrow represents the longitudinal force (F_x), basically one, which drives the vehicle forward. The dotted arrow corresponds to the vertical forces (F_z) on the tyre. The drag force (F_d) is in solid line arrow, oriented in the opposite direction of the longitudinal forces.

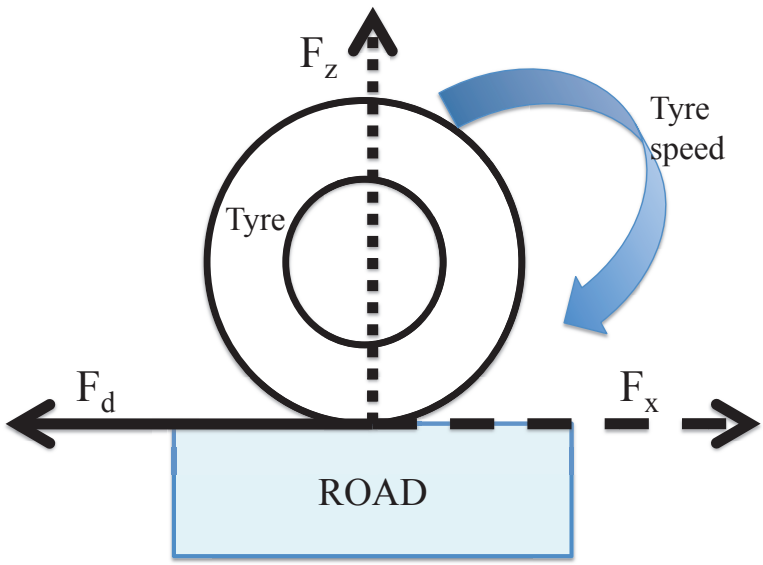

Figure 3.15: Parameters to be analysed in vehicle dynamics

Remarks 3.1

All resources available are used to build these various non deterministic (mathematical model of) HEV power-trains. That means literally some of the power-train's components such as DC/DC converter for instance are from MathWorks. It was reconfigured to meet the specification for instance ($300V$ to $500V$).

Note also that for simplicity some components (subsystems) in the proposed power-trains are unchanged, that allows comparing the four proposed power-train later. Also, this simplicity can affect the power-train performance as well. For example the Simulink model of the fuel cell has at least different parameters. But for this implemented FC HEV power-train model, only two parameters (fuel flow rate and air flow rate) are used.

3.2 Control strategies

This Section deals with different control strategies, which are implemented. Note that the control unit subsystem in Figure (3.2, 3.6, 3.9, 3.12) contains the supervisory (master) control unit and different controls units for a power-train components such as EM, ICE and Gen. Here, it will explain the re-configurable power-train controller platform. This power-train controller aims to control different HEV power-trains (can be plugged into different HEV power-trains) by re-configuring (play with parameters) this controller for each power-train with the objective of having a stable and driveable HEV on road.

3.2.1 Supervisory control

This controller is the master controller. The specification of this control strategy is as follows:

- Enable or disable the component (subsystem) controllers based on the power-train feedback information and the driver acceleration demand.
- Define the optimum operating point (the reference to reach) for different components of the power-train, in order to optimise the power-train activities.

This is one way to achieve a supervisory control for a stable and driveable vehicle. The block diagrams in Figure 3.16 describes the re-configurable power-train control platform, which is proposed (but it is first configured for the PS HEV power-train). The dotted and dashed arrows are the supervisory controller inputs. The quantity $u_1(t)$ in (3.1) is represented by the dotted arrow. The long dashed and double dotted arrow corresponds to $u_2(t)$ of (3.1). The dashed arrow represents $u_4(t)$ of (3.1). Finally the long dashed arrow is $u_3(t)$ of (3.1). Figure 3.15 demonstrates how the proposed power-train control operates.

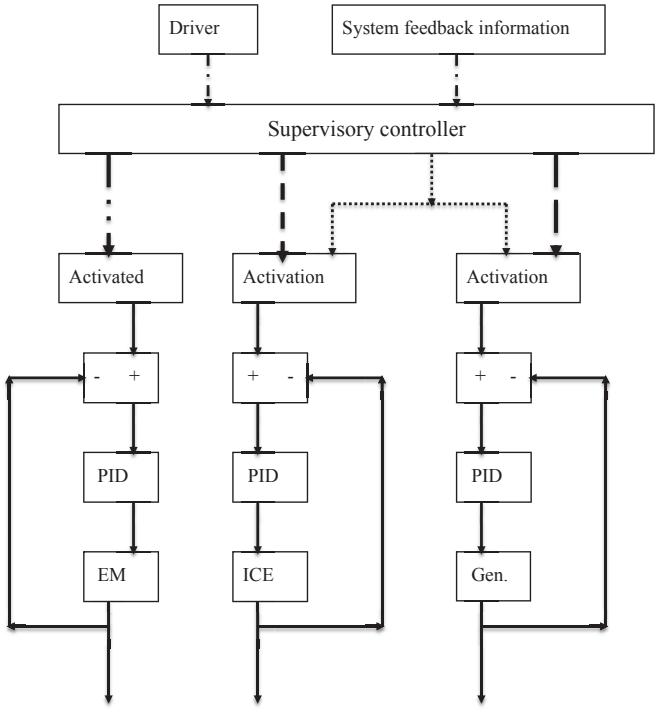

Figure 3.16: Proposed power-train control architecture

In general the control law for ICE based HEV may be represented as:

$$[u_1(t), u_2(t), u_3(t), u_4(t)] = f\{D_T(t), D_P(t), B_P(t), B_L(t), Em_{spd}(t), Gen_{spd}(t), Ice_{spd}(t)\} \tag{3.1}$$

Here $u_1(t)$, $u_2(t)$, $u_3(t)$ and $u_4(t)$ are the control actions f is a function, which takes different functions such as $D_T(t)$, $D_P(t)$, $B_P(t)$, $B_L(t)$, $Em_{spd}(t)$, $Gen_{spd}(t)$,$Ice_{spd}(t)$ as inputs. These inputs represent the "Driver" and the "System feedback information" in Figure 3.6. Note that the term function here, could mean: algebraic operation, logic operation, and/or look up table. The goal is to make the control strategy simple to understand.

$D_T(t)$ is driver torque demand function in $[Nm]$. It is computable within the System.

$D_P(t)$ is the driver power demand function in $[W]$. It is computable within the System.

$B_L(t)$ is the battery power limit function in $[W]$. It is computable within the System.

$B_P(t)$ is the battery recharge power function in $[W]$. It is computable within the System.

$Em_{spd}(t)$ is the EM speed function in $[rpm]$. It is measurable within the System.

$Gen_{spd}(t)$ is the Generator speed function in $[rpm]$. It is measurable within the System.

$Ice_{spd}(t)$ is the ICE speed function in $[rpm]$. It is measurable within the System.

The controller to enable or disable the power-train components controller is

$$u_1(t) = g\{D_P(t), B_P(t)\} \tag{3.2}$$

Note that the explanation of Equation (3.2) is given in control strategy 1, which is given in Appendix D.

Here g is a function, which takes different functions such as $D_P(t)$ and $B_P(t)$ as inputs to produce the control action $u_1(t)$. This control action acts like a switch. It enables or disables the component controller. Note that $u_1(t)$ is without units.

The following control strategy defines the EM reference torque.

Note that the explanation of Equation (3.3) is given in control strategy 2, which is given in Appendix D.

$$u_2(t) = h\{D_P(t), Em_{spd}(t), Ep(t)\} \tag{3.3}$$

where

$$Ep(t) = \chi\{Gen_P(t), B_P^*(t)\} \tag{3.4}$$

$Ep(t)$ is a function, which takes an input function such as generator power $Gen_P(t)$ is in $[W]$ and battery reference power $B_P^*(t)$ is in $[W]$.

$$B_P^*(t) = \phi\{B_L(t), B_P(t), D_P(t), Ice_{spd}(t)\} \tag{3.5}$$

The control strategy, which defines the generator reference speed in $[rpm]$ is:

$$u_3(t) = \psi\{D_T(t), B_P(t), B_L(t), Gen_{spd}(t)\} \tag{3.6}$$

Note that the explanation of Equation (3.6) is given in control strategy 3, which is given in Appendix D.

The following control strategy, which defines ICE reference speed in $[rpm]$ is:

$$u_4(t) = \lambda\{D_P(t), B_P(t)\} \tag{3.7}$$

Note that the explanation of Equation (3.7) is given in control strategy 4, which is given in Appendix D.

Remarks 3.2

Note also that this control strategy is designed for the power-split power-train. But since the parallel and series power-trains were proposed, this controller will readily (with a minor change) apply to the proposed series and parallel power-trains, in order to see their (series and parallel HEVs) responses to such control strategy. Note that this proposed platform (a re-configurable power-train controller) may not work properly for series and parallel HEVs power-train if it is not tuned correctly. Tune properly a controller needs time.

Figure 3.17 shows the proposed fuel cell power-train control strategy, which is implemented. The dashed arrow corresponds to $u_5(t)$ of (3.9). The doted arrow represents $u_6(t)$ of (3.9). Figure 3.17 illustrates how the power-train control operates in the proposed FC power-train.
In general the control law for FC based HEV could be given by:

$$[u_5(t), u_6(t)] = \Omega\{D_T(t), D_P(t), B_P(t), B_L(t), Em_{spd}(t), Fc(t)\} \tag{3.8}$$

where $Fc(t)$ is fuel cell information
The following control strategy allows defining the EM reference torque:
Note that the explanation of Equation (3.9) is given in control strategy 5, which is given in Appendix D.

$$u_5(t) = \Phi\{D_T(t), B^*_{Fcp}(t), Fc_P(t), Em_{spd}(t)\} \tag{3.9}$$

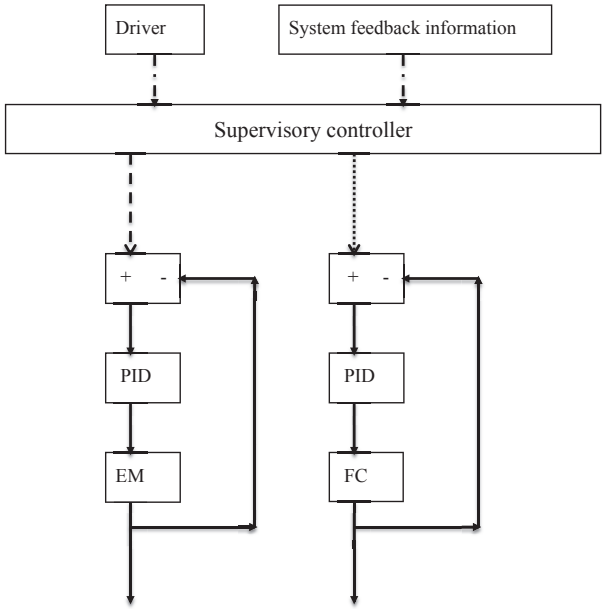

Figure 3.17: Proposed FC power-train control architecture

where

$$B^*_{Fcp}(t) = k\{B_P(t), B_L(t), B^*_{Fp}(t), Fc_P(t)\} \tag{3.10}$$

and

$$B^*_{Fp}(t) = x\{D_P(t), B_P(t)\} \tag{3.11}$$

and

$$Fc_P(t) = j\{I_{Fc}(t), V_{Fc}(t)\} \tag{3.12}$$

Here $I_{Fc}(t)$ and $V_{Fc}(t)$ are, respectively, the fuel cell current and voltage produced by proton exchange electrochemical reaction basically by the FC.

The following control strategy allows defining the FC reference current.

$$u_6(t) = \Delta\{D_P(t), B_P(t)\} \tag{3.13}$$

Note that the explanation of Equation (3.13) is given in control strategy 6, which is given in Appendix D.

3.2.2 Power-train components control

Components such as the EM ICE, generator are controlled via a PID controller. Their roles are as important as the supervisory controller. The PID controller aims to control these components to reach the set point, which are the references (torque and speed), defined by the supervisory controller. But for the EM and the generator flux-weakening controller (see Definition 6 in Appendix A) are adding to the PID controller, in order to weaken the i_d component of the phase current. The goal is to reach the maximum torque or speed. Note that a PID block provided by Simulink is used.

Remarks 3.3

In practice there is a need to measure and evaluate the input and output of the system, in order to optimise the system. Consequently it is necessary to define certain rules within the System. These rules will allow observing and measuring different measurable variables within the system (the system being a HEV power-train).

Some of the rules or limits are given as follows:

The battery power limit in $[W]$ is defined respect to this:

$$B_L(t) = \mu\{I_{Batt}(t), V_{Batt}(t), Batt_{VNominal}(t), Batt_{PNominal}(t)\} \tag{3.14}$$

where

$V_{Batt}(t)$ is battery voltage in $[V]$

$I_{Batt}(t))$ is battery current in $[A]$

$Batt_{VNominal}(t)$ is the battery nominal voltage in $[V]$

$Batt_{PNominal}(t)$ is the battery nominal power in $[W]$.

The battery recharge power in $[W]$ is obtained from:

$$B_P(t) = \Psi\{Batt_{soc}(t), Batt_{PNominal}(t)\} \tag{3.15}$$

where $Batt_{soc}(t)$ is the battery state of charge information.

The driver requested torque from the acceleration demand is respect to:

$$D_T(t) = sign(Acc_{Req}(t))Min(Max_T, actual_T(t)) \tag{3.16}$$

where $Acc_{Req}(t)$ is the requested acceleration from the driver lies in the range [-1 1]

without units. Max_T is a constant, which is set as a torque limit in $[Nm]$. This means whatever happens the requested torque will never be greater than that value. $actual_T(t)$ corresponds to the actual driver requested torque in $[Nm]$, which is:

$$actual_T(t) = \frac{Driving_{spd} Max_T}{Driving_{spd} \leq |\frac{Acc_{Req} 60}{2\pi}| < \infty} \tag{3.17}$$

where $Driving_{spd}$ is a constant in $[rpm]$.

Note that the EM control is about torque control compensated by a flux weakening controller in order to control the inverter output. Technically it is current control. The reason for this is the acceleration demand cannot be interpreted as voltage or current directly.

3.3 Conclusions

This Chapter has described the systems design (systems (HEVs power-trains) modelling and implementation) within Simulink. In effect, the specifications of each proposed HEV were presented in the HEV's architecture. Each component of the drivetrain of the HEV was clearly presented with their specifications. The Simulink implementation of the each proposed HEV power-train followed its architecture presentation, with the explanation of the composition of each subsystem implemented. It also introduced the proposed power-train control strategies, which were tested, but the results will be presented in next Chapter. The proposed power-train control platform, was a composition of two control levels, which are:

- the supervisory control level, which aimed to define the optimal operating point (the reference) of each main component involved in the hybridisation of the four-wheel vehicle, these components were the EM, the ICE and the generator, and the fuel cell. This supervisory controller takes inputs as the driver acceleration request and the HEV feedback information (vehicle speed, battery state of charge).

- in component level a simple PID control strategy were proposed. This PID had the objective to drive the main component involved in the hybridisation of the four-wheel drive to reach the optimal operating point computed by the supervisory controller.

In summary this Chapter 3 explains from systems (HEVs) specification to the systems implementation and testing (simulations).

The next Chapter 4 will present different simulation results and their analysis.

Basically, the impact of the proposed re-configurable power-train controller on four different power-trains will be discussed. The power flow, stability and driveability of the four different HEVs using this proposed control platform will be analysed.

Chapter 4

Simulation results

This Chapter discusses the simulation results of four different proposed power-trains under the power-train control strategies which have been proposed. The supervisory control action will be presented followed by power flow in the proposed power-trains. In that way some appreciation of the proposed power-train controller platform can be made. The vehicle handling responses will be also discussed. Basically, it is about analysing the vehicle stability and driveability (but the study will be focused only on the vehicle's tyres behaviour. Basically the forces acting on tyres are analysed). Instead of using a driving cycle to simulate the power-train, the driver acceleration profile will be used to simulate the four proposed HEV power-trains under the proposed re-configurable power-train controller. This Chapter is organised as follows:

- Section 4.1 will be concerned with PS HEV computer simulation results.
- The computer simulation results of the S HEV will be analysed in Section 4.2.
- Section 4.3 will present the P HEV computer based model simulation results.

- Finally the FC HEV computer simulation results will be discussed in Section 4.4. Note that the HEV stability and driveability, the flow of power through the power-train and the four-wheel drive HEV speed will allow the performance of the proposed platform to be evaluated. One of the goals of the HEV in this research is to drive the HEV power-train with the EM as long as possible by reducing the use of the ICE for as long as possible.

4.1 Simulation results for PS HEV power-train

This Section covers the simulation results of the proposed Power-split power-train under the proposed power-train control strategy. The results such as the driver acceleration profile followed by the proposed power-train control strategy performance will be presented. Then the flow of energy through this proposed PS HEV power-train will be discussed. Finally the vehicle road handling will be considered.

4.1.1 Acceleration and vehicle speed in PS HEV

This Section deals with the driver acceleration profile, which lies in the range [-1 1] and the vehicle speed on the straight line road.

Figure 4.1 displays on the upper plot the profile of the acceleration requested by the driver during $30s$, in percentage. Basically, the driver starts with a small acceleration request then increased to 0.5, which corresponds to 50% acceleration request at around $3s$. This is observable in the interval [5 7]s. Then the driver brakes, followed by a build up of acceleration demand, which reaches 1, which is

equivalent to 100% acceleration request, (full acceleration). The build up of acceleration request is observable between [10 17]s. After that the driver requests a gentle deceleration [17 22]s, followed by braking during [22 28]s. Then the driver requests a build up acceleration again during [28 30]s. The braking in the interval [7 10]s and [22 28]s will allow simulating the regenerative braking on this proposed PS HEV power-train. The lower plot is the vehicle speed in $[km/h]$. When the driver requests acceleration, the vehicle speed increases. This is observable in the intervals [0 8]s and [10 22]s. Then when the driver brakes (a negative acceleration) the vehicle speed decreases. This can be seen in the interval [8 10]s and [22 28]s. The dashed line in the lower plot shows the driver speed profile (it is the integration of the acceleration profile). This lower plot demonstrates that the four-wheel drive PS HEV speed follows the driver speed profile.

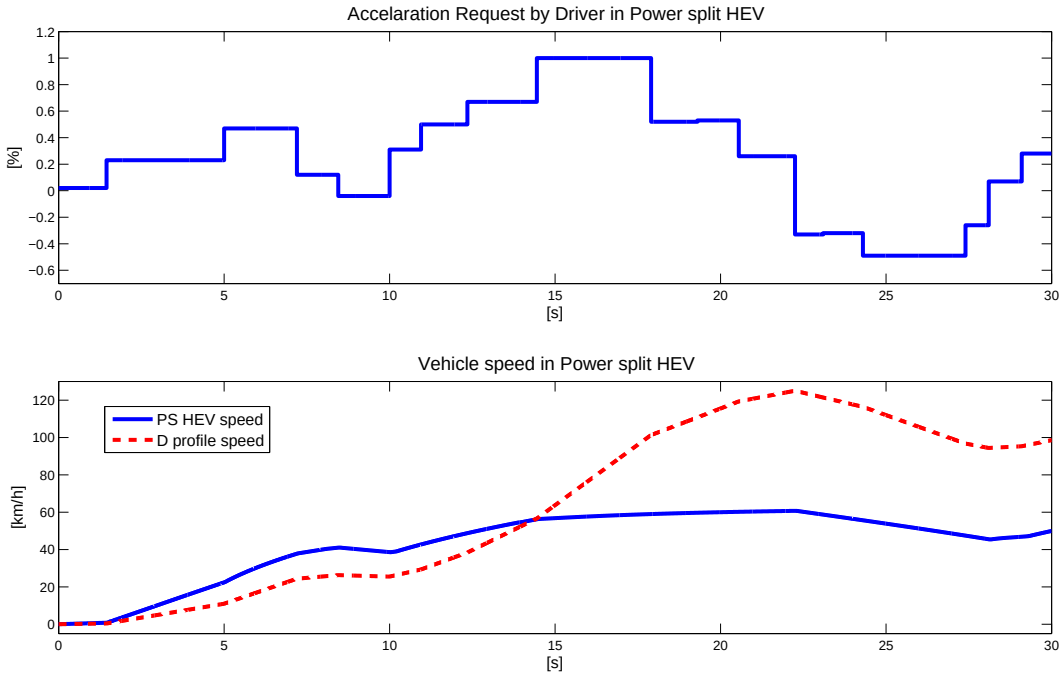

Figure 4.1: Acceleration requested and vehicle speed for PS HEV

Figure 4.2 shows the electrical and mechanical powers of the EM and the generator. The upper plot: In the solid line is the mechanical power of the EM, it is that, which drives the vehicle through the planetary gear. The dashed line represents the electrical power of the EM. It is the power which the EM uses to produce the mechanical power to drive the vehicle.

The solid line is slightly above the dashed line. The lower plot: the dashed line corresponds to the generator electrical power. The solid line is the generator mechanical power, which is used to produce the electrical power for providing electrical power to the EM charging the battery.

Note that the mechanical power curve is below the electrical power curve. These remarks demonstrate that there are losses during the power conversion from electrical to mechanical and vice versa. This problem can be addressed by optimising the proposed power-train components (the EM and the generator) controllers and improving the components (the EM and the generator) models.

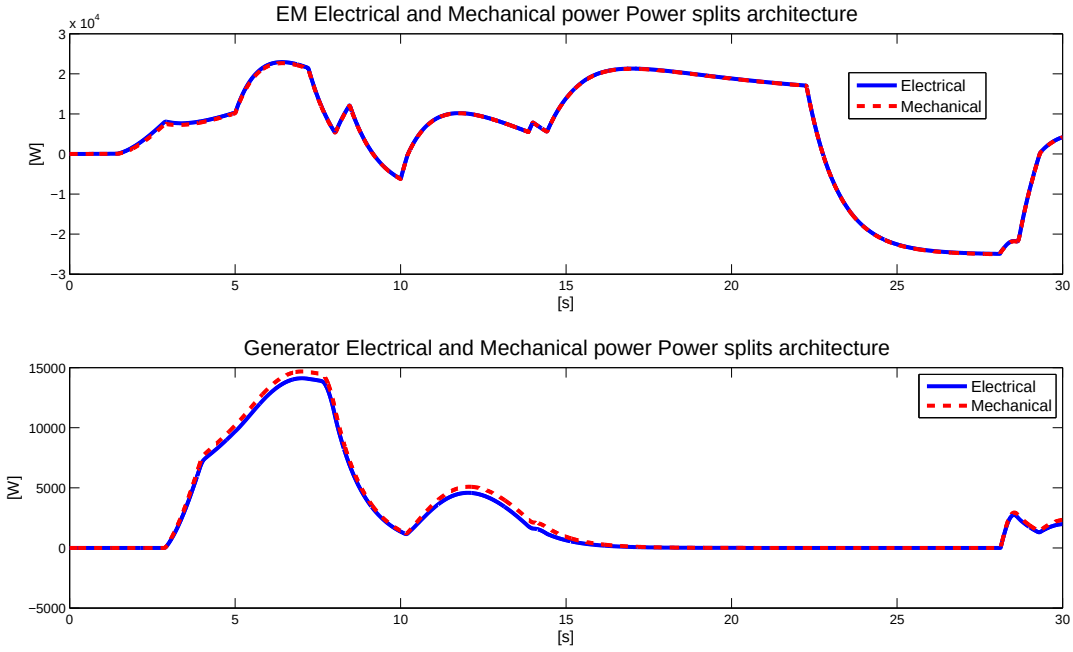

Figure 4.2: EM power (mechanical and electrical) comparison in PS HEV

Remarks 4.1

The plots in Figures (4.2, 4.13, 4.24, 4.34) are with respect to the following formulas:

$$EM_{Mech_{pow}}(t) = EM\_Tork(t)Em_{spd}(t) \tag{4.1}$$

where $EM_{Mech_{pow}}(t)$ is the mechanical power of the EM in $[W]$, $EM\_Tork(t)$ is in $[Nm]$ and $Em_{spd}(t)$ is in $[rpm]$

$$EM_{Elec_{pow}}(t) = I_{EM}(t)V_{EM}(t) \tag{4.2}$$

where $EM_{Elec_{pow}}(t)$ is the electrical power of the EM in $[W]$, $I_{EM}(t)$ is in $[A]$ and V_{EM} is in $[V]$

$$Gen._{Mech_{pow}}(t) = Gen.\_Tork(t)Gen_{spd}(t) \tag{4.3}$$

where $Gen._{Mech_{pow}}(t)$ is the mechanical power of the Gen. in $[W]$, $Gen.\_Tork(t)$ is in $[Nm]$ and $Gen_{spd}(t)$ is in $[rpm]$

$$Gen._{Elec_{pow}}(t) = I_{Gen.}(t)V_{Gen.}(t) \tag{4.4}$$

where $Gen._{Elec_{pow}}(t)$ is the electrical power of the Gen. in $[W]$, $I_{Gen.}(t)$ is in $[A]$ and $V_{Gen.}$ is in $[V]$

4.1.2 Controller performance in PS HEV power-train

This Section considers the robustness of the proposed power-train control strategy. Within this Power-split power-train, the supervisory controller outputs are $u_1(t)$, $u_2(t)$, $u_3(t)$ and $u_4(t)$.

Figure 4.3 displays the components controllers activation signal, the EM torque in $[Nm]$, the generator speed in $[rad/s]$ and the ICE speed in $[rpm]$. The upper plot corresponds to $u_1(t)$. It allows enabling the ICE and the generator controllers. Because the activation of the ICE requires the need for more power, therefore calls for electrical power as well. The battery provides the necessary power to the EM to run the vehicle. Note that the acceleration request at the beginning of the simulation is relatively small around 2%. When braking the components controllers activation signal is disabled, in order to disable the generator by allowing the regenerative braking to charge the battery. The lower plot: the solid line is the optimal reference torque for the EM. This torque is defined by the supervisory controller.

The dashed line is the actual (the output of the Simulink model) EM torque under the PID and flux weakening control. The component (EM) controller provides a satisfactory result, but it needs to be optimised.

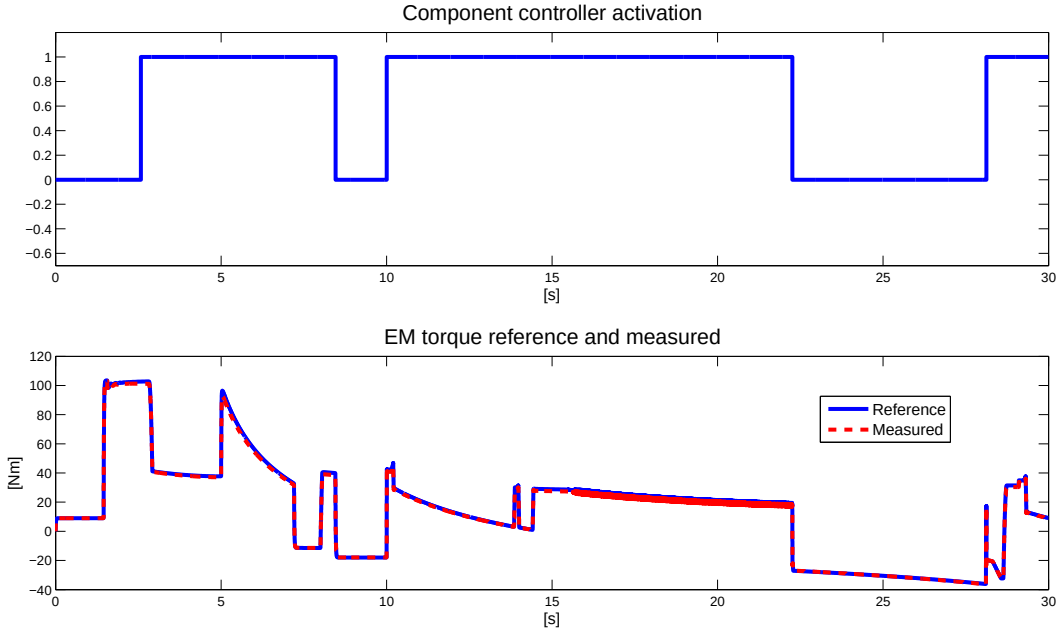

Figure 4.3: Supervisory control and component control performance for PS HEV

Remarks 4.2

- 'Measured' in the legend of Figures (4.3, 4.4, 4.14, 4.25, 4.35) are basically the output measurement of the Simulink model.

- the 'Reference' is computed with respect to Equation (5.7) in Appendix D.

Figure 4.4 displays the ICE speed in $[rpm]$ and the generator speed in $[rad/s]$. The upper plot: the solid line is the $u_3(t)$, which is the generator reference speed. This reference speed is defined by the master controller. The dashed line is the actual generator speed. The component (generator) controller provides satisfactory results. The lower plot: the solid line is the $u_4(t)$. The reference speed of the ICE is defined by the supervisory controller. The dashed line is the ICE actual speed. When

braking the ICE speed decreases. But the generator speed goes to zero (this is one of the advantages of Electric machine), because these components (the ICE and the generator) controllers were disabled by the supervisory controller. In other words the components controllers activation signal is disabled. Again, the components (the ICE and generator) controller provide satisfactory results. But there is a need to improve them.

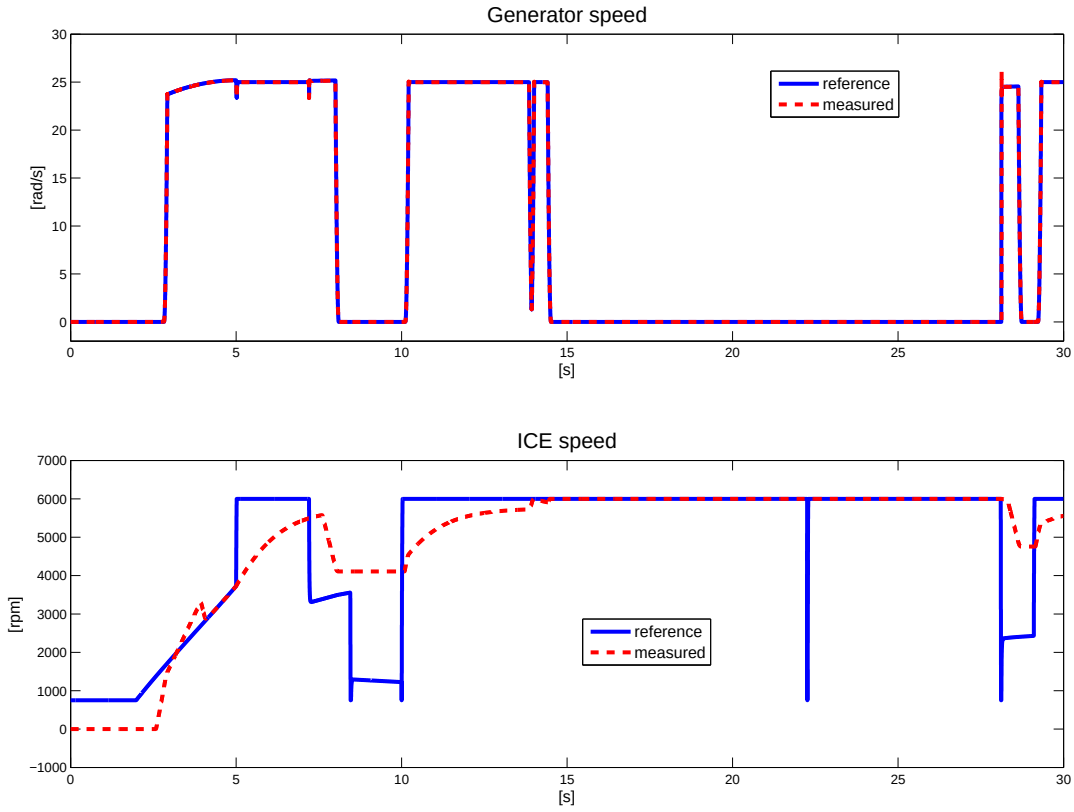

Figure 4.4: Supervisory control and component control performance for PS HEV

Remarks 4.3

- the 'reference' in the generator speed plot is computed respect to (5.13) in Appendix D.

- the 'reference' in the ICE speed plot is calculated respect to (5.14) in Appendix D.

4.1.3 Power and energy flow in PS HEV power-train

This Section discuss the flow of power and torque through the proposed Power-split power-train. Under the proposed power-train control strategy, Figure 4.5 shows the power flow through the PS HEV power-train. The requested power is in the light solid line. It cannot be met, probably due to the characteristics of this power-train components. The dark solid line is the battery power, which powers the EM. The dotted line is the ICE power, which is produced in this power-train. The dashed and dotted line is the generator power. The EM power is represented by the dashed line. Figure 4.6 displays the zoom ps1(power split 1), which is presented in Figure 4.5. The battery power curve is below the EM power curve. This may have two explanations: note that at the beginning $[0\ 3]s$ the EM drives the vehicle alone. Because in that time interval the ICE power is $0W$. It is the the battery, which provides electrical power to the EM, in $[0\ 3]s$. In that interval the EM Battery power curves are quasi similar. But as the requested power increases, the ICE starts working. A few milliseconds later the generator starts working to provide the extra power to the EM and charging the battery at the same time if required. The reason why the EM does not drop from $3s$ is that, the generator provides the additional power to the EM. Although, the result is satisfactory in the sense that the ICE produces the extra power to meet the requested power, the supervisory controller needs to be reviewed and optimised, similar to the PS HEV power-train the components controllers as well.

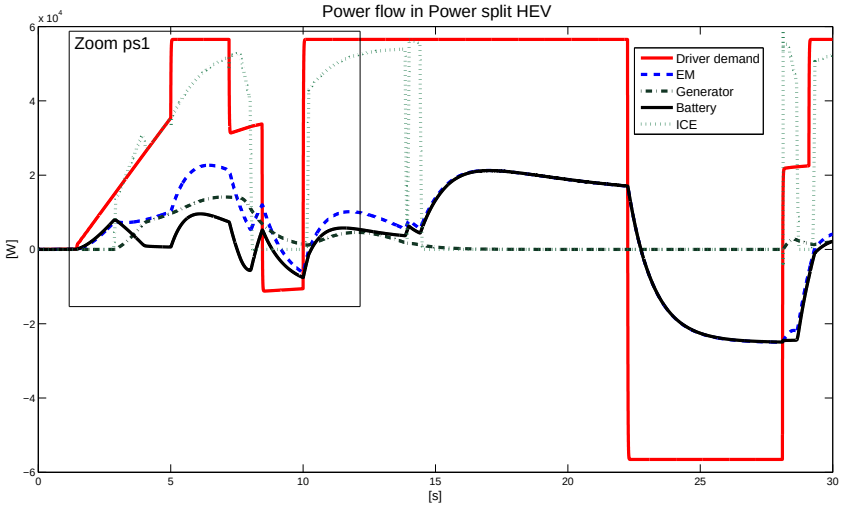

Figure 4.5: Flow of power (electrical and mechanical) in PS HEV

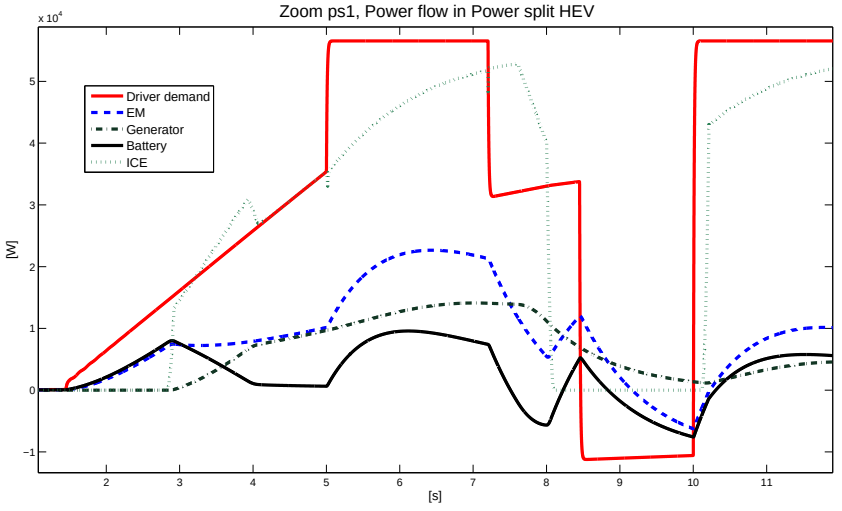

Figure 4.6: Zoom ps1, Flow of power (electrical and mechanical) in PS HEV

Remarks 4.4

The 'ICE power' is computed with respect to:

$$ICE(t) = ICE\_Tork(t)ICE_{spd}(t) \tag{4.5}$$

where $ICE(t)$ is the mechanical power of the ICE in $[W]$, $ICE\_Tork(t)$ is in $[Nm]$ and $ICE_{spd}(t)$ is in $[rpm]$.

Figure 4.7 displays the flows of torque through the proposed Power-split HEV power-train. The solid line is the requested power from the driver. The dashed line corresponds to the actual torque, which drives the vehicle. The dotted line represents the EM torque, which drives the vehicle. The EM starts driving the vehicle until the battery state of charge starts to fall. As consequence the EM torque is reduced until the generator begins to provide enough power to the EM. Figure 4.8 displays the zoom ps2 (power split 2), which is presented in Figure 4.17. The EM actual torque does follow that requested. The components (EM, generator and the ICE) controllers need to be optimised. At the beginning there are small oscillations. This may be the simulation initialisation error, or may be the component (the EM) controller gain which needs to be retuned. What is really interesting here is that it is clear that the ICE provides the extra torque close enough to the requested torque. Note that the EM (only) drives the vehicle in [0 3]s.

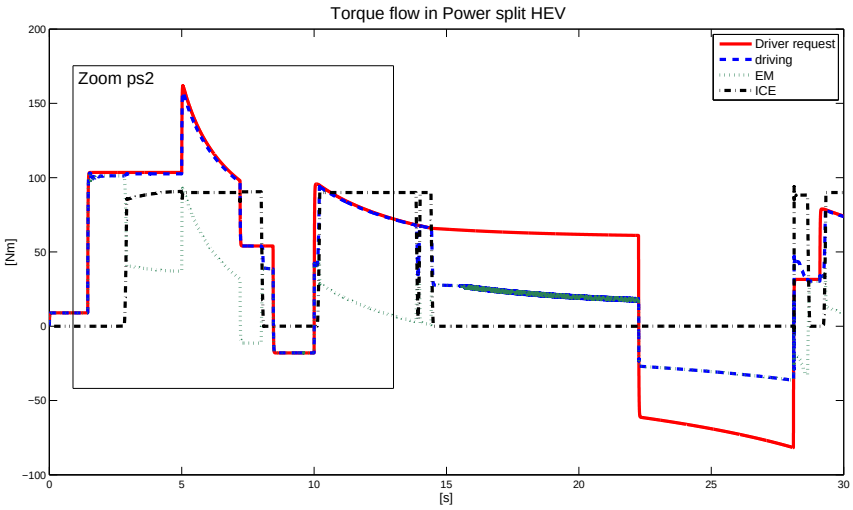

Figure 4.7: Flow of torque (electromagnetic and mechanical) in PS HEV

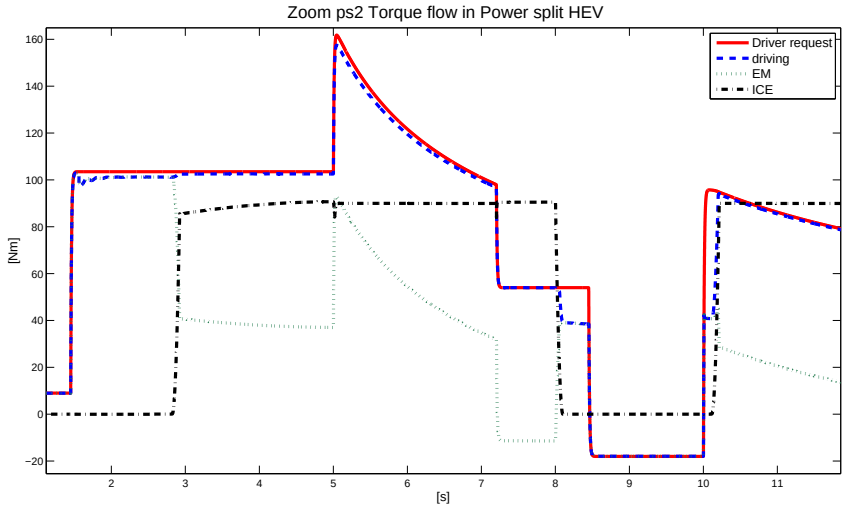

Figure 4.8: Zoom ps2, Flow of torque (electromagnetic and mechanical) in PS HEV

4.1.4 Energy cost in PS HEV power-train

This Section presents the energy cost. Basically, it is about fuel consumption estimation and the state of charge of the battery evolution during the driving time. Figure 4.9 displays on the upper plot the fuel rate in fuel-air mixture dynamism in the combustion chamber of the ICE. The spikes correspond to a sudden acceleration request by the driver. Note that the ICE starts consuming fuel from $3s$. Also in [5 7] s, [10 14]s, [28 30]s, there are a high acceleration demands so high fuel consumption. Nevertheless, the reconfigured model of fuel rate needs to be readjusted. The lower plot is the high voltage battery state of charge (SOC). The initial SOC is 46.7%. The SOC decreases due to the fact that at the beginning [0 3]s, the EM drives the vehicle using the battery. Then the SOC increases slightly. Because the generator starts working. Then the SOC decreases again because of the high acceleration request, so a high power demand. Note also that the SOC increases when the driver brakes. This is observable in [8 10]s and [22 28]s.

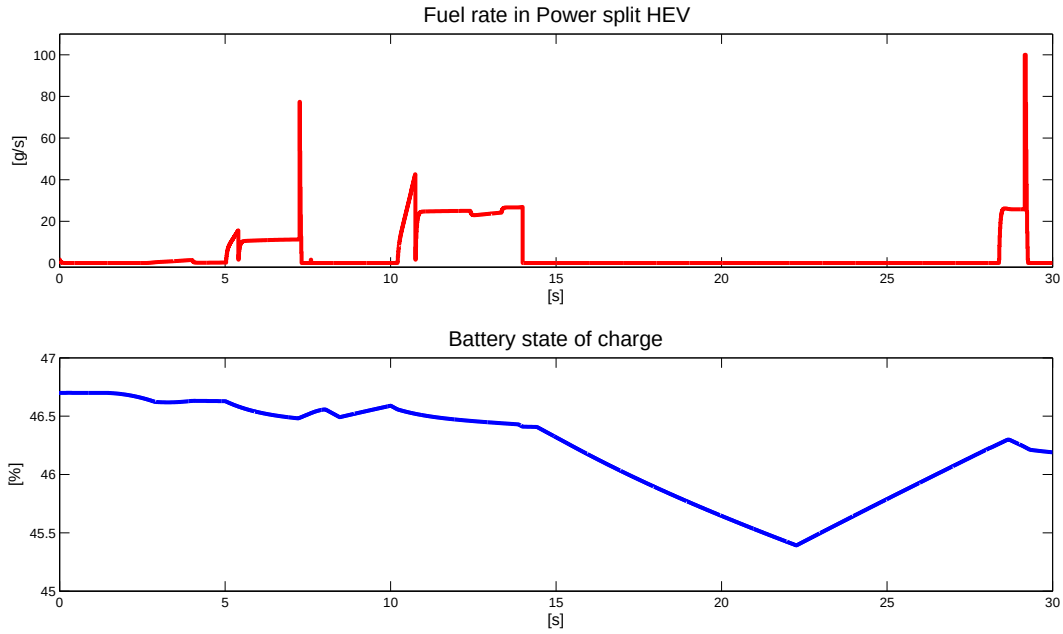

Figure 4.9: Energy (fuel and electric) cost in PS HEV

4.1.5 Vehicle dynamics information in PS HEV power-train

This Section deals with the vehicle handling, where the forces acting on the tyres and the tyres speed are analysed.

Figure 4.10 shows on the upper plot, the speed of the four wheels of the vehicle in *rpm*. The four wheels have almost the same speed. The speed increases, when the driver requests acceleration and decrease, when the driver brakes. The lower plot is the drag force (F_d). It is the force, which opposes the longitudinal force (F_x). This force is proportional to the vehicle speed. It is measurable within the system. It has to be smaller than the longitudinal force to allow the vehicle to move forwards.

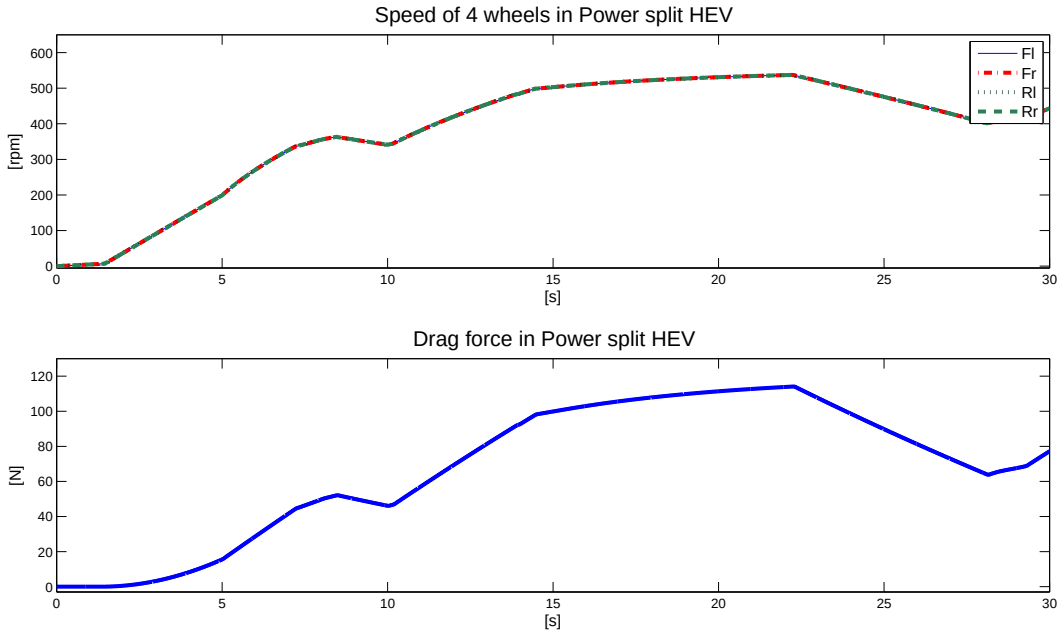

Figure 4.10: Tyres (4) speed and drag force in PS HEV

Figure 4.11 shows the vertical forces (F_z) and longitudinal forces (F_x) acting on the vehicle's tyres. The upper plot: the solid line shows the F_z acting on the two front tyres of the four wheels vehicle. The dashed line is the F_z acting on the two rear tyres of the vehicle. At the beginning of the simulation the F_z acting on the front tyres are larger (in value) than those acting on the rear tyres. Because the Engines is at the front the vehicle weights more than at the rear. The F_z acting on the front tyres decrease apparently when the vehicle starts accelerating at the same time the F_z acting on the rear tyres increase. This is due to the lift force effect on the vehicle. The lift force is proportional to the vehicle speed. Unfortunately, the lift force is not measurable within the system. When braking the value of the F_z acting on the front tyres increase. That is due to the fact that the vehicle front weighs more than the rear and when braking the rear of vehicle tends to lift up. That automatically increases the value of the F_z acting on the front tyres and F_z acting on the rear tyres decrease in value. This is observable in interval [8 10]s and [22 28]s. At high speed in [10 22]s the value of the F_z acting on the front tyres increases, whereas the value of the F_z acting on the rear tyres decreases. The lower plot: the dashed line is the longitudinal forces (F_x) acting on the rear tyres. The solid line is the longitudinal forces (F_x) acting on the front tyres of the vehicle. Those forces decrease and stay constant, with negative value, when the driver brakes. It is observable in [8 10]s and [22 28]s. The spike at 14s is due to a sudden high acceleration request. Note that F_x acting on the rear tyres when braking is slightly bigger (in value) than the F_x acting on the front tyres. However, overall the vehicle is stable and driveable except at the beginning there are some oscillations. This could be the simulation initialisation error or the influence of the component

(the EM) controller gain, because those gains influence the EM torque. The EM torque drives the vehicle, automatically it impacts on the vehicle tyres behaviours.

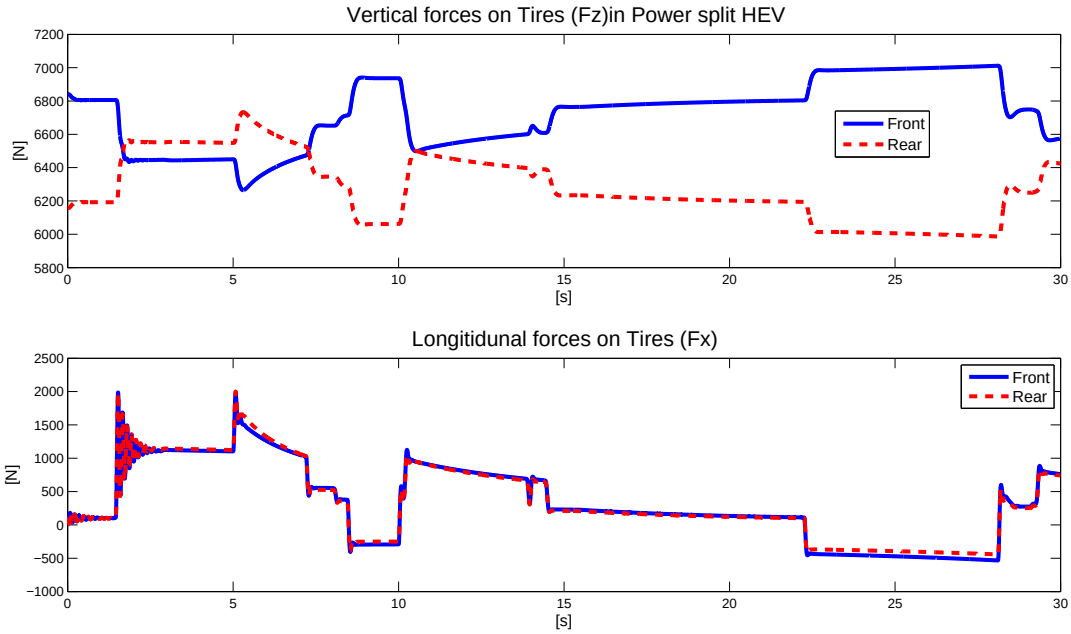

Figure 4.11: Vertical and longitudinal forces on PS HEV tyres

Remarks 4.5

In general there is a need to improve the system as whole (components modelling and controllers optimisation). Nevertheless, the results are satisfactory in the sense that the proposed power-train control allows the ICE and the EM to work together when it is required to. Also the tyres behaviours are satisfactory. Therefore the vehicle is stable and driveable under the proposed power train-controller strategy.

4.2 Simulation results for S HEV power-train

This Section covers the Matla/Simulink simulation results of the proposed series power-train under the control strategy, which is proposed. The results such as the driver acceleration profile followed by the proposed power-train control strategy performance are presented. The flow of energy through this power-train, and the vehicle handling responses are subsequently discussed.

4.2.1 Acceleration and vehicle speed in S HEV power-train

This Section deals with the driver profile and the vehicle speed on the straight line road. Figure 4.12 displays the driver acceleration profile and the vehicle speed. In effect the upper plot shows the profile of the acceleration requested by the driver during $30s$. The driver acceleration profile for this simulation is the same as in Figure 4.1. The lower plot is the vehicle speed in $[km/h]$. When the driver requests acceleration the vehicle speed increases. This is observable in the intervals [0 8]s and [10 22]s. The difference between Figure 4.1 and Figure 4.12 is the vehicle speed in Figure 4.12 reaches $40km/h$. But previously, in Figure 4.1, the vehicle speed reached $60km/h$. This is probably due to the power-train component characteristics. The dashed line in the lower plot shows the driver speed profile. This lower plot demonstrates that the four-wheel drive S HEV speed profile follows approximately the driver speed profile.

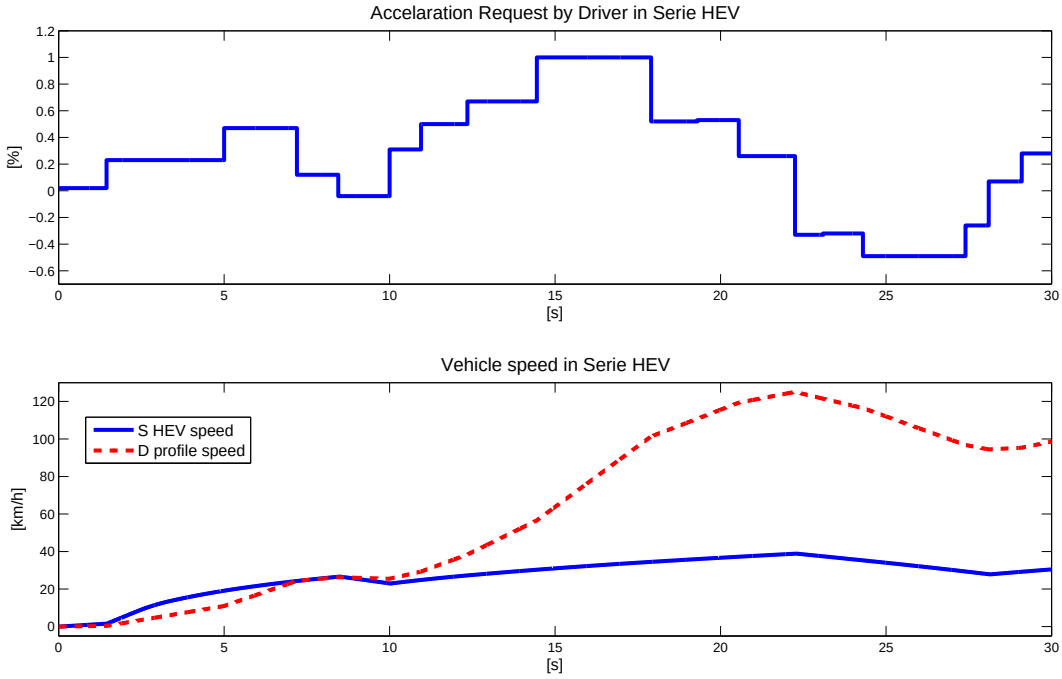

Figure 4.12: Acceleration requested and vehicle speed for S HEV

Figure 4.13 shows the mechanical and electrical power of the EM. In effect the solid line is the mechanical power of the EM. The dashed line represents the electrical power of the EM. It is the power which the EM uses to produce the mechanical power to drive the vehicle. Note that the mechanical power is lower than the electrical power. This demonstrates that there are losses during the power conversion from electrical to mechanical. This problem can be addressed by optimising the component (the EM) controller, also by improving the proposed power-train components models.

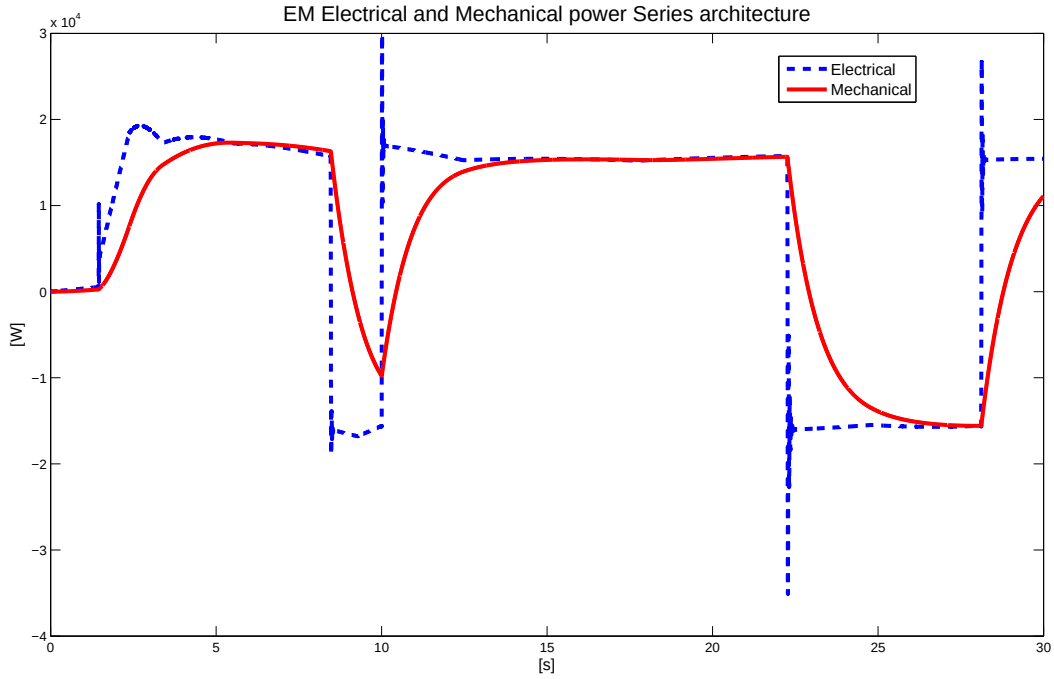

Figure 4.13: EM power (mechanical and electrical) comparison in S HEV

4.2.2 Controller performance in S HEV power-train

This Section discusses the robustness of the power-train control proposed. Within S HEV power-train the supervisory controller outputs $u_1(t)$, $u_2(t)$ and $u_4(t)$. Note that the ICE defines the generator reference speed.

Figure 4.14 displays the components controllers activation signal, the EM torque in $[Nm]$ and the ICE speed in $[rad/s]$. The upper plot corresponds to the subsystems (the generator and the ICE) activation signal. At the beginning the ICE is off [0 3]s. During that time the battery provides the necessary power to the EM to run the vehicle. Note that the acceleration request during that time is relatively small around 2%. When braking the activation signal is off in order to disable the generator by allowing the regenerative braking to charge the battery. The plot in the middle: the solid line is the optimal reference torque of the EM. It is defined by the supervisory controller. The dashed line is the actual EM torque under the PID and flux weakening control. The component (the EM) controller provides a satisfactory result, but it needs to be optimised. The lower plot: the solid line is the ICE actual speed. The dashed line corresponds to the generator actual speed. When braking the ICE and Generator speed decreases because their controllers were disabled by the master controller. In other words the activation signal is disabled. Again the component (the generator) controller provides a satisfactory result, but it needs to be improved.

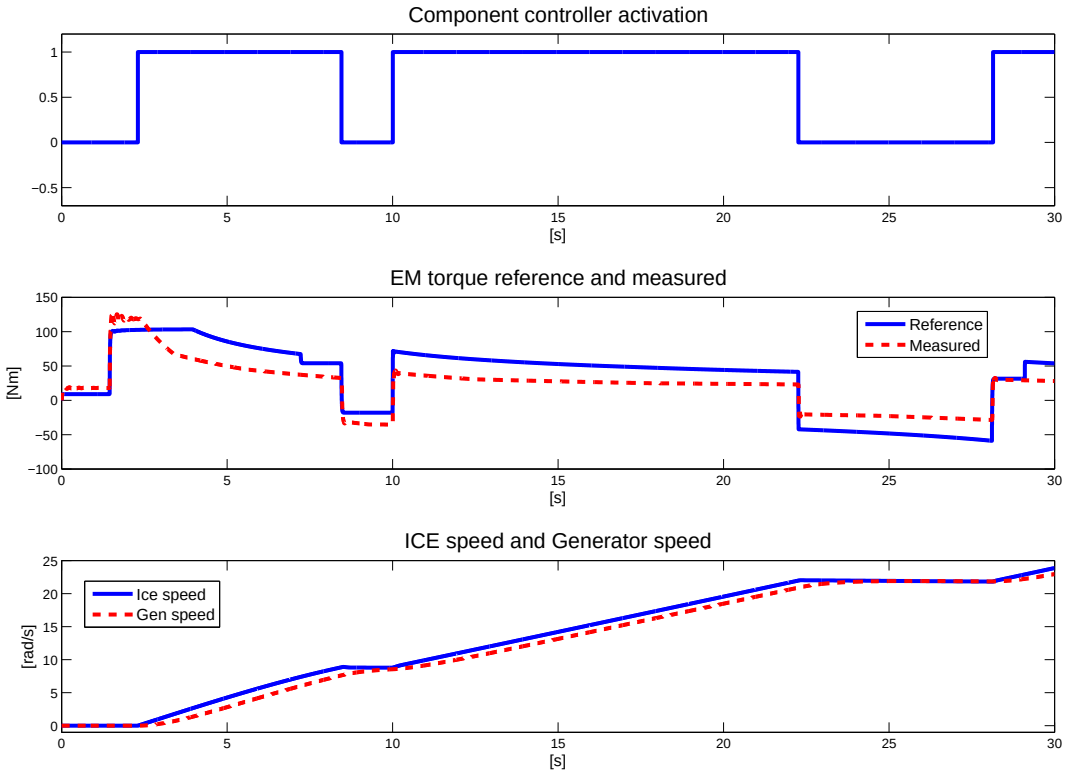

Figure 4.14: Supervisory control and component control performance for S HEV

4.2.3 Power and energy flow in S HEV power-train

This Section discusses the flow of torque and power through the proposed S HEV power-train, under the proposed power-train control strategy.

Figure 4.15 shows the power flow through the proposed S HEV power-train. The requested power is in dark solid line. It cannot be reached, probably because of the the power-train components specification. The light solid line is the ICE power which is produced. The dashed and dotted line is the generator electrical power and the dashed line is the EM power which drives the vehicle. The dotted line corresponds to the battery power. Figure 4.16 displays the zoom s1(S HEV's power train) which is presented in Figure 4.15. The battery power curve is above the EM power curve. This may have two explanations: first the supervisory controller needs to be reviewed by changing the range of the SOC of the battery and the battery power limit for this S HEV power-train. As mentioned before the proposed power-train control strategy is designed for PS HEV power-train. But series and parallel are the ICE based HEV and it is sample to test that control strategy on the series and parallel power-train. The second explanation is the battery needs to be re-specified in order to have an battery less than $25kW$ for this proposed series power-train.

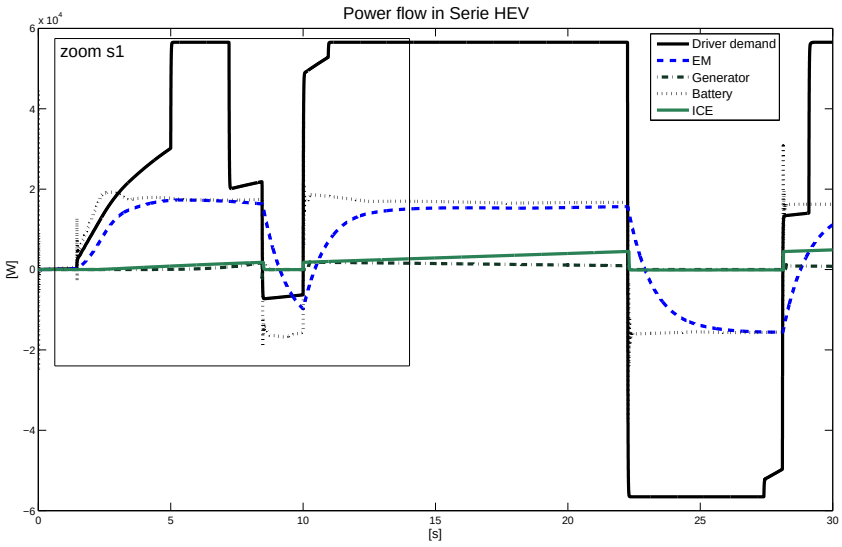

Figure 4.15: Flow of power (electrical and mechanical) in S HEV

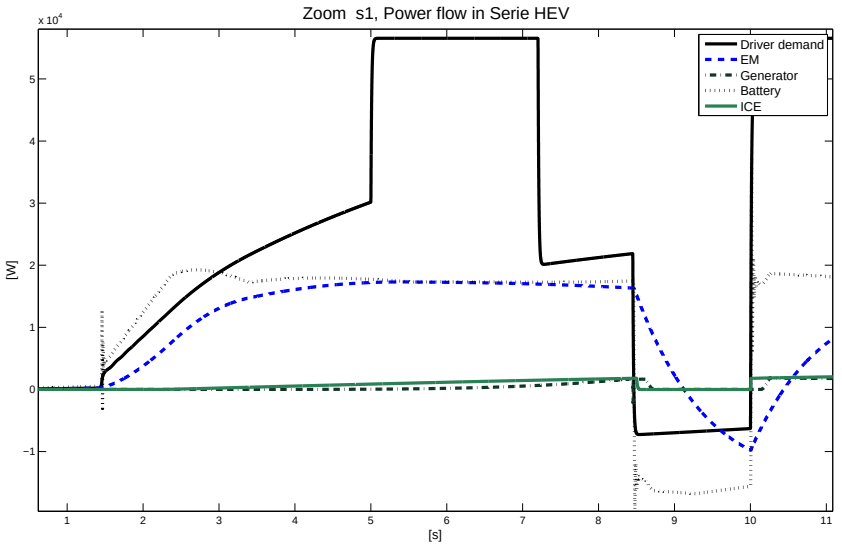

Figure 4.16: Zoom s1, Flow of power (electrical and mechanical) in S HEV

Figure 4.17 shows the flow of torque through the S HEV power-train. The upper plot: the solid line is the requested torque from the driver. The dashed line corresponds to the actual EM torque. The middle plot: the solid line is the requested torque from the driver. The dashed line is the torque, which drives the vehicle, in fact this torque has to be equal to the EM torque. Because the vehicle is driven by the EM only. The lower plot: the solid line is the torque requested by the driver. The dashed and dotted line is the generator torque. The ICE torque is in dotted line. Figure 4.18 displays the Section termed zoom s2 (series 2), which is presented in Figure 4.17. The EM actual torque does not follow that requested. The component (the EM) controller needs to be optimised and the EM model as well. The small oscillation at the beginning of the simulation is probably due to the simulation initialisation error or the EM PID gains, or the battery, which needs to be resized. The generator torque decreases when braking (negative acceleration), but not equal to zero, because the ICE cannot achieve zero spontaneously.

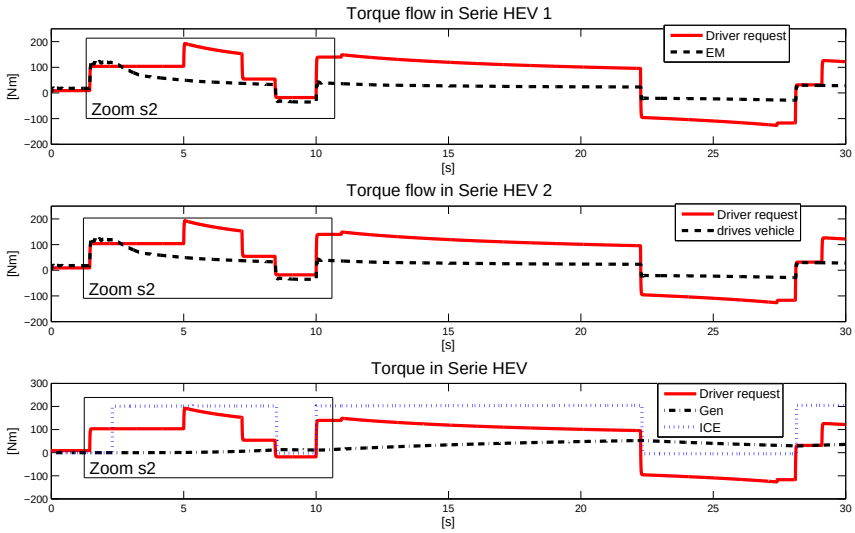

Figure 4.17: Flow of torque (electromagnetic and mechanical) in S HEV

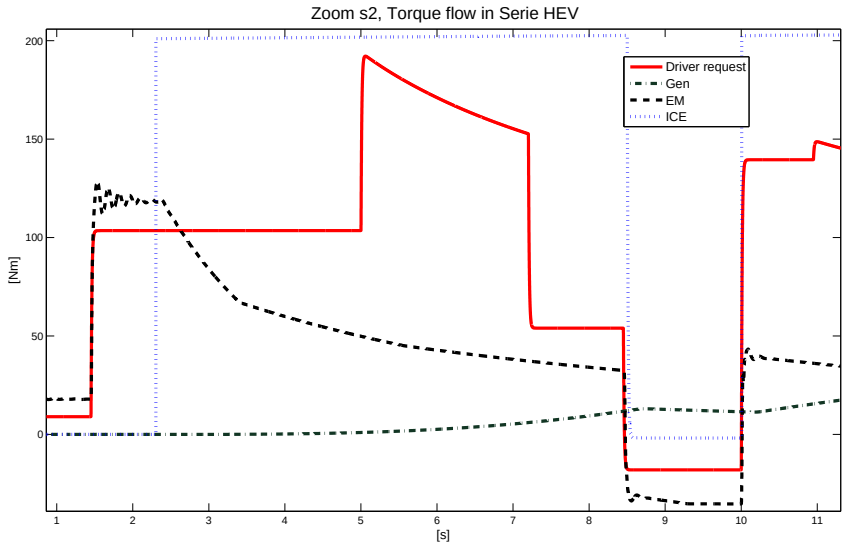

Figure 4.18: Zoom s2, Flow of torque (electromagnetic and mechanical) in S HEV

4.2.4 Energy cost in S HEV power-train

This Section presents the energy cost. Basically, it is about fuel consumption and the state of charge of the battery. Figure 4.19 displays on the upper plot the fuel rate in fuel-air mixture dynamism in the ICE. The spikes correspond to a sudden high acceleration request. Note that the driver acceleration profile signal is square-like wave. Nevertheless, the reconfigured model of fuel rate needs to be readjusted. The lower plot is the high voltage battery state of charge. The initial SOC is 46.7%. The SOC decreases when driving by accelerating, it is observable in $[0\ 8]s$ and $[10\ 22]s$. The SOC increases when the driver brakes, it can be noticed in $[8\ 10]s$ and $[22\ 28]s$.

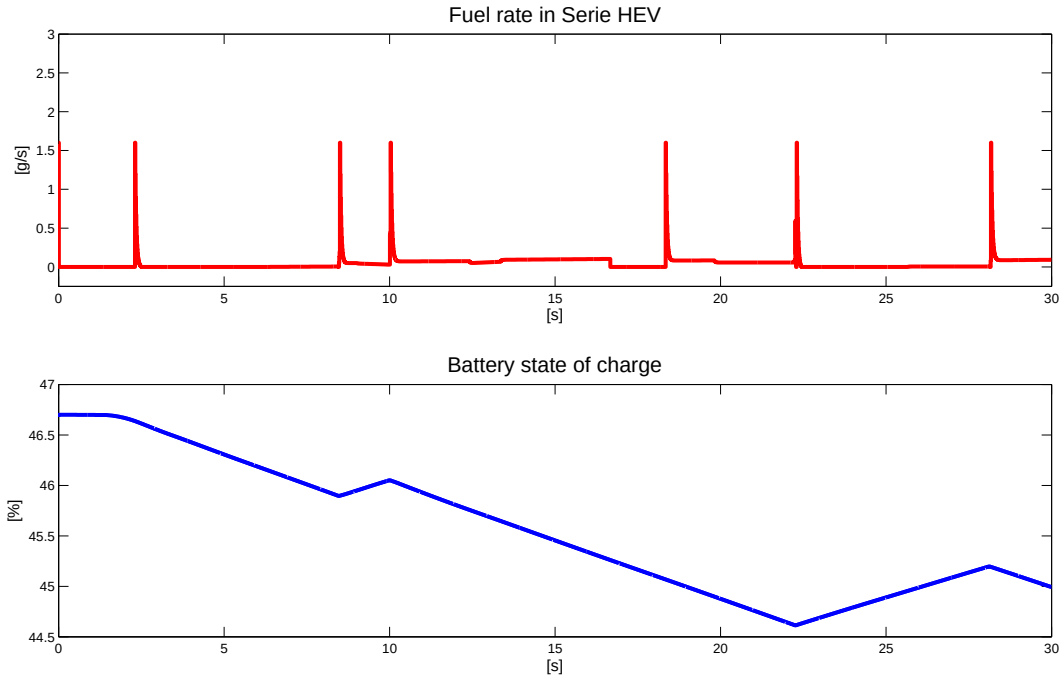

Figure 4.19: Energy (electric and fuel) cost in S HEV

4.2.5 Vehicle dynamics information in S HEV power-train

This Section deals with the vehicle handling, where the forces acting on the tyres and the tyres speed are analysed.

Figure 4.20 shows on the upper plot, the speed of the four wheels of the vehicle in $[rpm]$. The four wheels have almost the same speed. The wheels speed remain small respect to the results shown in Figure 4.10. The speed of the wheels increase when the driver requests acceleration. The tyres speed decrease when the driver brakes. The lower plot is the drag force (F_d). It is the force which opposes the longitudinal force (F_x). The value of the F_d in Figure 4.20 is small compared to its value in Figure 4.10.

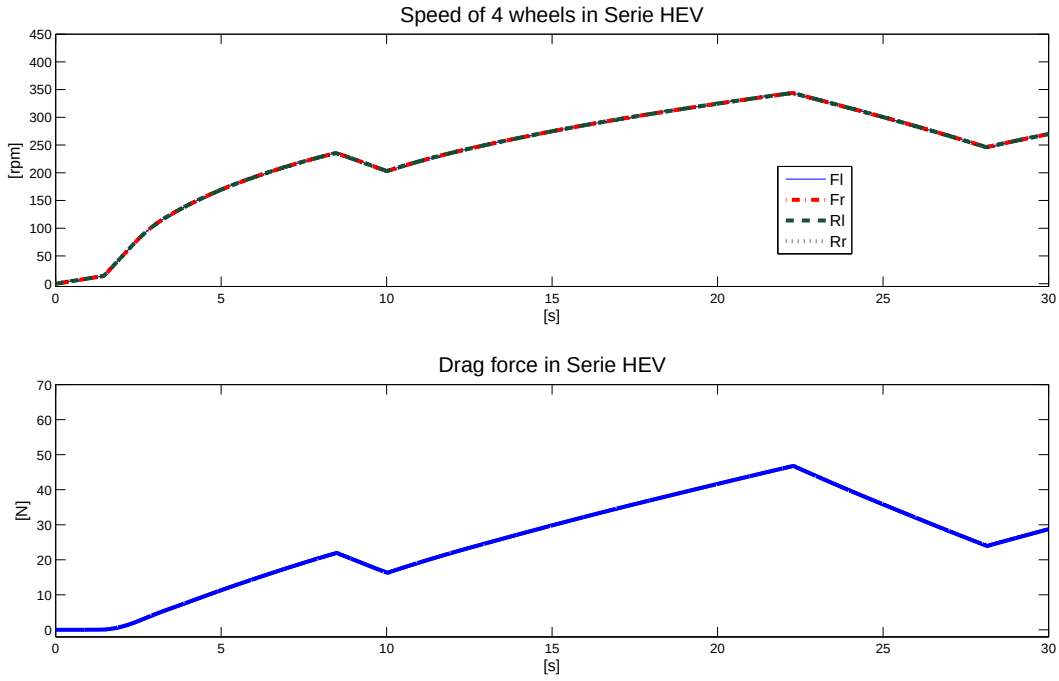

Figure 4.20: Tyres (4) speed and drag force in S HEV

Figure 4.21 shows the forces such as F_z and $F_x$which are acting on the vehicle's tyres. The upper plot displays the F_z which are acting on the two front tyres and on the rear tyres of the vehicle. The F_z decrease when the vehicle starts accelerating at the same time the F_z acting on the rear tyres increase. Probably because of the lift force effect. When braking the F_z acting on the front tyres increase. In effect, during a braking the rear of vehicle tends to lift up. Therefore the F_z, which are acting on the front tyres increase. The F_d, which are acting on the rear tyres decrease. The lower plot: the dashed line is the F_x acting on the rear tyres. The solid line is the F_x acting on the front tyres of the vehicle. In overall the vehicle is stable and driveable except at the beginning, there are some oscillation. This can be the simulation error or the PID gain or the battery influence on the EM torque, which automatically impacts on the vehicle tyres behaviours. The difference between Figure 4.21 and Figure 4.11 is: F_z acting on the front tyres increase smoothly in high speed and when the driver brakes. This is observable in [10 22]s, [8 10]s and [22 28]s. The F_z decrease smoothly as well in those interval. However the value of F_z in Figure 4.21 and Figure 4.11 are quasi similar. Because F_z is related to the vehicle body weight which does not change. At high speed in [15 22]s the value of the F_x in Figure 4.11 is relatively smaller than the value of the F_x in Figure 4.21.

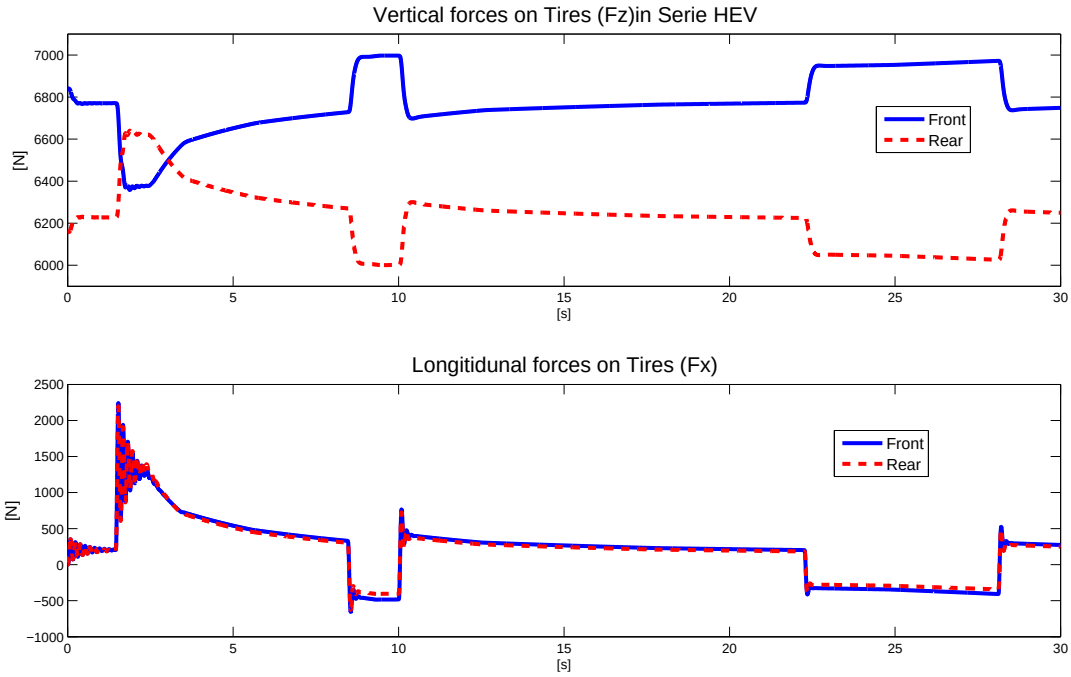

Figure 4.21: Vertical and longitudinal forces on S HEV tyres

Remarks 4.6

There is a need to resize different components of the proposed S HEV power-train. Components such as the battery, the ICE and the EM, without forgetting the optimisation of the supervisory controller and the components controllers. However, the results in general are satisfactory in sense that the proposed power-train control allows the ICE to work when is required, and the components (the EM, the generator) controllers work to achieve the master control demands. Also the tyres behaviour in this S HEV power-train are satisfactory. Therefore the vehicle is stable and driveable under the proposed power train-control method.

4.3 Simulation results for P HEV

This Section discuses the simulation (ran in Matlab/Simulink) results of the proposed parallel power-train under control strategy, which is proposed. The results such as the driver acceleration profile follow by the the proposed power-train control strategy performance are shown. The flow of energy through this power-train, and the vehicle handling response are subsequently discussed.

4.3.1 Acceleration and vehicle speed in P HEV power-train

This Section deals with the driver acceleration profile and the vehicle speed on the straight line road.

Figure 4.22 displays on the upper plot the driver acceleration profile. This profile to simulate this proposed power-train is the same profile used in the previous simulation. The lower plot is the vehicle speed in $[km/h]$. When the driver requests acceleration the vehicle speed increases. This is observable in the intervals [0 8]s and [10 22]s, and when the driver brakes (a negative acceleration), the four-wheel drive vehicle speed decreases. The difference here (Figure 4.22) compared to the previous results (Figure 4.12 and Figure 4.1) is that, the vehicle speed reaches $18km/h$ in Figure 4.22, but previously the vehicle speed reached $40km/h$ and $60km/h$. This is not realistic. This vehicle cannot be driven on the road. Note that the vehicle does not slow down in [22 28]s like in Figure 4.12 and Figure 4.1.

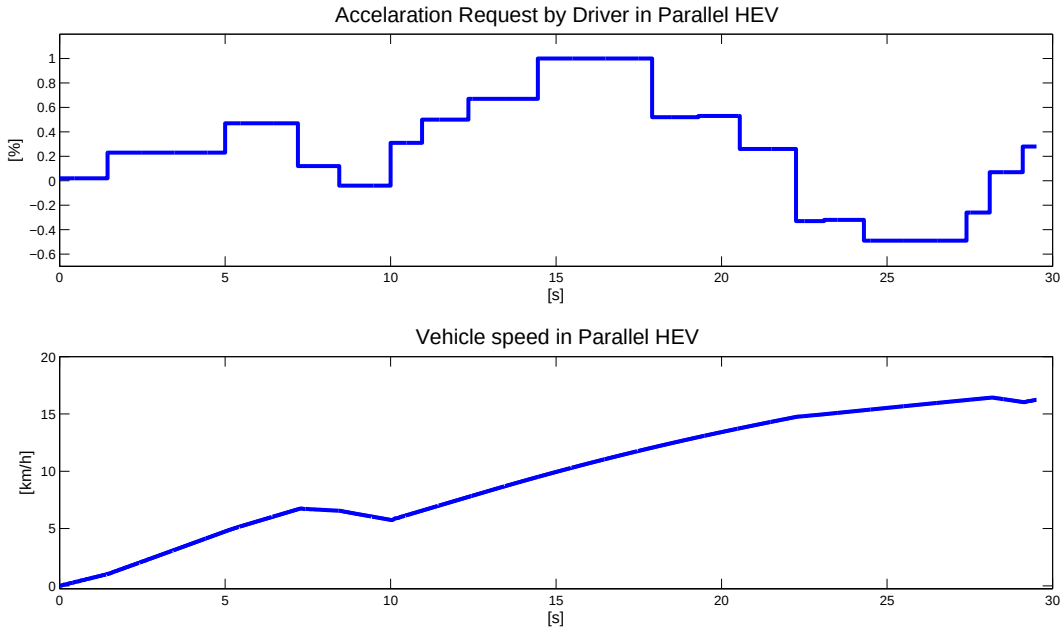

Figure 4.22: Acceleration requested and vehicle speed for P HEV

The dashed line in the lower plot of Figure 4.23 shows the driver speed profile. It is the integration of the acceleration profile. This lower plot demonstrates that the P HEV speed has approximately the same profile as the driver speed profile at the beginning.

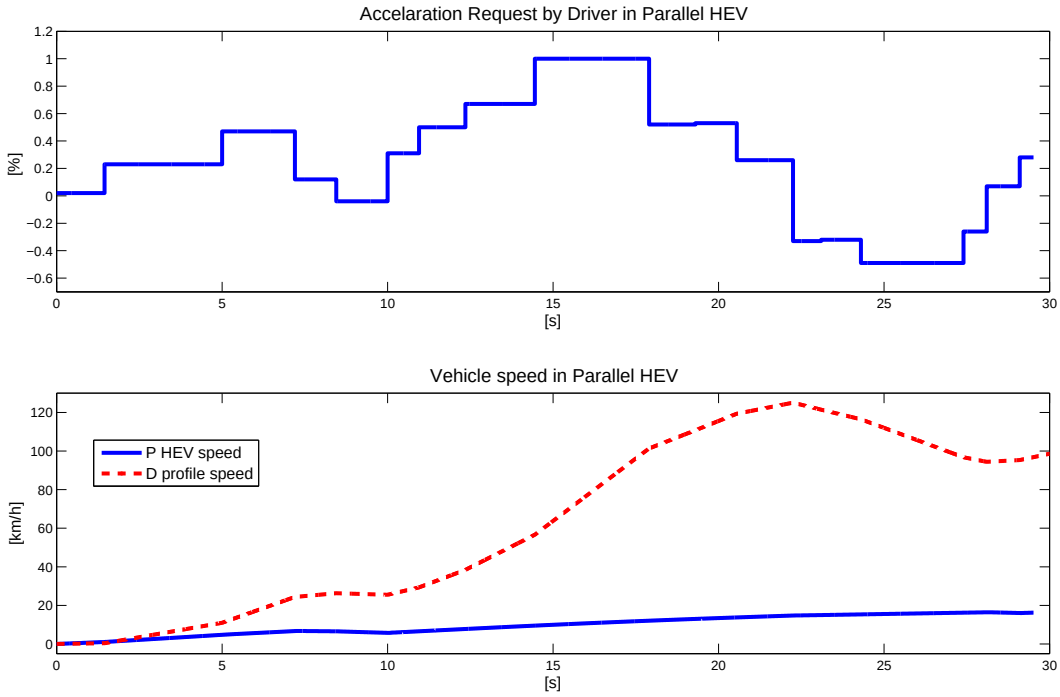

Figure 4.23: Speed requested and vehicle speed for P HEV

Figure 4.24 displays the electrical and mechanical power of the EM the generator. Upper plot: The solid line is the electrical power of the EM. This is the power, which the EM uses to produce the mechanical power (in dashed line) to drive the front wheels of the four-wheel drive vehicle. Note that the EM mechanical power curve is slightly below the The EM electrical power curve. The similarity of both

curves demonstrate an interesting characteristic of the EM. It is almost as if there are zero losses during the power conversion from electrical to mechanical. The lower plot: the dashed line is the mechanical power, which is used to produce the electrical power in solid line, for powering the EM and charging the battery. The electrical power curve is below the mechanical power curve. This means there are losses during power conversion. This problem can be solved by optimising the components (the EM, the generator) controller and the power-train components models as well.

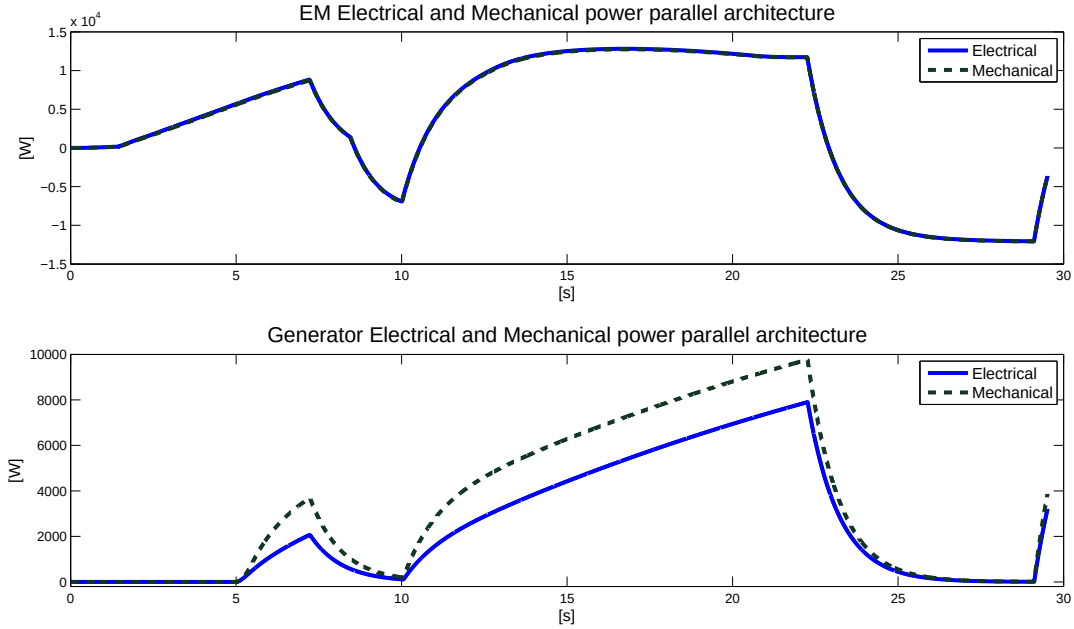

Figure 4.24: EM power (mechanical and electrical) comparison in P HEV

4.3.2 Controller performance in parallel power-train

This Section is about showing the robustness of the power-train control, which is proposed. More importantly this control strategy needs to be reconfigured properly for the P HEV power-train. Within this proposed P HEV power-train, the supervisory controller outputs are $u_1(t)$, $u_2(t)$, $u_3(t)$.

Figure 4.25 displays the components controllers activation signal, the EM torque in $[Nm]$ and the generator speed in $[rad/s]$. The upper plot corresponds to $u_1(t)$. It shows how the generator controller works when there is need. When braking the signal is off in order to disable the generator by allowing the regenerative braking to charge the battery. The middle plot: the solid line is the optimal reference torque for the EM. It is defined by the master controller, basically, it is $u_2(t)$. The dashed line is the actual EM torque under the PID and flux weakening control. The component (the EM) controller provides a satisfactory result but it needs to be optimised. The lower plot: the actual generator speed in $[rad/s]$ is in the solid line. The generator starts working from $5s$. When the driver brakes, the generator stops working. The dashed line is the reference speed defined by the supervisory controller. The component (the generator) controller provides satisfactory results, but there is a need to improve it.

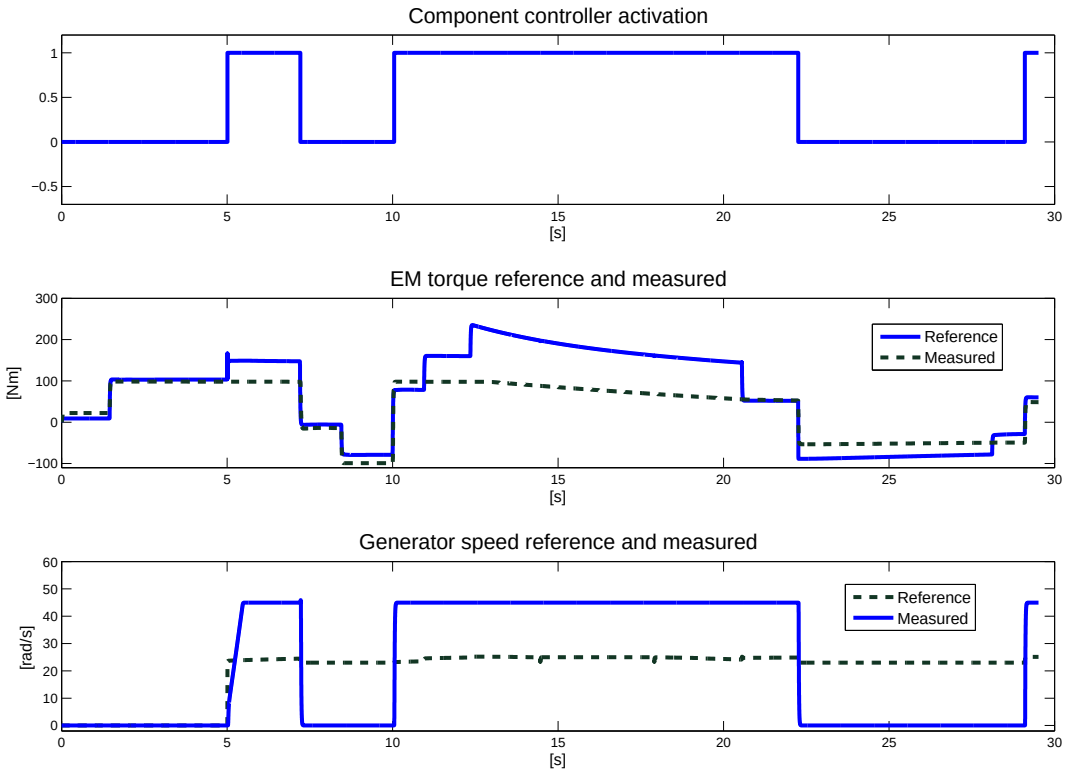

Figure 4.25: Supervisory control and component control performance for P HEV

4.3.3 Power and energy flow in P HEV

This Section presents the flow of power and torque through the proposed P HEV power-train, under the proposed power-train control strategy.

Figure 4.26 shows the power flow through the proposed P HEV power-train. The requested power corresponds to the light solid line. It cannot be met, probably due to the EM characteristics. The dark solid line is the generator power. The battery power starts providing the extra power to the EM from $5s$. The battery power, dashed and dotted line, powers the EM since at the beginning, it starts dropping because the requested power is higher. As the battery cannot deliver that power, the generator starts working. The dotted line is the ICE power which drives the rear wheels of the vehicle. The ICE produces more power than the EM does. The dashed line is the EM power, which drives the front wheels of the vehicle. Figure 4.27 displays the Section termed 'zoom p1 (parallel 1)' , which is presented in Figure 4.26. shows clearly the flow of power. The battery power curve is below the EM power curve. Since at the beginning the ICE power is larger than the EM power. This will mean that the rear wheels run faster than the front wheels. That may imply an instability of the vehicle (handling). Note also that The ICE controller needs to be reviewed, and it may be better to allow the supervisory controller defining the ICE reference speed or torque.

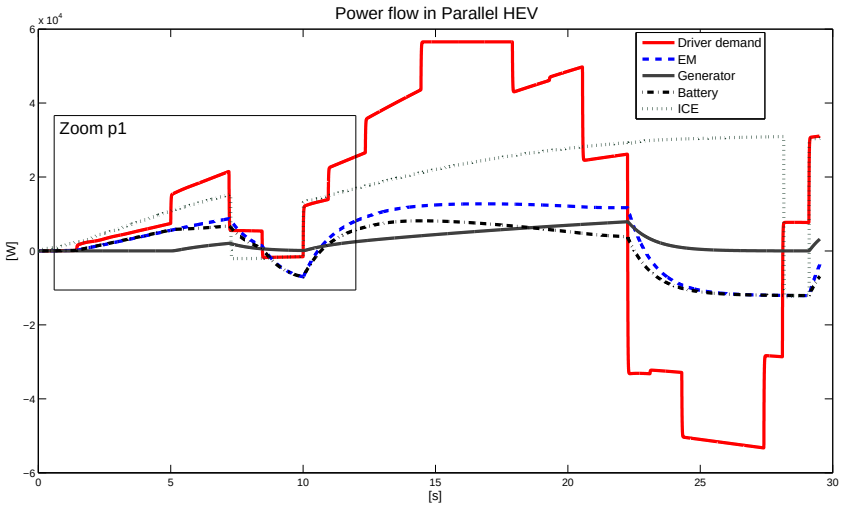

Figure 4.26: Flow of power (electrical and mechanical) in P HEV

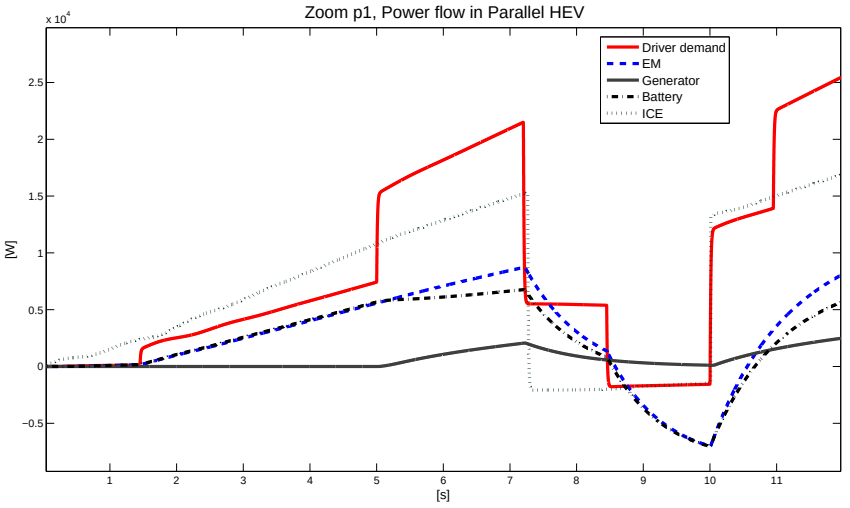

Figure 4.27: Zoom p1, Flow of power (electrical and mechanical) in P HEV

Figure 4.28 displays the flow of torque through the P HEV power-train. The upper plot: the solid line is the requested power from the driver. The dashed line corresponds to the EM actual torque, which drives the front wheels of the vehicle. The middle plot: The dashed line represents the actual torque, which drives the front wheels of the vehicle. In fact it has to be the same as the EM torque. That means there are zero losses during the torque transmission. The solid line is the requested torque by the driver. The lower plot: the solid line is the driver torque demand. The dashed and dotted line is the ICE torque, which is produced. The dotted line is the actual ICE torque, which drives the rear wheels of the vehicle. Figure 4.29 displays the Section called 'zoom p2 (parallel 2)', which is presented in Figure 4.28. Note that the produced ICE torque is different than the actual ICE, which drives the rear wheels of the vehicle. That demonstrates that there are losses during the torque transmission. It is probably due to the friction. This Figure 4.29 allows confirming that the vehicle with this P HEV power-train under this proposed power-train control strategy may have a stability (in terms of handling) problem at the beginning.

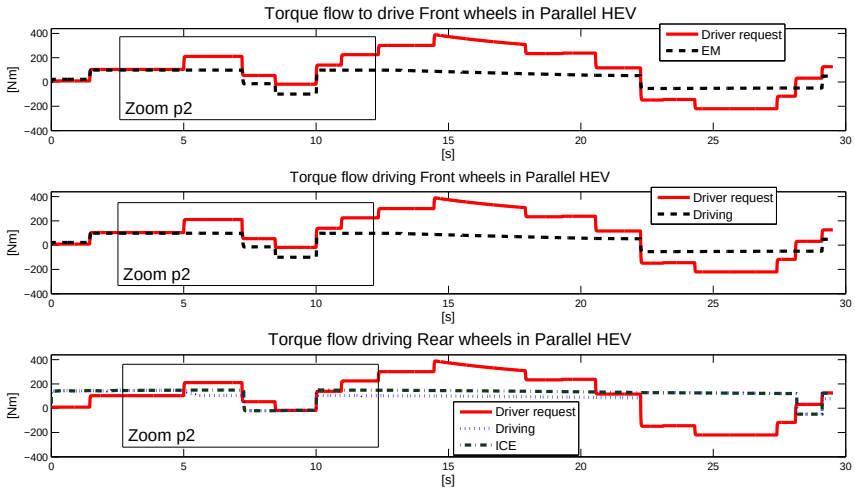

Figure 4.28: Flow of torque (electromagnetic and mechanical) in P HEV

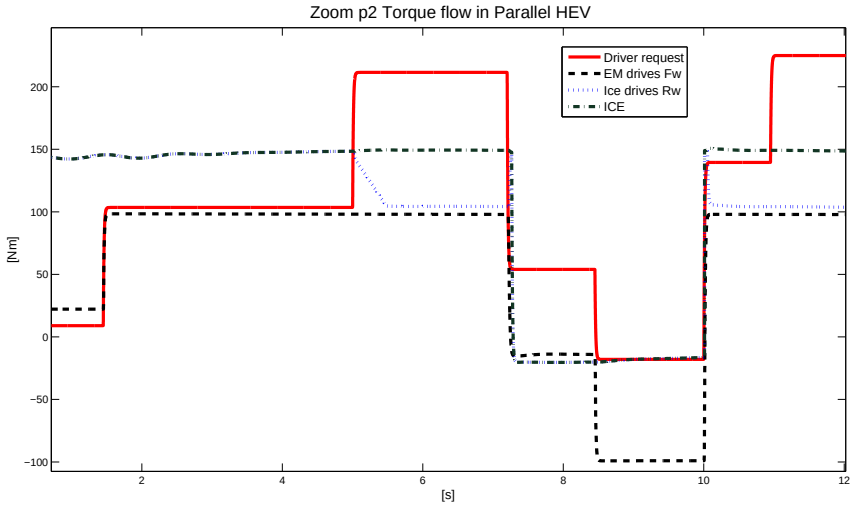

Figure 4.29: Zoom p2, Flow of torque (electromagnetic and mechanical) in P HEV

4.3.4 Energy cost in P HEV

This Section presents the energy cost. It is about fuel consumption estimation and the state of charge of the battery.

Figure 4.30 displays on the upper plot the fuel rate in fuel-air mixture dynamism in the combustion chamber of the ICE. The spikes correspond to a sudden high acceleration request. The reconfigured model of fuel rate needs to be readjusted. The lower plot is the high voltage battery state of charge. The initial SOC is 46.7%. The SOC decreases in the interval [0 7]s and [10 22]s. Because the battery provides power to the EM. The fact that it is constant in [7 8]s it is because of the generator starts working. Note that the SOC increases when the driver brakes.

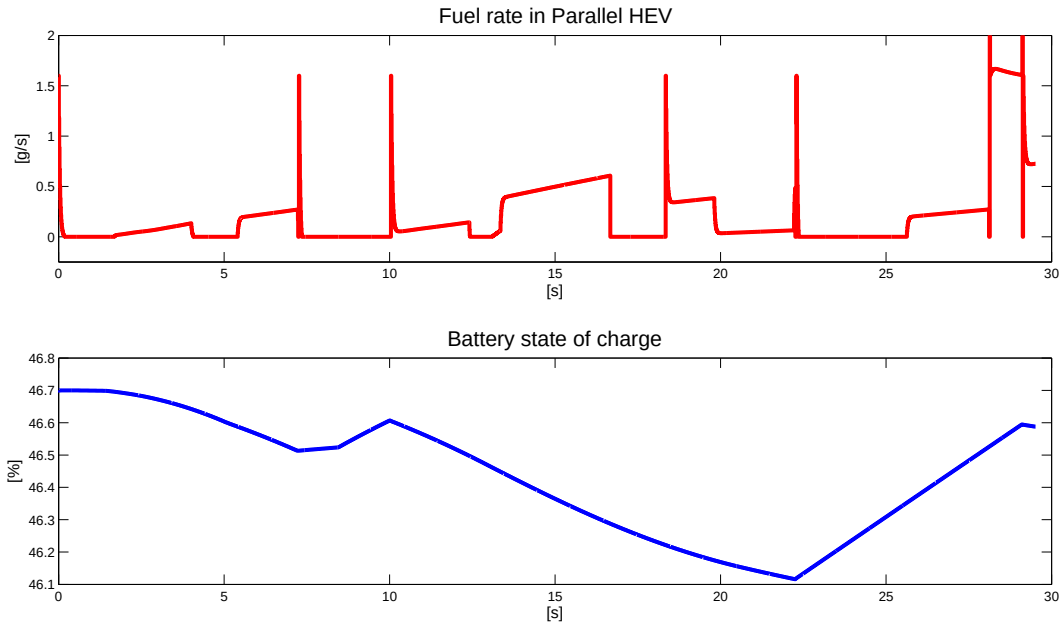

Figure 4.30: Energy (electric and fuel) cost in P HEV

4.3.5 Vehicle dynamics information in P HEV power-train

This Section discuss the vehicle handling, where the wheels speed and the forces acting on the tyres are analysed.

Figure 4.31 shows on the upper plot, the speed of the four wheels of the vehicle in $[rpm]$. The four wheels have slightly different speed this is clearly observable in the interval [22 28]s. This behaviour may explain the vehicle speed in Figure 4.22. It is also slightly observable in the interval [0 3]s and [7 10]s. The speed of the wheels increases when the driver requests acceleration. The tyres speed decrease when the driver brakes. But the tyres speeds do not decrease in [22 28]s. The lower plot is the drag force. It is the force which opposes the F_x. This force and the wheels speed are really small (in value) compared to the results in Figure 4.10 and Figure 4.20.

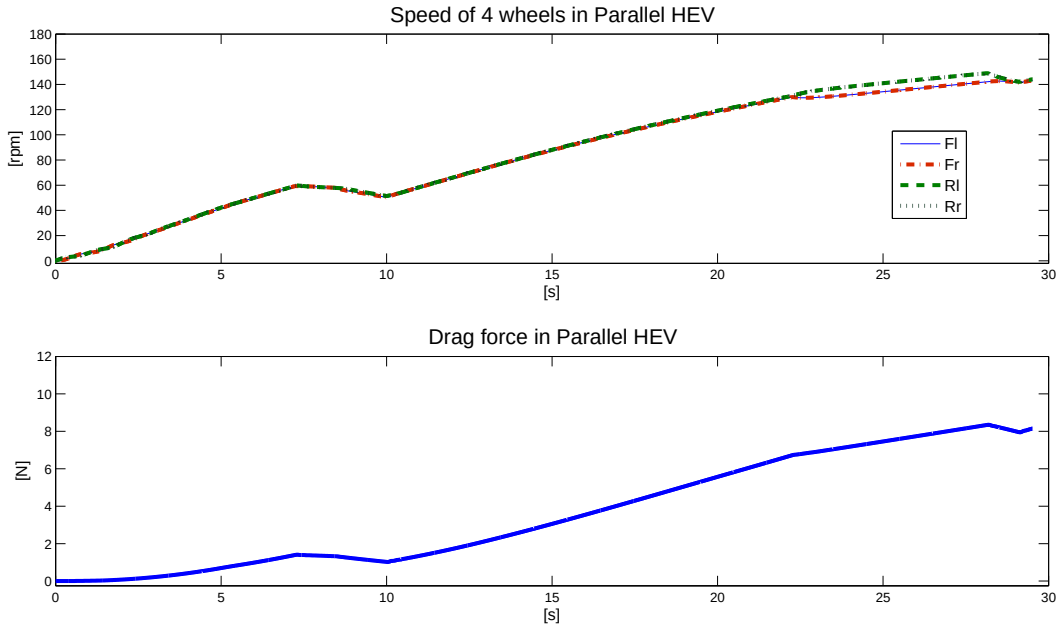

Figure 4.31: Tyres (4) speed and drag force in P HEV

Figure 4.32 shows the F_z and F_x acting on the vehicle's tyres. The difference between Figure 4.32 and (Figure 4.11, Figure 4.21) is that, the F_z acting on the front tyres decrease and increase slightly compare to the same results in others Figures (4.21, 4.11). The same remarks can be observed on the F_z acting on the rear tyres. The value of F_z in Figure 4.32 is small compared to the results in Figure 4.11 and Figure 4.21. The reason of the forces decreasing and increasing was explained previously in the same Section of previous power-train study. The lower plot: the dashed line is the F_x acting on the rear tyres. The solid line is the F_x acting on the front tyres of the vehicle. Notes that this behaviour of the tyres at the beginning is expected. This instability is due to the power-train control strategy, which needs to be configured appropriately for the P HEV power train.

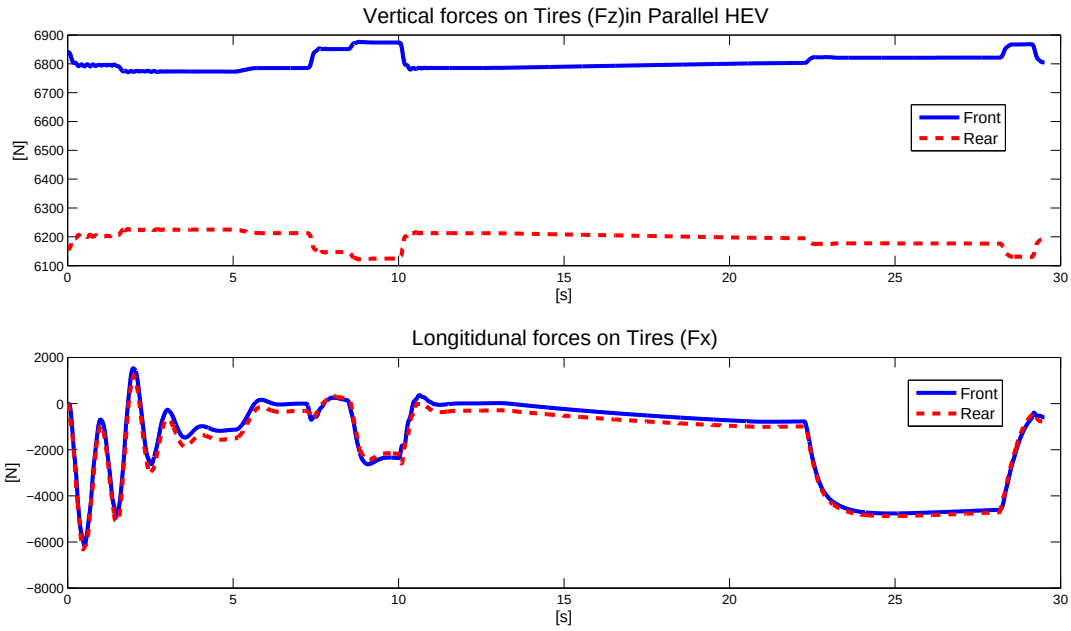

Figure 4.32: Vertical and longitudinal forces on P HEV tyres

Remarks 4.7

The proposed power-train control for the P HEV power-train really needs to be reviewed. Also the power-train components specifications needs to be reconsidered as well. The vehicle is not very stable on the road (because of the tyre behaviour) and it is not likely to be driveable under the proposed power train-control method.

4.4 Simulation results for FC HEV

This Section presents the simulation results of the FC HEV power-train under control strategy, which is proposed. The results such as the driver acceleration profile and the proposed power-train control strategy performance are discussed. Then the flow of energy through this FC HEV power-train and how the vehicle is handling on the road are subsequently analysed.

4.4.1 Acceleration and vehicle speed in FC HEV

This Section deals with the driver acceleration profile, the vehicle speed on the straight line road and the high voltage battery state of charge.

Figure 4.33 displays on the upper plot the acceleration profile of the driver during $30s$. Note that this profile is the same, which was used in the previous simulations. The middle plot is the vehicle speed in $[km/h]$. When the driver brakes (a negative acceleration) the vehicle speed decreases, it is observable in the intervals [8 10]s and [22 28]s. The vehicle speed here reaches $75km/h$. The lower plot is the battery state of charge. The battery SOC decreases in the intervals [0 7]s. Because the battery is the main power source for the EM during that time. The battery SOC starts increasing from $8s$, this is due to the regenerative braking, then the SOC decreases slightly. The reason of such small variation compared to the results in Figures (4.30, 4.19 and 4.9) is that the fuel cells are producing enough electrical power. Therefore, there is no need to use the battery too much. During the regenerative braking all the electric power and the FC extra power go to charge the battery. This is

observable in the interval [22 28]s. The SOC rises above the initial value 46.7%. The dashed line in the middle plot shows the driver speed profile (it is the integration of the acceleration profile). This middle plot demonstrates that the FC HEV speed profile is similar to the driver speed profile, which is the dashed line.

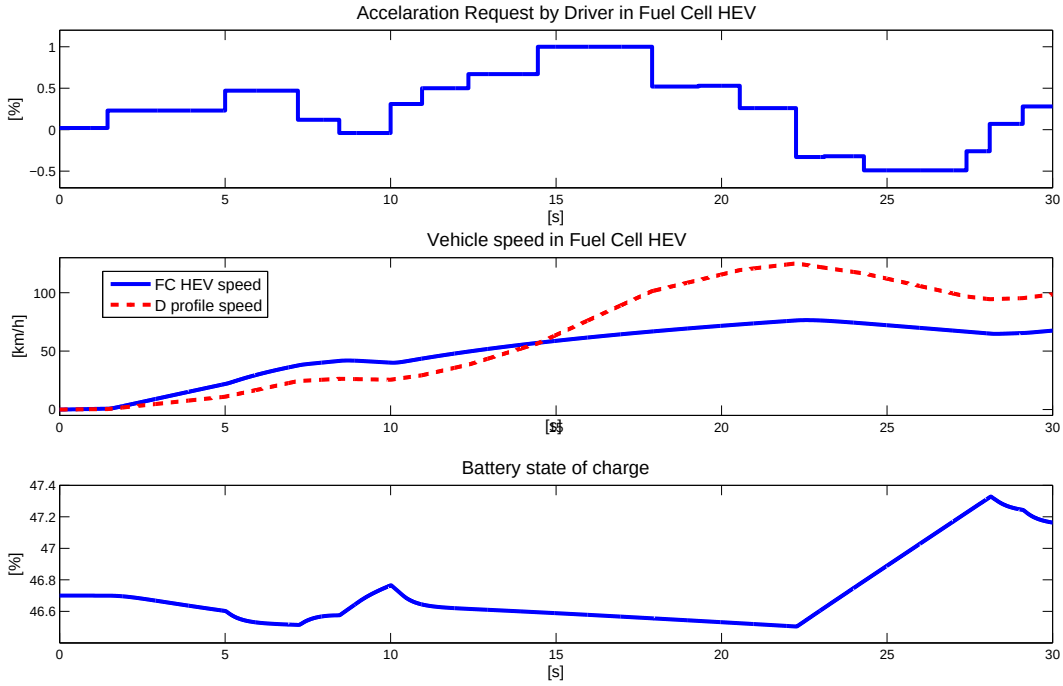

Figure 4.33: Acceleration requested and vehicle speed for FC HEV

Figure 4.34 shows the mechanical and electrical power of the EM. The dashed line is the mechanical power of EM. The full line represents the electrical power of EM. It is the power which EM uses to produce the mechanical power to drive the vehicle. Note that the mechanical power curve is below the electrical power curve. This demonstrates that there are losses during the power conversion from electrical to mechanical. This problem can be addressed by improving the components (the EM) controller and the model.

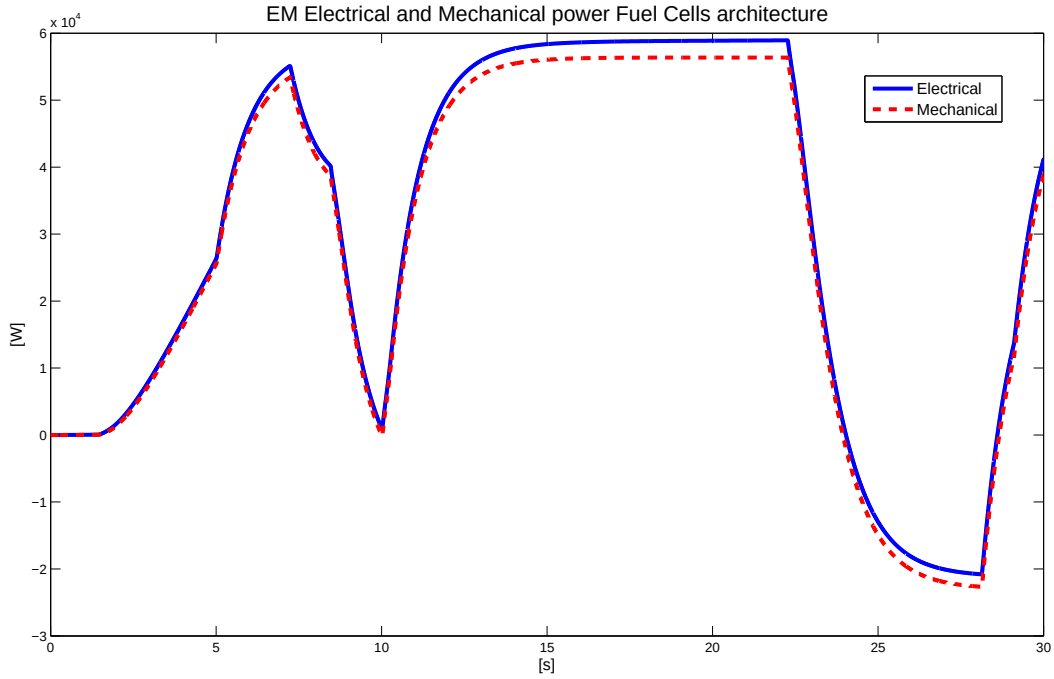

Figure 4.34: EM power (mechanical and electrical) comparison in FC HEV

4.4.2 Controller performance in FC power-train

This Section discusses the robustness of the proposed power-train control. Within the proposed FC HEV power-train the supervisory controller outputs are $u_5(t)$ and $u_6(t)$. Note that this control strategy controls only the EM torque ($u_5(t)$) and the FC produced current (by controlling the reaction), is the control $u_6(t)$.

Figure 4.35 shows the EM torque in $[Nm]$ and the FC current in $[A]$. The upper plot: the solid line is the reference torque defined by the supervisory controller for the EM. The dotted line is the EM actual torque. It is interesting how the component (the EM) controller regulates the EM torque. It is satisfactory result. The lower plot: the solid line is the reference current defined by the master controller. The dashed line is the actual current, which is produced by the FC reaction. The component controller needs to be optimised. Nevertheless, the results is satisfactory.

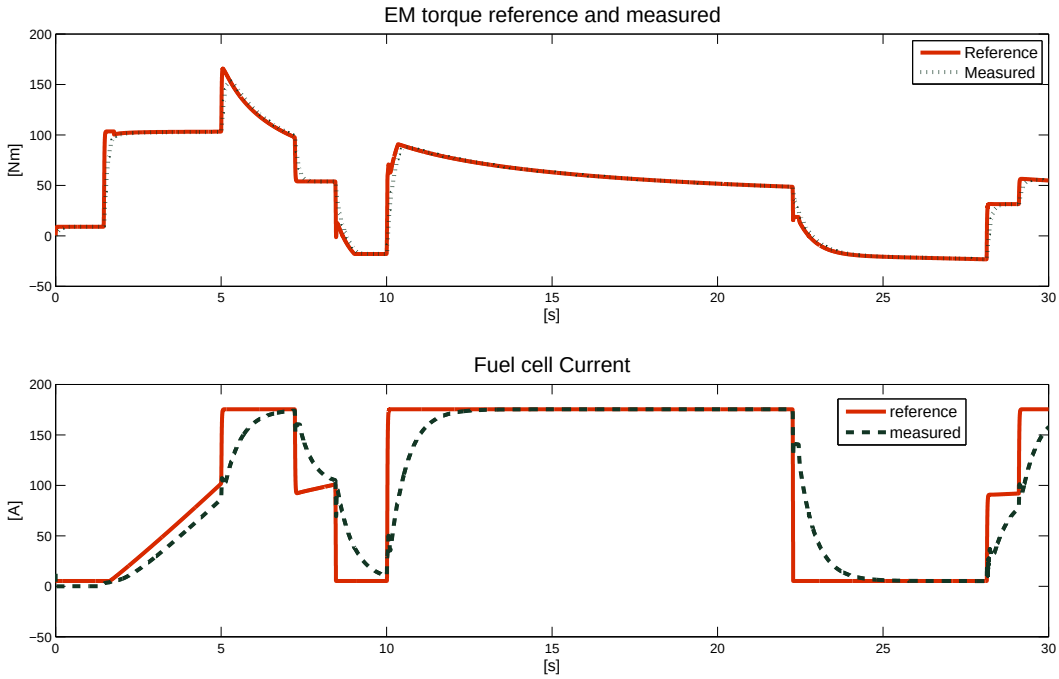

Figure 4.35: Supervisory control and component control performance for FC HEV

4.4.3 Power and energy flow in FC HEV

This Section deals with the flow of power and torque through the proposed FC power-train, under the proposed power power-train control.

Figure 4.36 shows the power flow through the power-train. The requested power is the solid line. The dashed line is the EM power, which drives the vehicle. The dashed and dotted line is the battery power. It starts providing power to the EM. That is the reason why the SOC decreases at the beginning of the simulation. The battery produces a small amount of power to compensate the FC power in the dotted line, to the EM, until the FC starts producing enough power. The extra FC power goes to the battery. This is observable in the interval [22 28]s.
Figure 4.37 shows the Section termed 'zoom fc1(fuel cells 1)', which is presented in Figure 4.36. It shows clearly the evolution the flow of power on this FC HEV drivetrain.

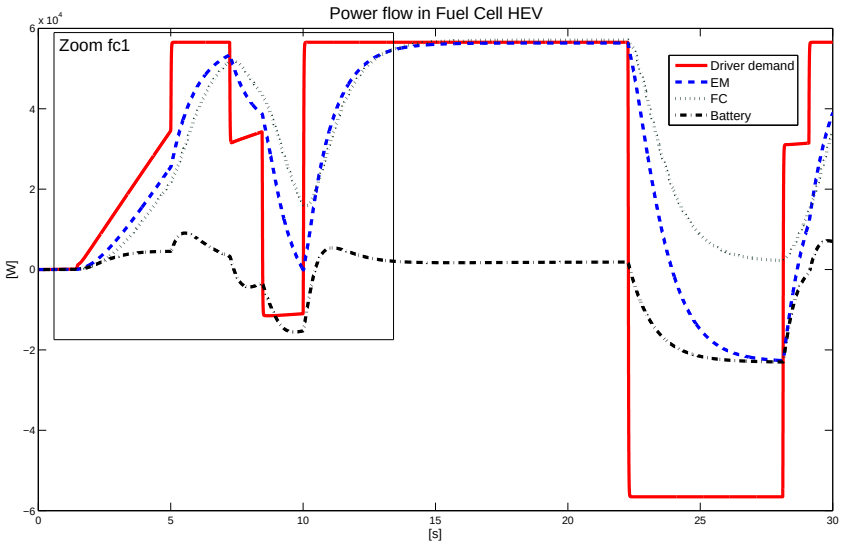

Figure 4.36: Flow of power (electrical and mechanical) in FC HEV

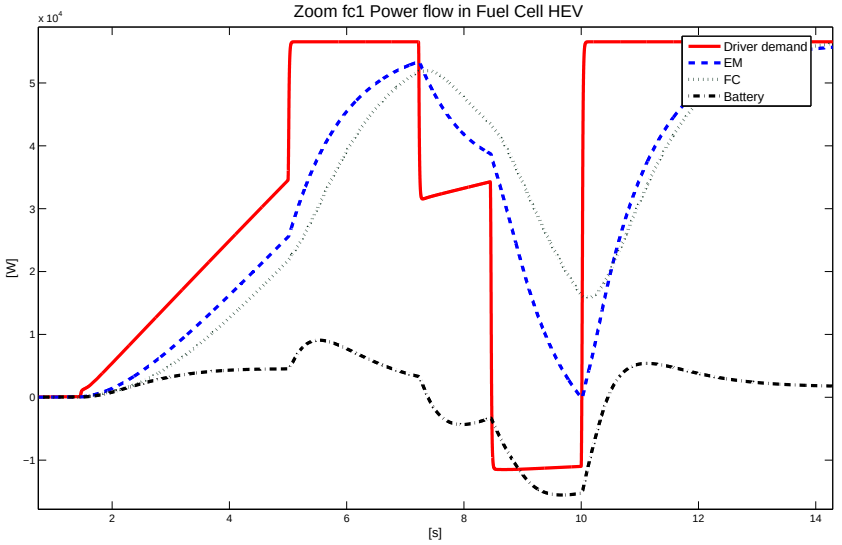

Figure 4.37: Zoom fc1, Flow of power (electrical and mechanical) in FC HEV

Figure 4.38 displays the flow of torque through the FC HEV power-train. The solid line is the requested torque from the driver. The dashed line is the EM torque defined by the master controller. The dotted line corresponds to the EM actual torque which drives the vehicle. Figure 4.39 shows the zoom fc2, which is presented in Figure 4.37. Note that the EM torque is not matched to the driver requested torque. But the result is satisfactory. However it needs to be optimised.

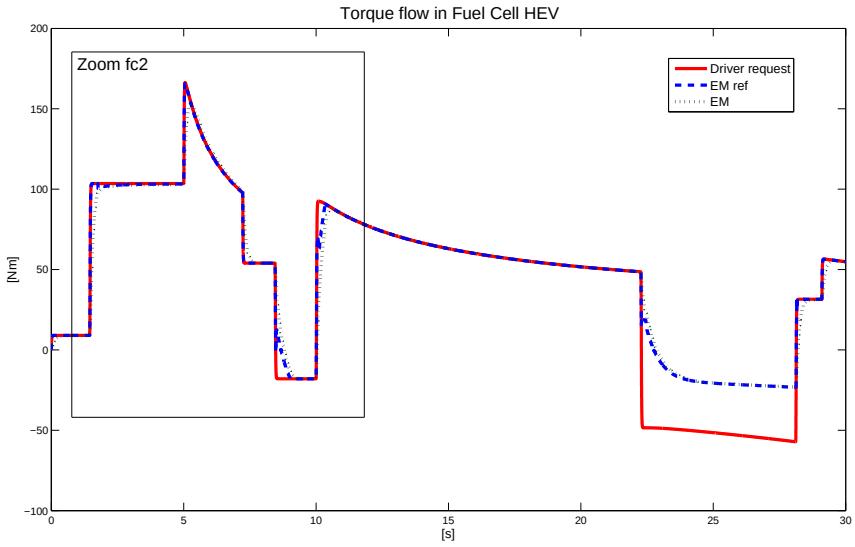

Figure 4.38: Flow of torque (electromagnetic and mechanical) in FC HEV

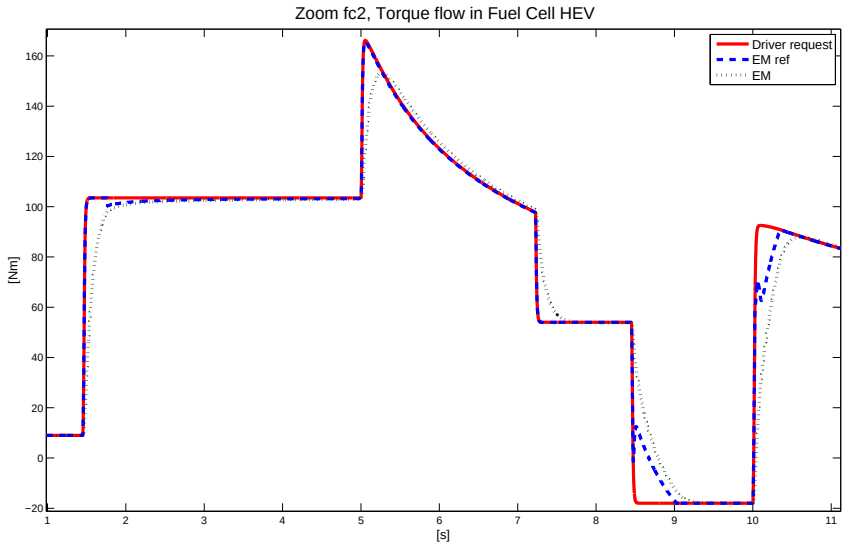

Figure 4.39: Zoom fc2, Flow of torque (electromagnetic and mechanical) in FC HEV

4.4.4 Vehicle dynamics information in FC HEV power-train

This Section deals with the vehicle handling, where the forces acting on the tyres and the tyres speed are discussed.

Figure 4.40 shows on the upper plot, the speed of the four wheels of the vehicle in $[rpm]$. The four wheels have approximately the same speed. The lower plot is the drag force (F_d). Note that the F_d and the wheels speed in Figure 4.40 are the biggest (in term of value) of all four simulations results (Figure 4.10, Figure 4.20, Figure 4.31 and Figure 4.40). F_d is proportional to the vehicle speed.

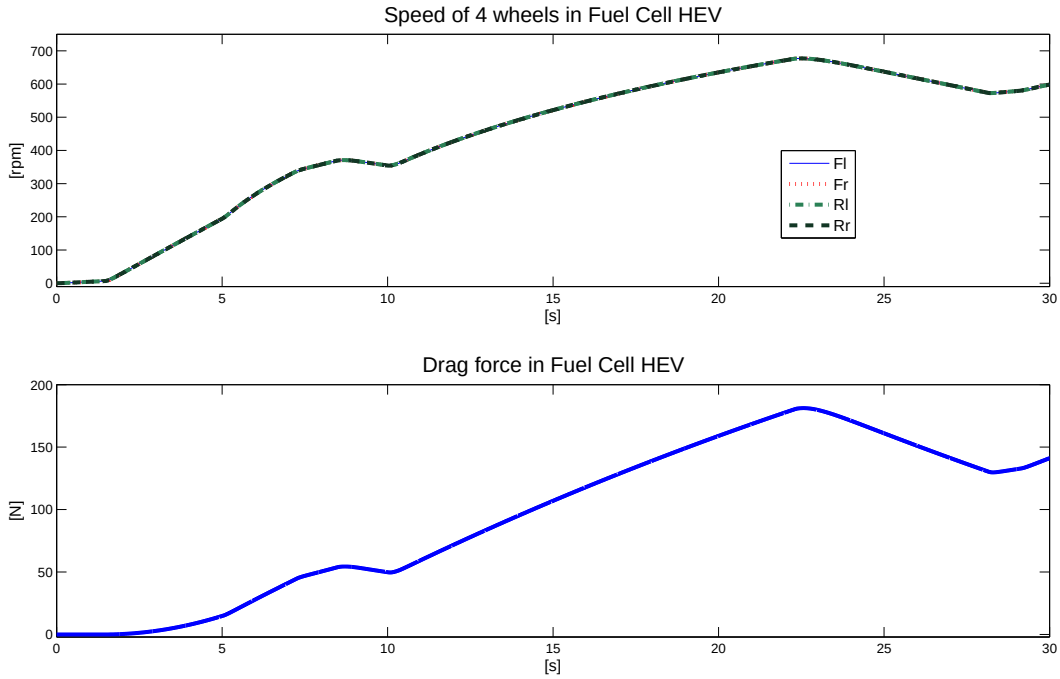

Figure 4.40: Tyres (4) speed and drag force in FC HEV

Figure 4.41 shows the F_z and the F_x acting on the vehicle's tyres. The upper plot: the solid line is the vertical forces acting on the two front tyres of the four wheels vehicle. The dashed line is the vertical forces acting on the two rear tyres of the vehicle. The F_z acting on the front tyres are larger in value than those acting on the rear tyres, because the front of the vehicle weighs more than the rear. At high speed in $[10\ 22]s$ the value of the F_z acting on the front tyres increases, whereas the value of the F_z acting on the rear tyres decreases. The lower plot: the dashed line is the F_x acting on the rear tyres. The solid line is the F_x acting on the front tyres of the vehicle. These forces decrease and stay constant, with negative value, when the driver brakes. Note that F_x acting on the rear tyres when braking is slightly larger (in value) than the F_x acting on the front tyres. The difference between the results in Figure 4.41 and (Figure 4.11, Figure 4.21 and Figure 4.32) are the smoothness of the F_z result in Figure 4.41. The oscillation of F_x at the beginning is decreased.

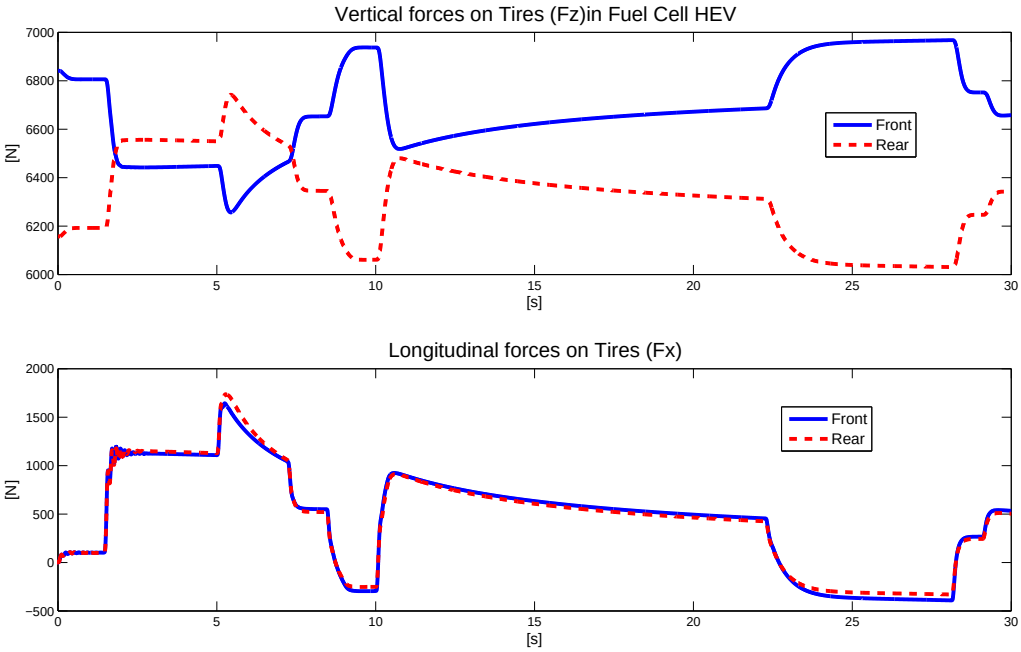

Figure 4.41: Vertical and longitudinal forces on FC HEV tyres

Remarks 4.8

The power-train control proposed for this FC HEV power-train shows an interesting result, in term of the flow of power and the vehicle handling.

4.5 Conclusions

This chapter has shown the simulation results of the four proposed HEV power-trains under the proposed power-train control strategies. The results were satisfactory for the PS HEV and the FC HEV power-train.

For the S HEV and the P HEV, the results were less satisfactory. In order to address that problem the power-train control strategy has to be reassessed appropriately for the S HEV and the P HEV.

The computer simulation results have highlighted the goals set in this research which are basically to drive the HEV with EM for as long as possible and reduce the use of the ICE for as long as possible (the flow of power results have gone some way to explained this). The goal is also to assure the driveability and stability of the HEV on the road (the vehicle dynamics results have explained this). In effect these computer simulation results have covered the supervisory control actions and the power-train control actions, without forgetting the subsystems control actions to the four-wheel drive HEV handling on the road. Some of the results are more satisfactory than others. This may be due to different incertitude for example accuracy in modelling and controller tuning. Incertitude such as the the accuracy of subsystems (Simulink blocks in Simscap, SimPowerSim tools box) cannot be ignored. Additionally the proposed power-train controller parametrization and tuning difficulty cannot be ignored either. Further work is required in order to properly tune the proposed power-train controller for a given specific HEV power-train.

Table 4.1 summarises the simulation results, and aims to qualify the results of the four different HEVs under a proposed power-train control platform. The results in Table 4.1 give some idea about what is required for improving the computer simulation results which are presented in Chapter 4.

Table 4.1: Comparison of simulation results for various HEV power-trains under the proposed power-trains control strategies

	PS HEV	**S HEV**	**P HEV**	**FC HEV**
Control	satisfactory results: supervisory and components level as well	satisfactory results: supervisory and components level as well	satisfactory results: supervisory and components level as well	satisfactory results: supervisory and components level as well
Stability and Driveability	quite satisfactory results	satisfactory results	unsatisfactory results	quite satisfactory results
Need to be done	optimised: the supervisory controller and components models	reconfigured: the supervisory and components controllers optimised the components models	reconfigured the supervisory and components controllers optimised the components models	optimised: the supervisory controller and components models

Chapter 5

Conclusions and further work

The main topic addressed by this thesis is the power-train control of four different HEV configurations. The implementation of the four approaches in Simulink has been satisfactory carried out, and has led to a valuable library of modules which can now be used by other researchers. The goal was to control the flow of power in the HEV power-trains and observe the stability and driveability of the vehicle on road, by designing a re-configurable power-train controller, which can be plugged into different HEV power-trains.

The goals were achieved in a step by step manner. Firstly the knowledge of various HEV power-trains architectures needed to be reviewed in order to propose different HEV power-trains models. A review of the different components (energy storage) such as battery, electric motors as well as the different control strategies was conducted. Combining this knowledge, different power-trains control methods were proposed. From the literature review, four different HEV power-trains models, were implemented in Simulink. The Simulink tools box such as SimPowerSystem,

SimDriveline, SimMechanics were used for modelling the components. In order to achieve the goal set in this research, which is power-train control and design for a stable and driveable HEV, the supervisory control strategy (the master controller), has been proposed. This controller defines the reference input to each subsystem component controller (subsystem for example EM torque). The supervisory controller also enables or disables each component (subsystem) activity. A PID controller is used to control each subsystem at the component level. The PID controllers are manually tuned.

The proposed re-configurable power-trains control strategies were initially configured for the PS HEV and FC HEV power-trains. But as the S HEV and P HEV are ICE based HEV, such as the PS HEV they were also included. It was acknowledged that the latter investigation was simplified, and the results were not so satisfactory. As consequence, further work is still required. The results of the ICE based HEV power-trains under the proposed power-train control are:

- For the PS HEV, the results were reasonably satisfactory in terms of control. Because the components controllers reach their goals (components outputs follow the reference defined by the master controller), the results were presented in Figure 4.3 and Figure 4.4 . The vehicle stability and driveability results were presented in Figure 4.11 and Figure 4.12 were also quite satisfactory. Finally Figures (4.5 to 4.8) show that an EM ran a four-wheel drive PS HEV for as long as possible. This will allow maximum fuel economy because the ICE is not running all the time. This will also allow minimum emission of pollutants because the ICE was inactive in the first $3s$ in the simulation.

- For the S HEV, the results were satisfactory in terms of control. Because the

components controllers reach their goals (components outputs aim to follow the reference), these results were presented in Figure 4.14. The vehicle stability and driveability results were also satisfactory. But not as good as in the PS HEV. These results were explained in subsection 4.2.5. Finally in the S HEV the ICE is used all the time, therefore both the emission of pollutants and fuel economy will not be optimal.

- For the P HEV, the results were less satisfactory in term of control. In effect, as subsection 4.3.2 has explained. The vehicle stability and drivability results were unsatisfactory, this can be seen directly in Figure 4.32. Finally in this four-wheel drive P HEV the ICE is used all the time, therefore as for the S HEV both the emission of pollutants nor fuel economy will not be optimal.

The results of the FC HEV under the proposed power-train control method:

- For the FC HEV, the results were interesting in terms of control. Because the components controller reach their goals. The components outputs follow the reference. The vehicle stability and driveability results were quite satisfactory as well. Here as only the EM drives the four-wheel drive FC HEV, there are zero emissions.

The re-configuration process for one particular HEV power-train requires for work to be carried out to achieve better results. The advantage of this re-configurable power-train controller is that it can be plugged into different HEV power-trains and provides a valuable modular approach, which can be built upon and used by other researchers in the future.

Further Work

Although this work has been focused mainly on power-train control, it would be interesting to improve the overall design and control (supervisory and component).

Design and modelling

For the design and modelling perspective:

- Firstly, clutch and transmission model need to be integrated to the model. The transmission can be manual or automatic. But it is better to start with manual by using Simulink black box.
- Second the auxiliary (radio, windows, etc.) power consumption model needs also to be added to the model. The idea is to see how these auxiliary powers affect the system as whole.
- Third, the model of a Super-capacitor (Ultra-capacitor) to replace the battery could be a welcome.
- Finally it will be useful to convert the European driving cycle (speed) into acceleration profile.

Control

For control perspective:

The incremental PID can be tested on each controllable component of the HEV power-train. For energy management, controllers such:

- Equivalent Consumption Minimisation Control Strategy (ECMCS) using a model-based instantaneous fuel minimisation technique can be useful for HEV. This

control strategy is mainly based on a cost function of electrical and fuel energies. Its performance is usually improved by adaptively tuning an equivalence ratio between the fuel and electricity. A ratio, which can be tuned according to the driving conditions and corrected as necessary to compensate large deviations in the battery SOC.

- An optimal sliding control can be considered, where it will assume an optimal fixed power demand. If it exists an optimal solution in effect that can satisfy the battery SOC constraint as well. That solution can be obtained by fast switching between the specified operating points of the ICE.
- Finally H∞ controller technique can also be considered for energy management in HEV power-train. However, this strategy can be real challenging, especially the computational times.

Optimisation

For optimisation perspective:

- The supervisory control strategy for each HEV power-train needs to be reviewed, for example by changing certain parameter value to increase the EM reference torque
- Improving the PID
- Testing different battery, with different nominal voltage and current rate
- Re-specified certain component of the power-train, for instance the ICE parameters

Appendix A

Definition 1 : Drivetrain : Also termed power-train, this term describes all of a vehicle's components that produce power and transmit power to the wheels, the engine, transmission, transfer case, drive shafts, differentials, axle shafts and wheel hubs [42].

Definition 2: power-train : group of components (engine, transmission, driveshafts, differentials) that generate power for propulsion purposes and deliver it to the road surface, water, or air [42]

Definition 3: Regenerative braking : The dissipative kinetic energy during braking is recaptured by applying negative torque to the electric motor. Basically it is an energy recovery mechanism, which reduces vehicle speed by converting some of its kinetic energy into a useful form of energy instead of dissipating it as a heat, in a conventional brake. This converted energy is stored for future use or fed into a power system of the vehicle. The amount of regenerative braking torque that can be added to the hydraulic braking torque is calculated by considering the electric motor torque characteristics, vehicle speed [42].

Definition 4 :

$$DOH = \frac{\frac{Battery}{motor(EM)}[kW]}{\frac{Battery}{motor(EM}[kW] + \frac{Engine}{Generator}[kW]} \text{ [43]} \tag{5.1}$$

Definition 5 : Random Markov process : is random process. In this process, there is some indeterminacy in its future evolution described by probability distributions. That means even if the initial condition is known there are many possibilities that the process might go to, but some of that possibility may be more satisfactory than others [44].

Definition 6 : The goal with this controller is to allow the EM producing maximum torque. But the main component of the torque is proportional to $q - axis$ component of the armature current. Therefore, it is convenient to control the inverter-fed PMSM by keeping the direct, d-axis, current component to be $i_d = 0$ as long as the inverter output voltage doesnt reach its limit. At that point, the motor reaches its maximum speed.

Appendix B

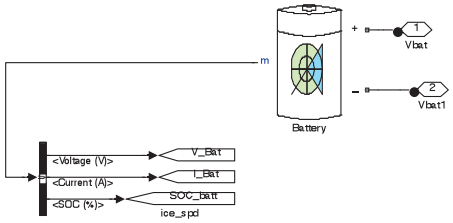

Figure 5.1: High Voltage battery subsystem breakdown

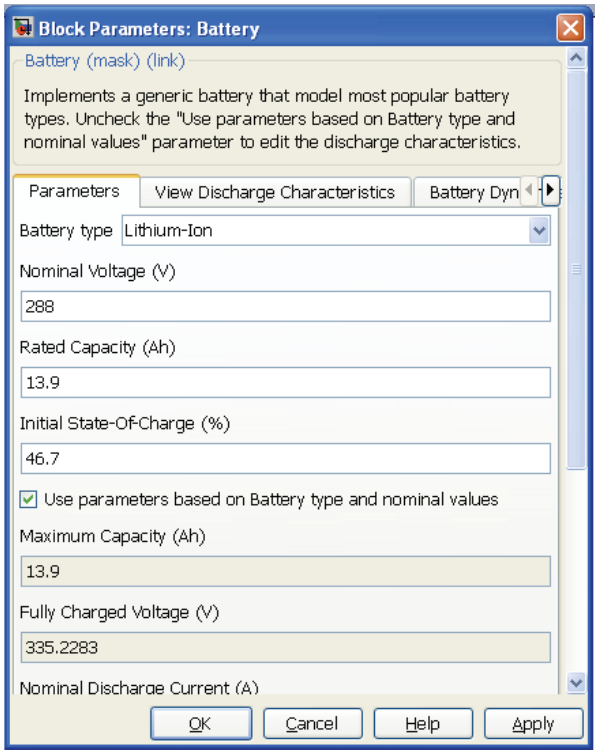

Figure 5.2: Battery configuration interface

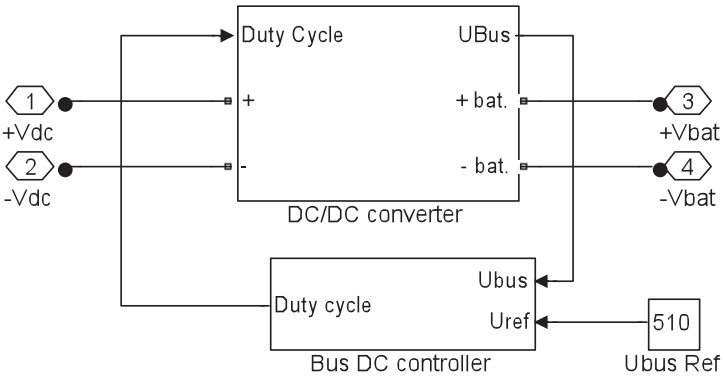

Figure 5.3: DC/DC Converter subsystem breakdown

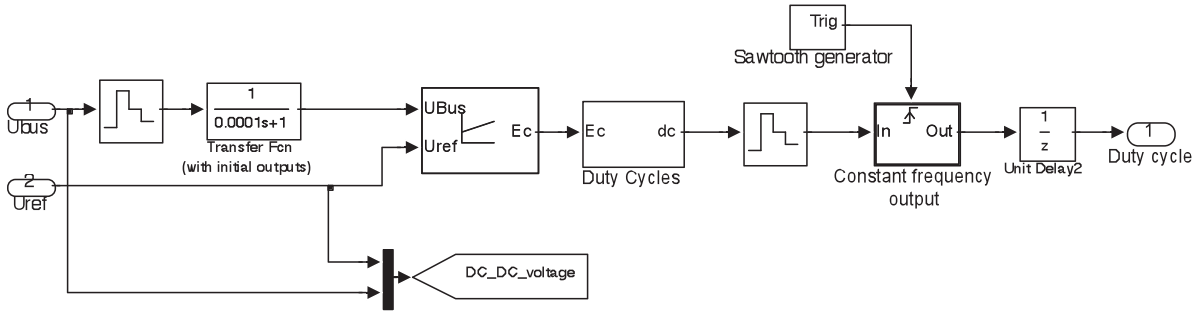

Figure 5.4: Bus DC controller subsystem of the DC/DC Converter breakdown

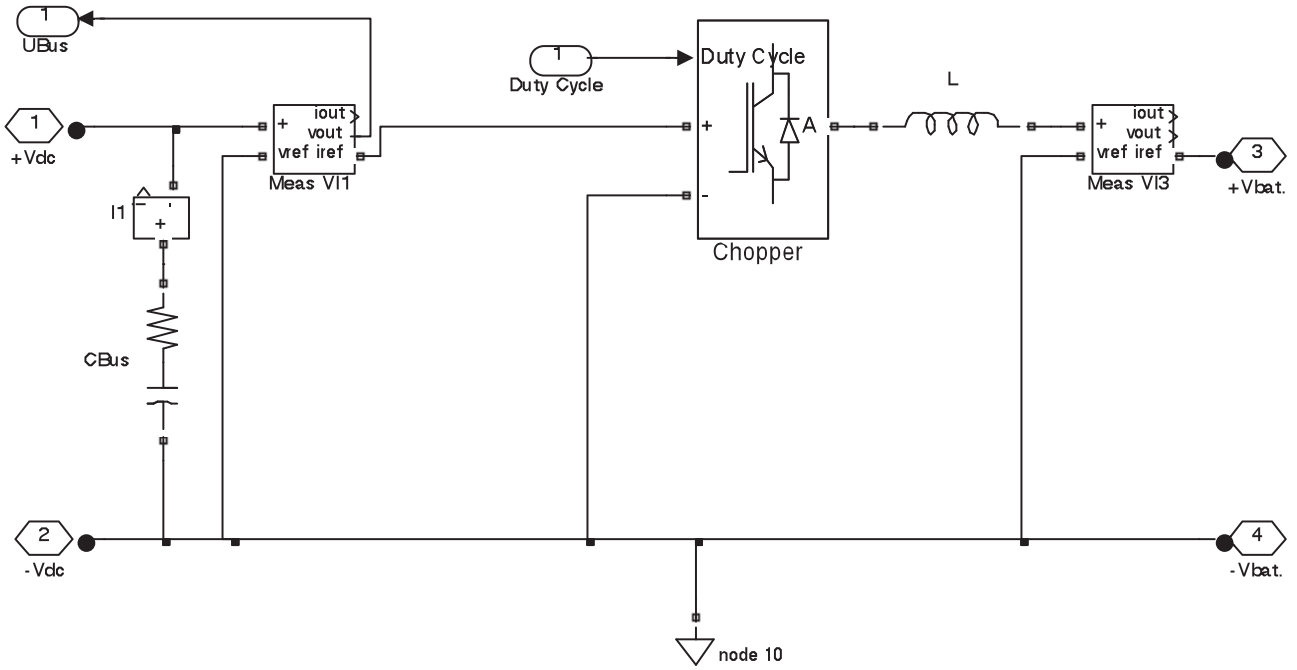

Figure 5.5: DC/DC converter subsystem of the DC/DC Converter breakdown

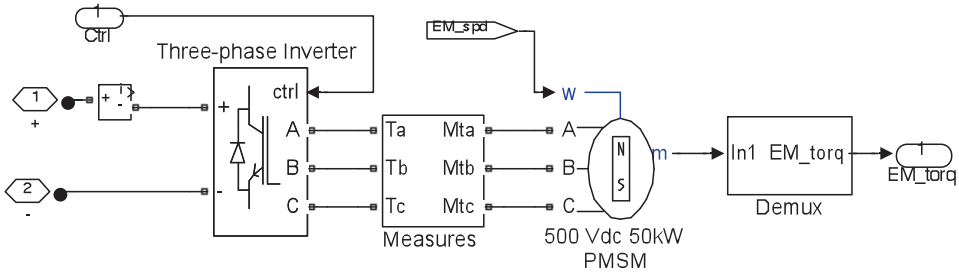

Figure 5.6: EM subsystem breakdown

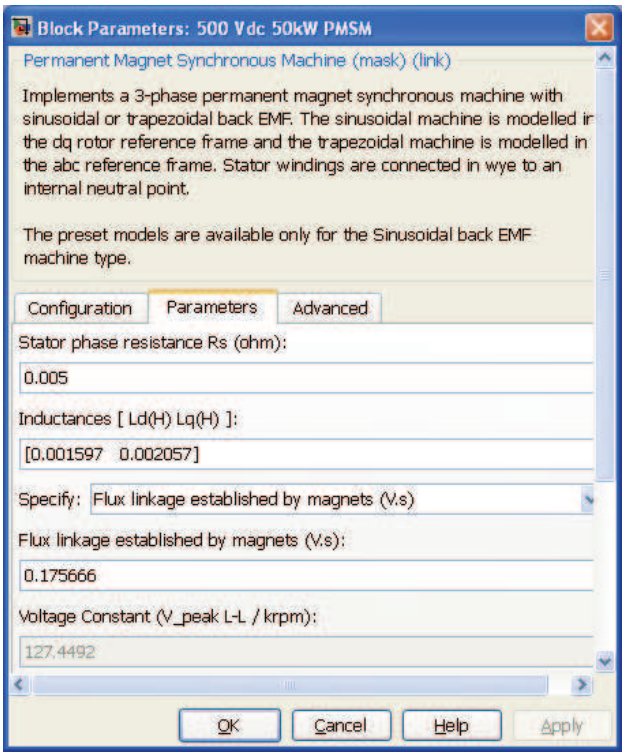

Figure 5.7: EM (PMSM) configuration interface

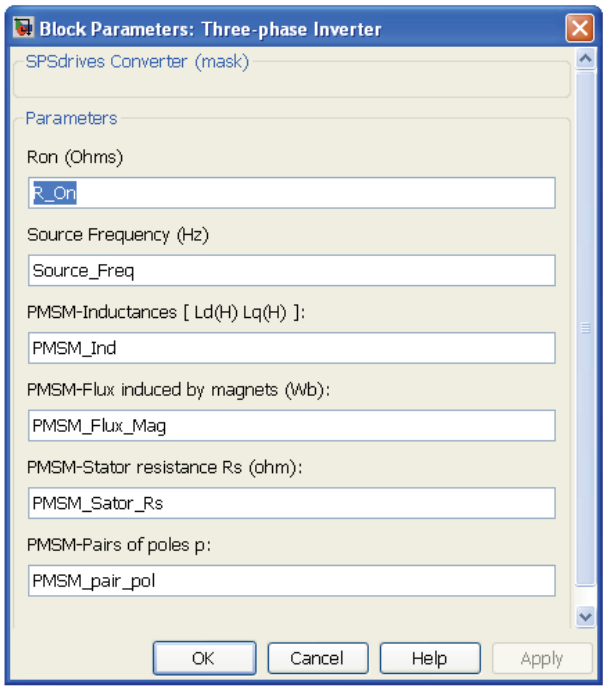

Figure 5.8: EM, three phase inverter configuration interface

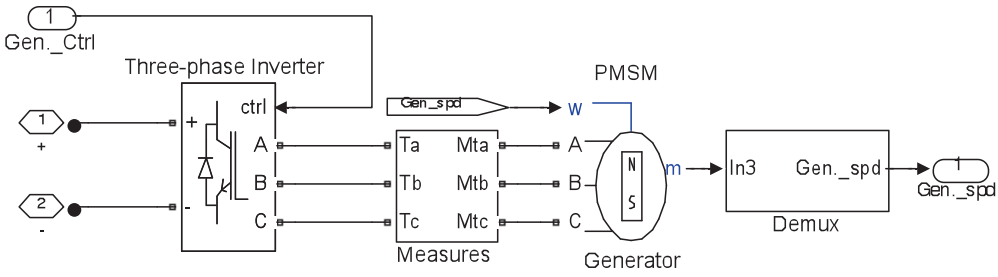

Figure 5.9: Gen. subsystem breakdown

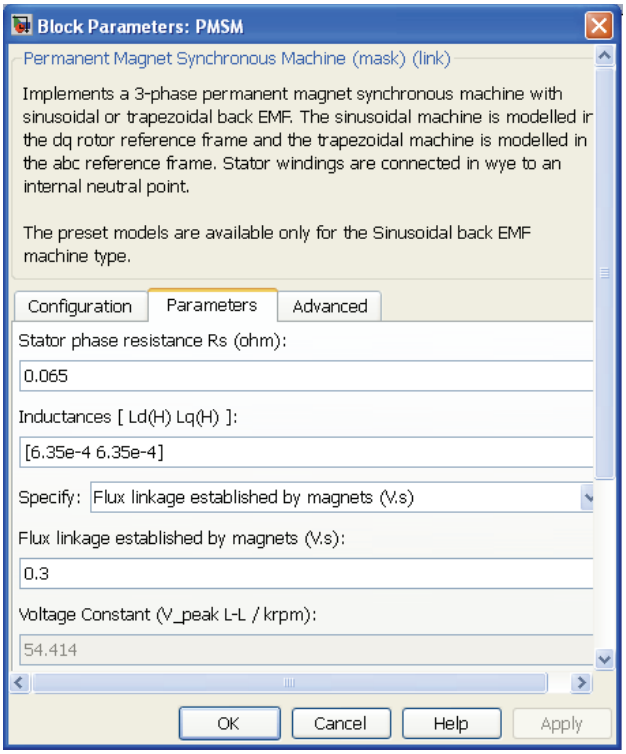

Figure 5.10: Gen. (PMSM) configuration interface

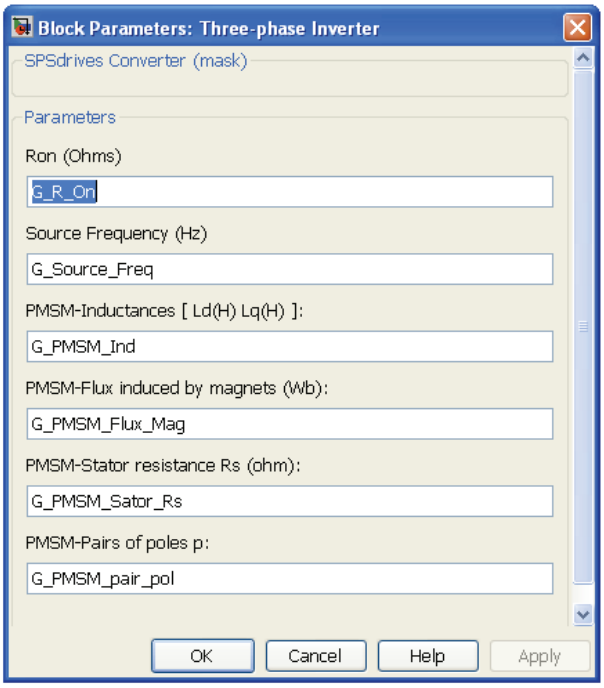

Figure 5.11: Gen., three phase inverter configuration interface

Appendix C

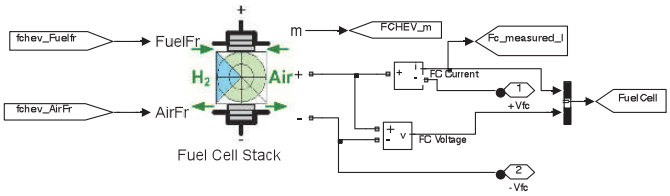

Figure 5.12: FC reaction subsystem breakdown

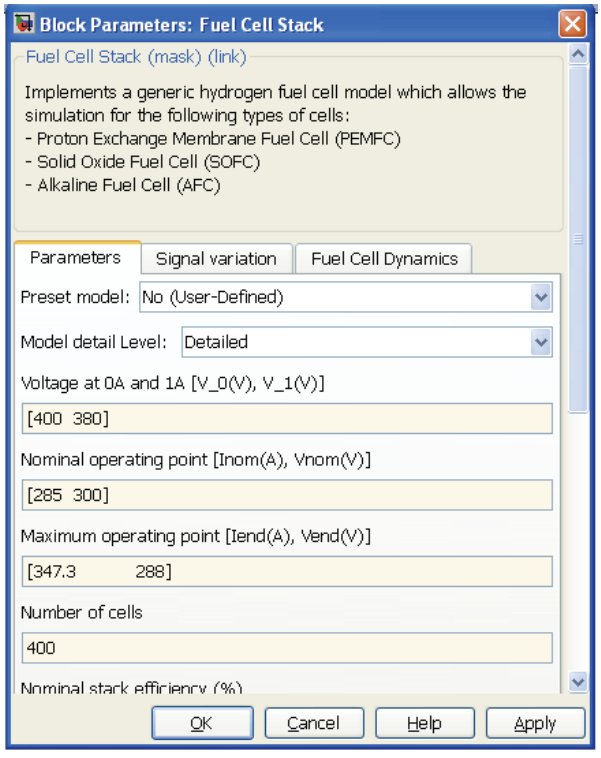

Figure 5.13: Fuel cell Stack configuration interface

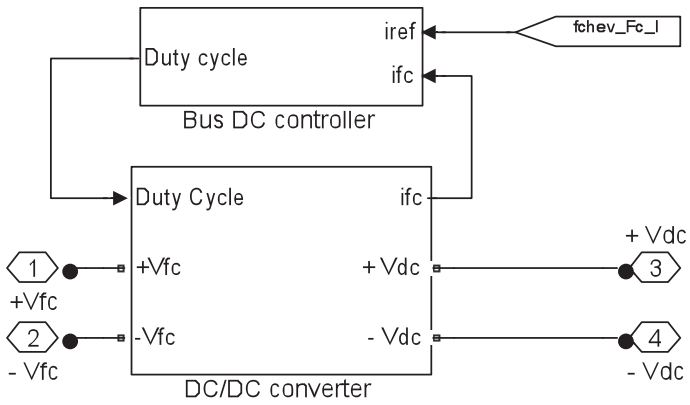

Figure 5.14: FC, DC/DC converter subsystem breakdown

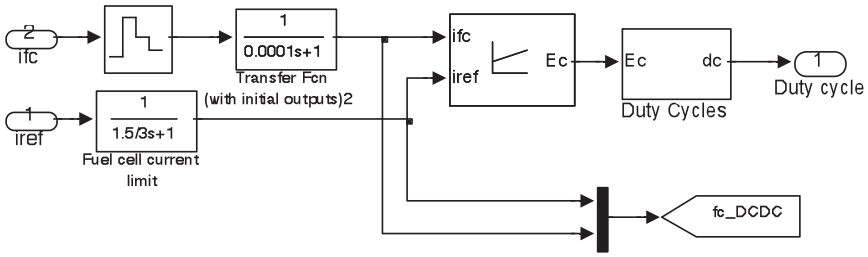

Figure 5.15: FC, Bus DC controller subsystem breakdown

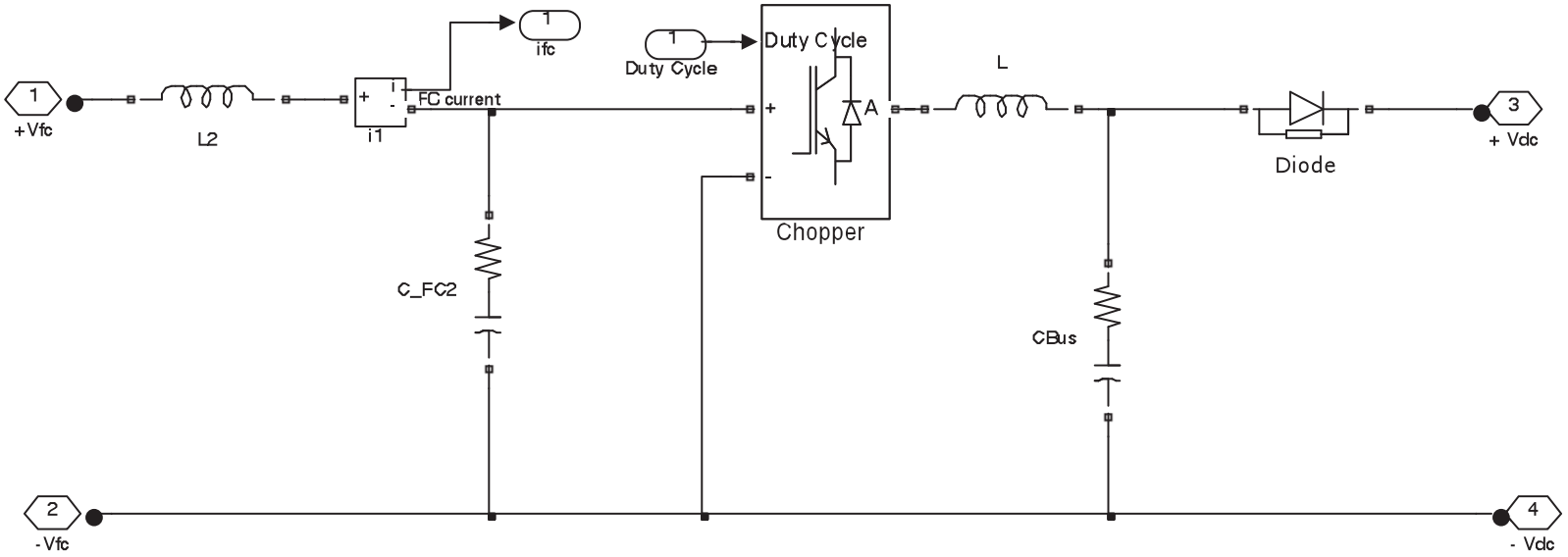

Figure 5.16: FC, DC/DC converter subsystem breakdown

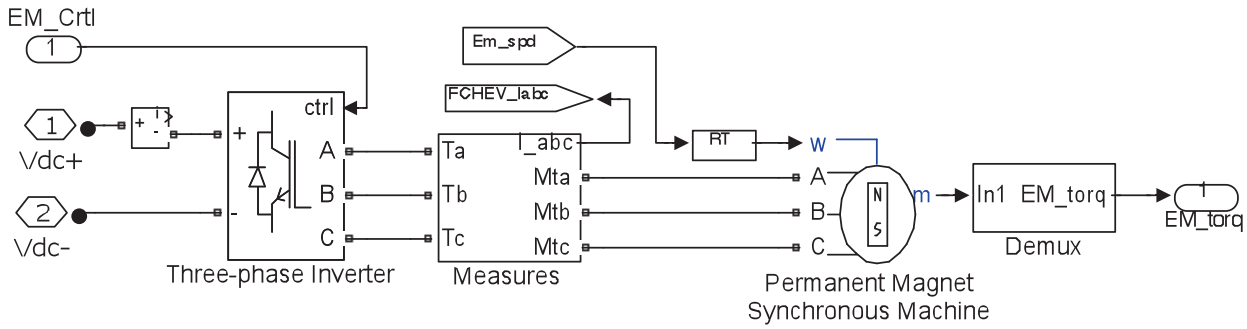

Figure 5.17: FC, EM subsystem breakdown

Appendix D

Control strategy 1

This control strategy is basically an explanation of Equation (3.2) in Chapter 3, which is:

$$u_1(t) = g\{D_P(t), B_P(t)\} \tag{5.2}$$

where g is a function, which takes different functions such as $D_P(t)$ and $B_P(t)$ as inputs to produce the control action $u_1(t)$; $u_1(t)$ is without units.
Here

$$D_P(t) = DriveShaft_{spd}(t)D_T(t) \tag{5.3}$$

where $DriveShaft_{spd}(t)$ is the conversion into $[rpm]$ the total torque which drives the four wheels of the HEV, and

$$D_T(t) = sign(Acc_{Req}(t))Min(Max_T, actual_T(t)) \tag{5.4}$$

with

$$actual_T(t) = \frac{Driving_{spd}Max_T}{Driving_{spd} \leq |\frac{Acc_{Req}60}{2\pi}| < \infty} \tag{5.5}$$

where $Driving_{spd}$ is a constant in $[rpm]$.
The implementation in Simulink is given in Figure 5.18.

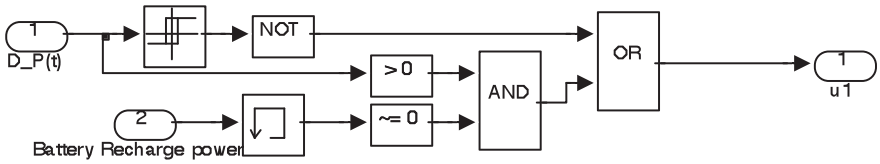

Figure 5.18: Simulink implementation of $u_1(t)$

Here the 'Battery Recharge power' is calculated as shown in Figure 5.19.

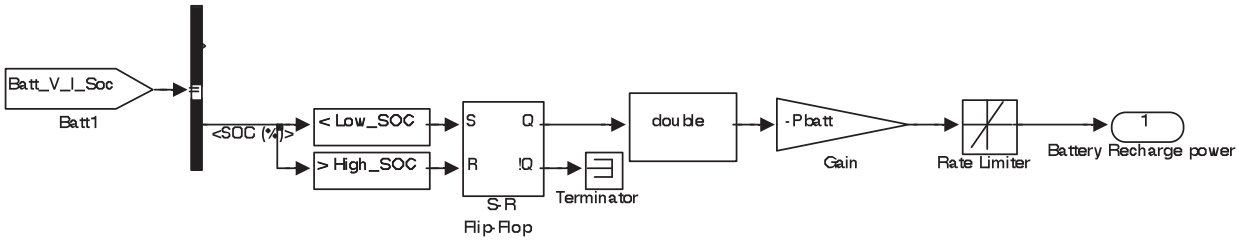

Figure 5.19: Simulink implementation of Battery Recharge power

Control strategy 2

This control strategy is an explanation of (3.3) in Chapter 3, which is:

$$u_2(t) = h\{D_P(t), Em_{spd}(t), Ep(t)\} \tag{5.6}$$

This (5.6) is basically the following equation.

$$u_2(t) = \frac{Batt_{pow}(t) + Gen._{pow}(t)}{EM_{spd}(t)} \tag{5.7}$$

where

$$Batt_{pow}(t) = Batt_{Recharge_{pow}}(t) + Batt_{Ref_{pow}}(t) \tag{5.8}$$

with

$$Batt_{Ref_{pow}}(t) = \Delta_{ICE_{pow}}(t) - \Delta_{ICE\_Tork} ICE_{spd}(t) \tag{5.9}$$

Here $-a \leq \Delta_{ICE_{pow}}(t) \leq a$ and a is a constant in $[W]$ and

$$\Delta_{ICE_{pow}}(t) = D_P(t) - Batt_{Recharge_{pow}}(t) \tag{5.10}$$

and

$$\Delta_{ICE\_Tork}(t) = \frac{\Delta_{ICE_{pow}}(t)}{ICE_{spd}(t)} \tag{5.11}$$

finally

$$Gen._{pow}(t) = [Gen_{spd}(t)\Delta_{ICE\_Tork}(t)]l\% \tag{5.12}$$

where l is a constant without units.

Control strategy 3

This control strategy is an explanation of Equation (3.6) in Chapter 3, which is:

$$u_3(t) = [\Delta_{ICE\_Tork}(t)]l\% \tag{5.13}$$

where l is a constant without units.

Control strategy 4

This control strategy is the explanation of (3.7) in Chapter 3, which is:

$$u_4(t) = [\Delta_{ICE_{spd}}(t)]\nu\% \tag{5.14}$$

Where $spd_1 \leq \Delta_{ICE_{spd}}(t) \leq spd_2$ and spd_1 and spd_2 are constant in $[rpm]$ and ν is a constant without units.

Note that $\Delta_{ICE_{spd}}(t)$ is a look up table. It implemented in Simulink as is shown in Figure 5.20.

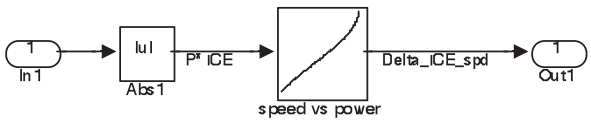

Figure 5.20: Power-split HEV Simulink implementation of $\Delta_{ICE_{spd}}(t)$

Control strategy 5

This control strategy is an explanation of Equation (3.9) in Chapter 3, which is:

$$u_5(t) = \Phi\{D_T(t), B^*_{Fcp}(t), Fc_P(t), Em_{spd}(t)\} \tag{5.15}$$

This (3.9) is basically the following Equation.

$$u_5(t) = \frac{Fc_P(t) + FcBatt_{pow}(t)}{EM_{spd}(t)} \tag{5.16}$$

where $u_5(t)$ is in $[rpm]$ and (3.12) corresponds to:

$$Fc_P(t) = V_{Fc}(t)I_{Fc}(t) \tag{5.17}$$

where $I_{Fc}(t)$ and $V_{Fc}(t)$ are, respectively, the fuel cell current and voltage produced by proton exchange electrochemical reaction.

$$FcBatt_{pow}(t) = (D_P(t) - Batt_{Recharge_{pow}}(t) - Fc_P(t) \tag{5.18}$$

Control strategy 6

This control strategy is an explanation of (3.13) in Chapter 3, which is basically a look up table as is shown in Figure 5.21.

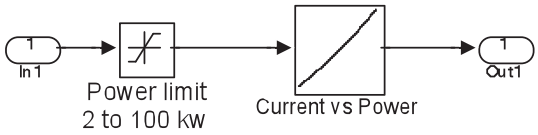

Figure 5.21: Power-split HEV Simulink implementation of $u_6(t)$

References

[1] **Yuliang Leon Zhou**. 2007, *Modeling and simulation of hybrid electric vehicles*, thesis, master of applied science, University of Victoria

[2] **Yusuf Gurkaynak**. 2007, online visited 03/2010, *Adaptive Energy Management of Hybrid and Plug-in Hybrid Electric Vehicles Using Artificial Intelligence* , literature review and research on the PhD disertation

[3] **Karen L. Butler, Mehrdad Ehsani, Preyas Kamath**. November 1999, *A Matlab-Based Modeling and Simulation Package for Electric and Hybrid Electric Vehicle Design*, IEEE transactions on vehicular technology, vol. 48, No. 6, pp 1770-1778

[4] **A.N.F.A.** 1997, online, visited 03/2010, *Le vhicule lectrique*, dossier technique

[5] **H Lee, H Kim**. 23 August 2004, *Improvement in fuel economy for a parallel hybrid electric vehicle by continuously variable transmission ratio control*, School of Mechanical Engineering, Sungkyunkwan University, Suwon, South Korea, pp. 43-51

[6] **Jeffrey Gonder. Tony Markel**. April 16-19, 2007, *Energy Management Strategies for Plug-In Hybrid Electric Vehicles*, National Renewable Energy Laboratory, NREL/CP-540-40970. Posted with permission. Presented at the 2007 SAE World Congress, Detroit, Michigan

[7] **G-Q Ao, J-X Qiang, H Zhong, X-J Mao, L Yang, and B Zhuo**. 3 June 2008, *Fuel economy and NOx emission potential investigation and trade-off of a hybrid electric vehicle based on dynamic programming*, Institute of Automotive Electronic Technology, Shanghai Jiao Tong University, Shanghai, Peoples Republic of China. Proc. IMechE Vol. 222 Part D: J. Automobile Engineerin, pp 1851- 1864

[8] **D-H Kim, J-M Kim, S-H Hwang, and H-S Kim**. 13 July 2007, *Optimal brake*

torque distribution for a four-wheel-drive hybrid electric vehicle stability enhancement, School of Mechanical Engineering, Sungkyunkwan University, Suwon, Republic of Korea

[9] **Ivan Arsie, Marco Graziosi, Cesare Pianese, Gianfranco Rizzo, Marco Sorrentino**. *Optimization of Supervisory Control Strategy for Parallel HybridVehicle with Provisional Load Estimate*, department of Mechanical Engineering - University of Salerno, pp 483-488

[10] **N. Bhoopal, G. Venu Madhav, and Dr. J. Amarnath**. November 2009, *DSP Based Control Hybrid Electric Vehicle*, institute of Technology, Dept. of EEE, Narsapur, Medak, Andhra Pradesh, India. International Journal of Recent Trends in Engineering, Vol 2, No. 8

[11] **Yann Guezennec, Giorgio Rizzoniand Gabriel Choi**. April 3- 4, 2003, *Supervisory Control of Fuel Cell Vehicles* , presentation powerpoint, Ohio State University Center for Automotive Research

[12] **Mohsen Mohammadian , Mohammad Taghi Bathaee**. 2005, *Motion control for hybrid electric vehicle*,K.N.Toosi University of Technology Tehran, Iran

[13] **Sylvain Pagerit, Aymeric Rousseau, Phil Sharer**. online visited 02/2010, *Global Optimization to Real Time Control of HEV Power Flow: Example of a Fuel Cell Hybrid Vehicle*

[14] **W. Lhomme, Ph. Barrade, Ph. Delarue, A. Bouscayrol**. 2-6 April 2005, *Maxximum control Structure of a series hybrid electric vehicle using supercapacitors*

[15] **Steven J. Boyd**. August 28, 2006, *Hybrid Electric Vehicle Control Strategy Based on Power Loss Calculations*, thesis Master of Science Mechanical Engineering, Virginia Polytechnic Institute and State University

[16] **Kerem Koprubasi**. 2008, *Modeling and control of hybrid electric vehicle for drivability and fuel economy improvement*, Dissertation for phd degree, Ohio State

University

[17] **John M. Miller**. 2004, *Propulsion systems for hybrid vehicles*. IEE Power and Energy Series 45. The Institution of Electrical Engineers.

[18] **Jonas Hellgren and Karin Jonasson**. online visited 01/2010, *'Comparison of Two Algorithms for Energy Management of Hybrid Powertrains*, Department of Machine and Vehicle Systems Chalmers University of Technology, Gteborg, Sweden, Department of Industrial Electrical Engineering and Automation, Lund University, Sweden

[19] **Westbrook. M.**, 2001 *The Electric Car:Development and future of battery, hybrid and fuel-cell cars*. IEE Power and Energy Series 38, ed. A. Johns and D. Warne, London, United Kingdom: Institution of Electrical Engineers.

[20] **Musardo, Cristian, Staccia, Benedetto, Bittanti, Sergio, Guezennec, Yann, Guzzella, Lino, Rizzoni, Giorgio**. February 2004, *An adaptive algorithm for hybrid electric vehicles energy management*, Technical paper for students and young engineers, FISITA world automotive congress, Barcelona.

[21] **Meisel, J**. 2006, *An analytic foundation for the Toyota Prius THS-II powertrain with a comparison to a strong parallel hybrid-elecric powertrain*, in SAE 2006 World Congress, Detroit, MI.

[22] **Karden, E., et al**. 2007, Energy storage devices for future hybrid electric vehicles. Journal of Power Sources, 168(1): pp. 2-11.

[23] **Christian Tallner, Simon Lannetoft**. 2005, *Batteries or supercapacitors as energy storage in HEVs?* , Dept. of Industrial Electrical Engineering and Automation Lund University, CODEN:LUTEDX/(TEIE-5194)/1-71

[24] **Markel, T. and A. Simpson**. 2005, *Energy storage systems considerations for grid-charged hybrid electric vehicles*, Chicago, IL, United States: Institute of Electrical and Electronics Engineers Computer Society, Piscataway, NJ 08855-1331, United States.

[25] **Kotz, R. and M. Carlen**. 2000, *Principles and applications of electrochemical capacitors*, Electrochimica Acta, 45(15-16): pp. 2483-2498.

[26] **Rufer, A. and P. Barrade**. Sep 30-Oct 4 2001, *A supercapacitor-based energy storage system for elevators with soft commutated interface* in 36th IAS Annual Meeting -Conference Record of the 2001 Industry Applications, Chicago, IL: Institute of Electrical and Electronics Engineers Inc.

[27] **Arulepp, M., et al**. 2006, *The advanced carbide-derived carbon based supercapacitor*, Journal of Power Sources, 162(2 SPEC ISS): pp. 1460-1466.

[28] **Dr. John M. Miller, VP Systems Applications and Integration**. 20 October 2008, *Ultracapacitors for PHEV? Application and Systems Engineering Perspective*, PowerPoint, Maxwell technologies, IEEE Southeastern Michigan Section

[29] **Anstrom, J.R., et al**. 2005, *Simulation and field-testing of hybrid ultra-capacitor/battery energy storage systems for electric and hybrid-electric transit vehicles*, Austin, TX, United States: Institute of Electrical and Electronics Engineers Inc., Piscataway, NJ 08855-1331, United States.

[30] **C. Musardo, G. Rizzoni, Y. Guezennec, and B. Staccia**. 2005, *A-ECMS: An adaptive algorithm for hybrid electric vehicle energy management*. European Journal of Control, 11(4-5), Fundamental Issues in Control, Special Issue.

[31] **Y. Zhu, Y. Chen, G. Tian, H. Wu, and Q. Chen**. 2004, *A four-step method to design an energy management strategy for hybrid vehicles*, In Proceedings of the American Control Conference, volume 1, pp 15661

[32] **G. Paganelli, G. Ercole, A. Brahma, Y. Guezennec, and G. Rizzoni**. 2000, *A general formulation for the instantaneous control of the power split in charge-sustaining hybrid electric vehicles*, In Proceedings of the 5th Intl. Symposium on Advanced Vehicle Control, pp 7380

[33] **P. Pisu, K. Koprubasi, and G. Rizzoni**. 2005, *Energy management and driveability control problems for hybrid electric vehicles*, In Proceedings of the IEEE International Conference on Decision and Control / European Control Conference, pp 182430

[34] **S. Jeon, S. Jo, Y. Park, and J. Lee**. 2002, *Multi-mode driving control of a parallel hybrid electric vehicle using driving pattern recognition.* Journal of Dynamic Systems, Measurement, and Control, 124(1):14149

[35] **V. H. Johnson, K. B. Kipke, and D. J. Rausen**. online, visited 02/2001, *HEV control strategy for real- time optimization of fuel economy and emissions.* In SAE Proceedings, number 2000-01-1543.

[36] **C.C. Lin, H. Peng, and J.W. Grizzle**. 2004, *A stochastic control strategy for hybrid electric vehicles*, In Proceedings of the American Control Conference, volume 5, pages 471015

[37] **E. D. Tate, J. W. Grizzle, and H. Peng**. Dec 5, 2007, *Shortest path stochastic control for hybrid electric vehicles*, International Journal of Robust and Nonlinear Control. published online

[38] **X. Wei, L. Guzzella, V. I. Utkin, and G. Rizzoni**. 2007, *Model-based fuel optimal control of hybrid electric vehicle using variable structure control systems*, Journal of Dynamic Systems, Measurement, and Control, 129(1):13-19

[39] **P. Pisu and G. Rizzoni**. 2004, *H-inf control for hybrid electric vehicles. In Proceedings of the 43rd*, IEEE Conference on Decision and Control, volume 4, pp 3497-502

[40] **M. Koot, J.T.B.A. Kessels, B. de Jager, W.P.M.H. Heemels, P.P.J. van den Bosch, and M. Steinbuch**. 2005, *Energy management strategies for vehicular electric power systems*, IEEE Transactions on Vehicular Technology, 54(3):771782

[41] **Tony Markel and Keith Wipke**. January 9, 2001, *Modeling grid-connected hybrib electric vehicles using ADVISOR*, NREL: center for transportation technologies and

systems Annual Battery Conference Long Beach, California. National Renewable Energy Laboratory Golden, Colorado

[42] **Chan-Chiao Lin, Huei Peng and J. W. Grizzle. Jason Liu and Matt Busdiecker**. 2003, *Control System Development for an Advanced-Technology Medium-Duty Hybrid Electric Truck'*, SAE International, University of Michigan and Eaton Corporation

[43] **Tony Markel and Andrew Simpson**. September 8, 2005, *Energy Storage System Considerations for Grid-Charged Hybrid Electric Vehicles*, Powerpoint, presented atIEEE Vehicular Power and Propulsion Conference

[44] web site, visited 04/2010, *http://en.wikipedia.org/wiki/Stochastic*